Cape Peninsula University of Technology

BIODIESEL PRODUCTION FROM EDIBLE OIL WASTEWATER SLUDGE WITH BIOETHANOL USING HETEROGENEOUS NANO-MAGNETIC CATALYSIS

by

ILUNGA WIGHENS NGOIE (211280224)

Thesis submitted in fulfilment of the requirements for the degree

Doctor of Engineering: Chemical Engineering,

in the Faculty of Engineering

at the Cape Peninsula University of Technology

Supervisors: Prof. Daniel Ikhu-omoregbe, Dr Pamela J. Welz and A/Prof Oluwaseun O. Oyekola

Bellville campus

2019

DECLARATION

I, Ilunga Wighens Ngoie, declare that the contents of this dissertation/thesis represent my own unaided work, and that the dissertation/thesis has not previously been submitted for academic examination towards any qualification. Furthermore, it represents my own opinions and not necessarily those of the Cape Peninsula University of Technology.

Signed **Date**

ABSTRACT

Currently, most sludge from the wastewater treatment plants of edible oil factories is disposed to landfills, but landfill sites are finite and potential sources of environmental pollution. Production of biodiesel from wastewater sludge can contribute to energy production and waste minimization. However, conventional biodiesel production is energy- and waste-intensive. Generally, biodiesel is produced from the transesterification reaction of oils with alcohol (i.e. methanol, ethanol) in the presence of a catalyst. Homogeneously catalysed transesterification is the conventional approach for large scale production of biodiesel as reaction times are relatively short. Nevertheless, homogenous catalysis presents several challenges such as high probability of soap formation in the presence of water and free fatty acids, and difficulty of separation and reusability. The current study aimed to reuse wastewater sludge from the edible oil industry as a novel feedstock for both monounsaturated fats and bioethanol to produce biodiesel. Preliminary results have shown that the fatty acid profile of the oilseed wastewater sludge is favourable for biodiesel production with 48% (w/w) monounsaturated fats; the residue left after the extraction of fats from the sludge contains sufficient fermentable sugars, after steam explosion followed by an enzymatic hydrolysis, for the successful production of bioethanol [29% (w/w)] using a commercial strain of *Saccharomyces cerevisiae.* A novel nano-magnetic catalyst was synthesised from mineral processing alkaline tailings, mainly containing dolomite originating from cupriferous ores using a modified sol-gel technique. The biodiesel produced from the wastewater sludge performed well. The thermal efficiency was 30.75% (compared to 28.4% and 26.95 for conventional biodiesel and petroleum-based commercial diesel, respectively). The fuel consumption was higher than commercial diesel at a maximum brake power of 12.8 kW (0.15 and 0.31 kg/kW.h for commercial diesel and wastewater sludge biodiesel respectively) but it was more environmentally friendly in terms of gaseous emissions - both fuels showed a linear decrease in emissions proportionate to the increase in engine speed, reaching averages of 51.5 ppm/g/h and 89.9 ppm/g/h nitrous oxides, respectively at 2000 rpm, and 249.3 ppm/g/h and 310.4 ppm/g/h carbon monoxide, respectively at 800 rpm. Both the catalytic properties and reusability of the catalyst were investigated. A maximum biodiesel yield of 88% was obtained, which dropped to 61% after the fourth transesterification reaction cycle. The proposed approach has the potential to reduce material costs, energy consumption and water usage associated with conventional biodiesel production technologies. It may also mitigate the impact of conventional biodiesel production on food and land security, while simultaneously reducing waste.

ACKNOWLEDGEMENTS

I am, first and foremost, thankful to God, Maker of all things, Most High, Father of our Lord and Saviour Jesus Christ. Without His wonderful grace and unending love, my study and good health during this period in Cape Town (South Africa) would not have been possible.

My extended acknowledgment and gratitude goes to my supervisors, namely, Dr Pamela J. Welz, A/Prof Oluwaseun O. Oyekola and Prof. Daniel Ikhu-Omoregbe for their guidance and assistance during the entirety of this project. Such academic rigour as may be found in this thesis is largely due to their constant refusal to let me get away with certain things, while their unerring sense of when to intervene, and how, and when not to, has taught me much not only as a student researcher but also as a tutor.

My sincere appreciation also goes to the Water Research Commission of South Africa (WRC-Project K5/2404) and the Council for Scientific and Industrial Research (CSIR/HCD-IBS programme) for funding this project, and the Cape Peninsula University of Technology for the opportunity. The content does not necessarily reflect the views and policies of the funding organisations.

Thank you all for making this research project such a great success.

DEDICATION

I would like first of all to dedicate this final dissertation to the Most-High, my God who gave me life and necessary strength, hope and intelligence to accomplish this work by His Love and Grace.

This dissertation is also dedicated to my outrageously loving and supportive wife, Cleopatra (Van Ster) Ngoie, to my boys, Jayden and Dilian, and especially to my beautiful daughters, Tiffany, Marie-Jeanne and Zarah-Kate. May this thesis be a source of inspiration for you. Special feeling of gratitude to my loving parents, Felix and Marie-Jeanne Ngoie, whose words of encouragements, prayers and push for tenacity still ring in my ears; to my sister Lisette and brothers Gusthalaure, Radelphe and Guemraphel, who have never left my side and are very special.

This thesis is also dedicated to my Godfather Prophet Joshua Mwansa and brother Bhytha for their prayers, words of motivation and words of comfort over my life as well as my family. In the same line, dedicating this thesis to my wise father in-law, Charles Daniels, my loving mother in-law, Florencia Daniels, Uncle Henry Roussow, Suzan Nyema, Tantine Georgette, Papa Toussaint and Maman Charlotte Mande, as well as the whole Van Ster family for their advices, compassion, love and care both physically and spiritually.

To my fellow colleagues, friends and brothers from the Congolese community of engineers in Cape Town, who have assisted me in so many ways on and off-campus, I dedicate this work. Most importantly, Aime Kabwe, Lagouge Tartibu, Butteur Ntamba Ntamba, Ladislas Kangaji, Paul Senda, Carl Mubenga, Fabrice Nebesse, Popaul Kaumba, Daniel Okundji, Bathe Kabamba, Emmanuel I-Muaka and Steeve Tshilumbu.

I also dedicate this dissertation and give special thanks to friends and cousins who have always been there to cheer me up and motivate me during my challenges: Patrick Kabale, Yves Lubovya, Walter and Gay Hendricks, Ayrton Daniels, Charles Daniels, Lorenzo Daniels, Kim Daniels, Yannick Kabale, Yvon Mbayo, Pablo Mulondayi, Francis Mbongo, Papy Nkaniabo, Patrick Mwanza, Sampi Dieya, Leon and Stephanie Jantjies, Jack Mwamba, Shane Hanson, George Okita, Jerry Ilunga Privato and Mickael Mukuta.

To everyone at the BTB research group (CPUT), you have been amazing: Dr Le Roes-Hill, Dr Welz, Ashton, Tony, Kim, Alaric, Robyn, Chandre, Gareth, Bulelwa, Monde and Thandeka.

Finally, to everyone who could not find his/her name mentioned above, be sure that in every single thing that you had contributed to make this work a success, I deeply thank you from the bottom of my heart and may you appreciate my feelings of gratitude.

May God bless you all.

Table of Contents

LIST OF FIGURES

LIST OF TABLES

ABBREVIATIONS AND SYMBOLS

ASTM: American Society for Testing and Materials

ADP: Abiotic Depletion Potential

AP: Acidification Potential

BET: Brunauer Emmett Teller

BF_3: Boron Trifluoride

BGL: β-glucosidase

BJH: Barrett-Joyner-Halenda

BTB: Biocatalysis and Technical Biology Research Group

CBH: Cellobiohydrolase

CBU: Cellobiase Unit

CFU: Colony forming unit

CHTs: Hydrotalcites

CPUT: Cape Peninsula University of Technology

CMCO: Catalyst obtained by co-precipitation method

CMSG: Catalyst obtained by sol-gel method

CO: Carbon monoxide

DPS: Dry pretreated sludge

EDX: Energy dispersive X-Ray spectroscopy

EtOH: Ethanol

EN: European normalisation

EOWWS: Edible oil wastewater sludges

EP: Eutrophication potential

FAAEs: Free acid alkyl esters

FAMEs: Free acid methyl esters

FAEEs: Free acid ethyl esters

FAETP: Fresh water aquatic ecotoxicity potential

FFAs: Free fatty acids

FPU: Filter paper unit

GC: Gas chromatography

GC-FID: Gas chromatography flame ionisation detection

GHGs: Greenhouse gases

GWP: Global warming potential

HHV: High heating value

HPLC: High performance liquid chromatography

HTP: Human toxicity potential

IC: Internal combustion

KF: Potassium fluoride

KOCH3: Potassium methoxide

LCA: Life cycle assessment

MAETP: Marine aquatic ecotoxicity potential

MEOH: Methanol

MgO: Magnesium oxide

$NaOCH_3$: Sodium methoxide

NOx: Nitrogen oxides

OD: Optical density

OWS: Oilseed waste sludge

POCP: Photochemical oxidation potential

ROE: Residues after oil extraction

RSM: Response surface methodology

SD: Standard deviation

SEM: Scanning electron microscopy

SHF: Separate hydrolysis-fermentation

SSF: Simultaneous saccharification-fermentation

TEFP: Terrestric ecotoxicity potential

TEM: Transmission electron microscopy

TS: Titanium Oxide supported on silica (TiO_2/SiO_2)

TSA: Tryptic soy agar

TSB: Tryptic soy broth

VOP: Vanadyl phosphate ($VOPO_4.2H_2O$)

XRD: X-Ray diffraction

ZVINPs: Zero valent iron nanoparticles

CHAPTER ONE: INTRODUCTION

Oilseed processing and refining to produce oil generates significant quantities of wastewater, organic solid waste and inorganic residues. Organic solids consist mainly of seeds and husks. Wastes, residues, and by-products may be used for producing commercially viable products or for energy generation (Olkiewicz *et al*., 2012; Kumar *et al*., 2015).

Currently, most edible oil industries use landfilling as a simple means of waste disposal. Collection and transportation account for 75 percent of the total cost of solid waste management. Landfilling has a potentially adverse impact on the environment, including problems such as flies, odour, air pollution, unsightliness, windblown litter, as well as pollution of the water system and landfill gas generation. Conversion of waste to energy as a form of resource recovery is a viable route for managing organic waste matter (DWA, 2016).

Biodiesel is a biodegradable, renewable fuel, consisting of mono-alkyl esters of fatty acids (Meher *et al*., 2006; Demirbas, 2016). This fuel offers many advantages over conventional diesel made from fossil fuels including higher flash point, higher cetane number, lower viscosity, higher lubricity, increased biodegradability, and environmental friendliness due to lower carbon monoxide emissions (Centi and Perathoner, 2008).

Generally, biodiesel is produced from the transesterification reaction of oils with alcohol in the presence of a catalyst. The alcohols typically used are methanol, ethanol, propanol or butanol. Methanol is preferred because of its low price and availability (Xie and Yang, 2007).

Homogeneously catalysed transesterification is the conventional approach for large-scale production of biodiesel as reaction times are relatively short (McNeff *et al.*, 2008). Nevertheless, homogenous catalysts present the following challenges: high possibility of soap formation in the presence of water and free fatty acids; they cannot be reused since some of the catalyst is consumed during the reaction, and the separation of the remaining catalyst from the product is difficult (McNeff *et al.*, 2008). Conversely, heterogeneous catalysts do not present separation and environmental problems, but the reactions they mediate are characterised by low reaction rates (Kouzu *et al.*, 2007). The low rate can be attributed to mass transfer restrictions. There is thus a need to employ catalysts that will minimise this and avoid the use of centrifugation separation which is energy-consuming (Kouzu *et al.,* 2007).

1.1 Research problem

Currently, most edible oil waste sludge is disposed of in landfills, but landfill sites are finite and potential sources of secondary environmental pollution. In addition, the world is currently

facing an energy crisis and global warming. Production of biodiesel from waste sludge can contribute to energy production and waste minimization. However, conventional biodiesel production is energy- and waste-intensive.

1.2 Aim and objectives

The aim of the project was to produce biodiesel from wastewater sludge generated from edible oil industries using a synthesised nano-magnetic heterogeneous catalyst. The primary objectives were:

a) To extract monounsaturated oils from oilseed waste sludge;

b) To produce bioethanol from lignocellulosic oilseed waste by microbial fermentation;

c) To synthesise a nano-magnetic heterogeneous catalyst from cupriferous mineral processing gangue;

d) To produce biodiesel through a heterogeneous transesterification process.

1.3 Delineation

The aim of the study, further, was to produce biodiesel from oilseed waste sludge from a canola seed oil processing industry. This included bioethanol production, catalyst synthesis, and optimisation of the transesterification process. Further logistics, costing and the building of a pilot plant will form part of future work.

CHAPTER TWO: LITERATURE REVIEW AND THEORY

2.1 Overview on biodiesel and its production

Crude oil is one the most abundant energy resources and has a high heating value. It is relatively inexpensive and there is no need for new pre-use of production technologies. Many of the locations where crude oil can be drilled at low cost have been depleted, and it is now being mined off-shore and from tar sands (International Energy Agency [IEA], 2016).

Oil refinery technology is mature, which implies that production of products like diesel and petrol, and global distribution networks are well-established (Renewable Energy Policy Network for the 21st Century [REN21], 2017). According to International Energy Agency (IEA, 2017), by the fourth quarter of 2018, the global crude oil demand will surpass the psychological barrier of 100 million barrels per day (m.bbl/day), with almost half of the rise in demand of 1.4 m.bbl/day coming from China and India.

The renewable energy policy network for the 21st century stated in the current annual report (REN21, 2017) that the direct route by which the transport sector contributes to greenhouse gas (GHG) emissions is through the combustion of fossil fuels.

Fossil fuels contain a substantial amount of carbon, and when they are burned in the presence of oxygen they form carbon dioxide, the most extensive GHG by volume. Small amounts of methane (CH_4) and nitrous oxide (N_2O) are also generated during combustion of fuels in the transport sector (REN21, 2017 and Althor *et al*., 2016).

The latest South African GHG inventory, an official submission to the United Nations Framework Convention on Climate Change (UNFCCC), was published in 2014. The latest data, for 2010, suggest that energy used in transportation contributed a total of 47 Mt CO_2 which is approximately 8.8% of South Africa's GHG emissions (excluding emissions from agriculture, forestry and land use) (Althor *et al.,* 2016 and Department of Environmental Affairs [DEA], 2016).

To convert emissions of a gas to its CO_2 related concentration, the emissions are multiplied by a factor known as the global warming potential or GWP. For example, the 100-year GWP of methane (CH_4) is 25. This also implies that methane is 25 times "worse" than CO_2, on a per kilogram basis, in terms of the warming it generates over a 100-year period (DEA, 2016).

In response to this increasing demand, together with related disadvantages of fossil fuels, alternative liquid fuels have become the subject of significant research interest for the following reasons:

- Biodiesel is renewable: biofuels are vast resources since the raw materials for their production can be replenished through renewable sources (Fulton *et al*., 2004).
- Biodiesel can reduce carbon emissions: direct carbon emissions from combustion of biodiesel are minimal relative to fossil fuels (Bailis *et al*., 2005).
- Biodiesel can improve energy security: countries with surplus agricultural land can produce their own fuel and reduce their dependence on foreign sources for energy (Hazell and Pachauri, 2006).
- Biodiesel has physical and chemical properties similar to liquid fuel from crude oil: Several physical and chemical characteristics of biodiesel such as specific energy density, viscosity, and combustion characteristics are similar to gasoline or diesel manufactured from crude oil (Fulton *et al*., 2004 and Ugarte, 2006).

Table 1: Major benefits of biodiesel over fossil fuels (Fulton et al., 2004)

Environmental impacts	Reduction of GHGs; reduction of air pollution; higher combustion efficiency; easily biodegradable; carbon neutral.
Energy security	Domestically distributed; reduced dependence on imported petroleum; renewable; fuel diversity.
Economic impacts	Sustainability; increased number of rural manufacturing jobs; increased farmer income; agricultural development.

The biodiesel market has been witnessing continuous growth and development across the world over the past few years. Governments across the world, especially those affected by volatile oil prices and production levels, are committing large resources to the development of this sector in an attempt to reduce their dependency on oil (REN21, 2017 and IEA, 2016).

Biodiesel production depends on the nature and quality of the feedstock. These include plant crops, crop residues, agricultural and municipal waste (Association of Official Analytical Chemists [AOAC], 2005 and Olkiewicz *et al*., 2012).

Transesterification is the conventional method for biodiesel production. It is a chemical process by which vegetable oils (e.g. soybean, canola, palm) can be converted to methyl or ethyl esters of fatty acids (biodiesel) using an alcohol (i.e. methanol or ethanol) in the presence of a catalyst (Demirbas, 2003) (Figure 1) or without a catalyst (Darnoko and Chernyan, 2000).

Non-catalytic reactions are fast but require high pressure (35-60 MPa) and high temperature (250-400°C) to be driven to completion. Although the products can be easily separated since there is no catalyst, the process requires high capital investment because of the operating conditions (Kusdiana and Saka, 2004).

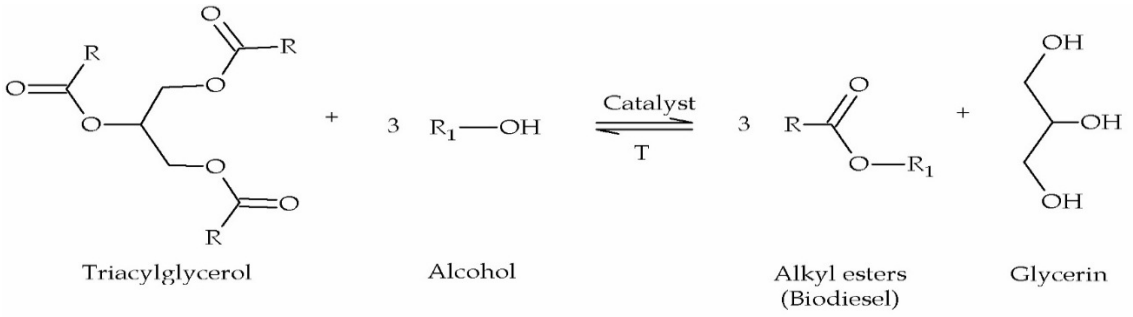

Figure 1: Transesterification reaction (R, R1: Alkyl chains with different lengths and/ or saturation degrees) (Darnoko and Cheryan, 2000)

Transesterification also results in the production of glycerol, a chemical compound with diverse commercial uses. Commercial biodiesel is currently produced by transesterification using homogeneous catalysts (i.e. acid or alkali solutions). In either case, the process requires both high purity raw materials (triglyceride from biomass) and an additional step for catalyst separation from the product. These requirements increase the cost of biodiesel production and consequently its price. High purity fats and refined oils tend to cost more than alternative, less pure feedstocks. The main impurities in the triglyceride feed, if it is not virgin plant oil, are typically free fatty acids (FFAs) and water. Homogeneous alkali catalysts are very sensitive to water and FFAs in the feedstock (Souza *et al*., 2016; Darnoko and Chernyan, 2000). Therefore, feed pretreatment is required. Pretreatment increases the cost of employing catalysed transesterification methods, which make low cost feedstocks less attractive (Lotero *et al*., 2005). Further, the strict regulations on the aromatic and sulphur content of diesel fuels results in higher production costs, as removal of aromatics from the distillate fractions requires capital-intensive processing equipment (Karmee *et al*., 2015).

At the end of the transesterification reaction, two liquid phases exist, a biodiesel layer and a glycerol layer. The glycerol layer contains most of the catalyst, which must be removed if pure glycerol is to be produced as a by-product. The trace amount of the catalyst in the ester layer needs to be removed by washing, which is increasingly being performed in a closed loop process to avoid generating large volumes of wastewater (Figure 2). The water reuse cycle relies on evaporation, which requires additional energy (Bobade *et al*., 2011).

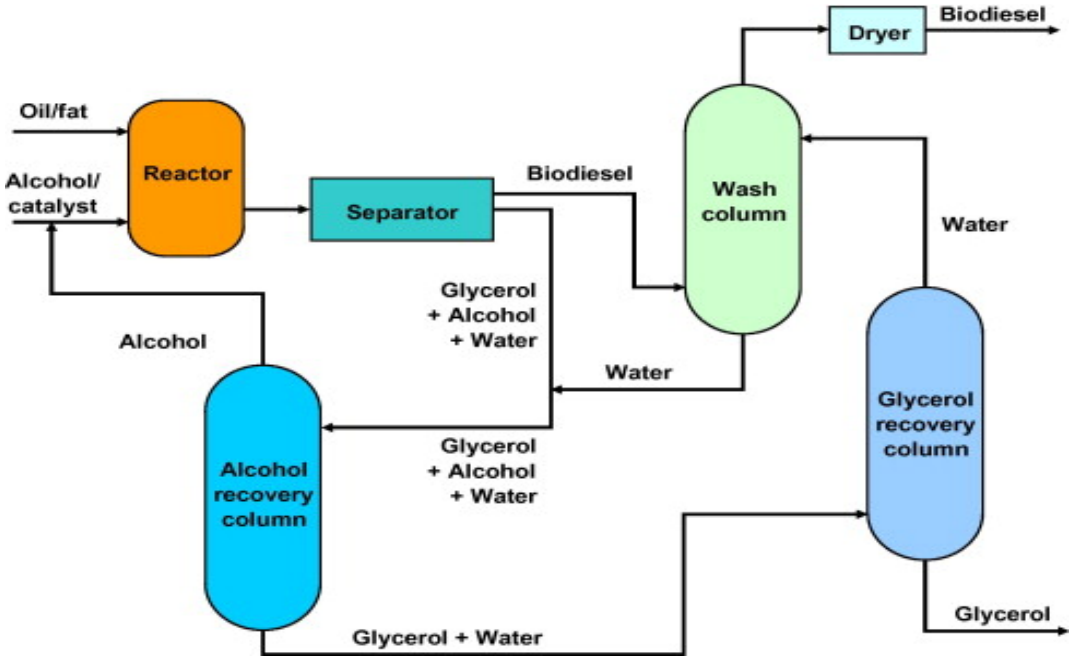

Figure 2: Conventional biodiesel production using alcohol and homogeneous catalysis (adapted from Demirbas, 2003)

In heterogeneously catalysed processes, once the biodiesel is produced, the catalyst can be regenerated and reused. Many separation techniques can be used for solid-liquid separation, with centrifugation being the most common. However, due to its high energy consumption, it is not economical on an industrial scale (Hu *et al.*, 2011). The use of magnetic catalysts and consequent magnetic separation is an alternative energy-efficient option. The drawbacks of conventional biodiesel production highlight the need to investigate a sustainable approach with the potential for cost competitive biodiesel production (Demirbas *et al*., 2016).

2.2 Feedstock

Although the biodiesel industry has experienced tremendous growth, raw material supplies have served as a natural brake and created a strain on margins for biodiesel producers. The surge in commodities prices is a result of numerous factors, including expanding domestic and global biofuel production capacity, low commodity stocks due to global weather situations, increased energy and transportation costs, and the strength of global food demand (REN21, 2017; Figiel and Hamulczuk, 2014).

Plant-derived vegetable oils are considered the most efficient raw materials for the production of biodiesel because of their biodegradable, non-toxic, environmentally friendly and renewable nature. The major economic factors to consider with regards to feedstock are the price of raw material, transport, collection, and oil extraction, which makes up around 75-80% of the total

operating costs (Karmee *et al*., 2015). The type of agricultural feedstock that can be grown locally differs significantly from country to country, based on regional climatic conditions and soil fertility (Hazell, 2006). In addition to vegetable oils (edible and non-edible), researchers have also evaluated animal fats, algal oil and even waste cooking oils to produce biodiesel (Table 2). It is difficult to critically compare research results in terms of feedstock as most processes employ different catalysts and/or reaction conditions.

Vegetable oils represent the main lipid feedstock for biodiesel production. They are renewable in nature and environmentally friendly, with the possibility of being produced on a large scale. Different vegetable oils, including edible and non-edible oils, as well as waste vegetable oils have been tested as feedstocks for biodiesel production. Vegetable oil can be obtained from more than 350 different oil-bearing crops (Souza *et al*., 2017 and Demirbaş, 2009).

Oils are extracted mainly from seeds and fruits of plants and consist of mixtures of organic compounds (Singh *et al*., 2014), in addition to free fatty acids, phospholipids, carotenes, tocopherols, water and other impurities. Oils derived from animal fat (e.g. pork and poultry fat, beef tallow, and fish oil from the meat and fish industries) contain high concentrations of saturated fatty acids, which negatively affect the quality of their methyl esters during biodiesel production at low temperatures (Balat *et al.*, 2011).

Although microalgae, considered to be the third-generation feedstock, have shown potential for high biomass growth and lipid productivity, and can be grown on non-arable land, there are some constraints that must be overcome in order to make biodiesel production from this source economic and sustainable: the composition of microalgal oil varies between species, often resulting in poor conversion of oil to biodiesel; high quantities of non-oil substances may be present; and the oil-extraction processes are costly (Singh *et al*., 2014).

The price of feedstock constitutes approximately 70-85% of the total biodiesel production costs, when even the least expensive refined vegetable oils are used (Souza *et al*., 2017; Demirbaş, 2016 and Knothe *et al*., 2005). The cost of biodiesel from a particular vegetable oil is dependent on a number of factors, including the oil content, and the geography, climate, and soil conditions (which affect the yield per hectare) (Figiel and Hamulczuk, 2014; Atabani *et al*., 2012; Gui *et al*., 2008 and Knothe *et al*., 2001).

Another important criterion that should be considered when choosing the feedstock for biodiesel production is the composition of the oil. The composition of oil will subsequently determine the properties and the quality of obtained biodiesel, but also will affect the choice of the production technology. Fatty acids vary in carbon chain length and in the number of

unsaturated (double) bonds. The percentage and type of fatty acid composition depends mainly on the plant species and their growth conditions (Atabani *et al*., 2013).

2.2.1 Edible oils

Currently, more than 95% of biodiesel produced globally is from edible vegetable oils, such as rapeseed, soybean, sunflower and palm as reported by the United States department of agriculture (USDA, 2017). Edible oils are readily available because of abundant agricultural production, and impurities are minimal. These factors, together with the relative ease of processing and high quality of biodiesel obtained, make them the most suitable raw material for biodiesel production (Demirbas *et al*., 2016), Edible oils are considered to be the first-generation biodiesel feedstock. The oil content and yield, fatty acid composition and other properties of edible oils are given in Table 2.

2.2.1.1 Soybean oil

Soybean is an annual crop from the Leguminosae family. It is one of the world's most important sources of plant protein and edible oil for both humans and animals (Milazzo *et al*., 2013). The major producers of soybean oil are the United States, Brazil and Argentina, and this oil is now the world's second largest oilseed in terms of total oil production (IEA, 2016).

With high protein content (about 40%), which is commonly used for animal feed, soybean is the highest yielding source of vegetable protein (up to 50%) globally (Milazzo *et al.*, 2013). The drawbacks of soybeans when compared to oilseeds oil as a biodiesel feedstock is the low oil content (15 to 22 wt.%) and its yield (3.6 t/ha) (Issariyakul and Dalai, 2014; Milazzo *et al*., 2013). The major fatty acids in soybean oil are oleic (C18:1), linoleic (C18:2) and linolenic (C18:3). Soybean-derived biodiesel is prone to oxidation because of the high polyunsaturated fatty acid content (63 wt.%) of soybeans (Table 2) (Milazzo *et al*., 2013). This problem can be overcome, since soybean oil is often modified by traditional plant breeding, chemical, or genetic manipulation, which have been used to modify the fatty acid composition of soybean oil in order to improve its oxidative or functional properties (Wang, 2002). Soybean biodiesel offers enhanced biodegradation, reduced toxicity, increased flash point and lubricity and lower emissions in comparison to other types of biodiesel produced using sunflower oil, canola oil and rapeseed oil (USDA, 2017 and Milazzo *et al.*, 2013).

2.2.1.2 Rapeseed and canola oil

Rapeseed is a bright-yellow flowering member of the family Brassicaceae (mustard or cabbage family), first cultivated in India almost 4000 years ago. According to the United States Department of Agriculture, rapeseed was the third-leading source of vegetable oil in the world in 2015, after palm and soybean oil; it was the world's second largest source of protein meal (USDA, 2017). Early rapeseed cultivars had high levels of erucic acid (C22:1) in the oil and high levels of glucosinolates in the meal, components that were considered to be a health concern (Przybylski and Mag, 2002). This was the reason for plant breeding programs initiated in Canada, which led to the first low-erucic acid cultivars of *Brassica napus* and *Brassica rapa* (Przybylski and Mag, 2002). By definition, canola should contain less than 2% erucic acid in the oil and less than 30 *μ*mol/g glucosinolates in the air-dried, oil-free meal (Przybylski and Mag, 2002). Rapeseed oil was used in the very first efforts to promote biodiesel as a fuel obtained from renewable sources. Rapeseed and canola seeds have oil content over 40 wt.% in which the dominant fatty acids include oleic acid (C18:1), linoleic acid (C18:2) and (for rapeseed) erucic acid (C22:1) (Issariyakul and Dalai, 2014).

The type of fatty acid in the feedstock oil determines the biodiesel characteristics, and a higher percentage of unsaturated fatty acids will result in biodiesel having better cold flow properties (Atabani *et al.*, 2013). Due to its high content of oleic acid (about 64 wt.%) biodiesel produced from rapeseed and canola oil has very good cold flow properties (Gui *et al*., 2008), making this biodiesel suitable fuel for use during the winter. However, according to Milazzo *et al.* (2013), biodiesel from rapeseed oil is not compatible with diesel oil particulate filters because it is difficult to achieve effective compression in the combustion chamber to generate sufficient energy output. Also, rapeseed require the application of high levels of nitrogenous fertilisers for growth, which is incorporated into the seeds and is released as the GHG/N_2O during combustion (Althor *et al*., 2016).

2.2.1.3 Sunflower oil

The sunflower is a plant native to the Americas, where it was domesticated long before the arrival of European explorers (Gupta, 2002). Sunflower oil is the fourth most important vegetable oil in the world and accounts for approximately 10% of the total world’s consumption of plant-derived edible oil (Balalić *et al*., 2012). Oil is derived from the seed of the sunflower plant, which contains 48-52% of high quality edible oil (Balalić *et al*., 2012). Usually, sunflower oil is comprised of up to 90% unsaturated fatty acids (combined oleic, C18:1, and linoleic, C18:2) and approximately 10% saturated fatty acids (palmitic, C16:0, and stearic, C18:0) (Zheljazkov *et al*., 2011). Several varieties of sunflower oilseeds have been developed by standard plant breeding methods, mainly to vary the amount of oleic and linoleic acid. Besides

the traditional sunflower oil with linoleic acid content of 65-70 wt.% of the oil, there are mid-oleic acid varieties (55-70% oleic acid and 15-35 wt.% linoleic acid) and high-oleic acid varieties (>80 wt.% oleic acid and only 5-9 wt.% linoleic acid) (Gupta, 2002). The high content of linoleic acid in traditional sunflower oil leads to less stability of the biodiesel to oxidation than biodiesel from canola oil, soybean oil or coconut oil (Souza *et al*., 2016).

2.2.1.4 Palm oil

The oil palm (*Elaeis guineensis*) originated from Africa and was introduced to East Asia as an ornamental plant in 1884 (Lin, 2002). Another species of oil palm, *Elaeis oleifera*, originated from Central and South America, but its oil is more unsaturated, and this species gives less oil yield, making it uneconomical to plant on a commercial scale (Lin, 2002). The oil palm is the most efficient oil-producing plant, with about 5.4 L of oil per hectare per year (Lin, 2002), which is five to ten times higher than oil yields from soybeans, sunflower or rapeseeds. Palm oil recently overtook soybean oil and now takes the first place in the list of oils produced in the world. Two south-east Asian countries dominate production of palm oil: Indonesia with 56% and Malaysia with 32% of all palm oil production (USDA, 2017).

Two types of oil, with different fatty acid composition and oil yield, are obtained from the oil palm fruit (*Elaeis guineensis*): palm oil from the mesocarp (palm oil in the narrow sense) and palm kernel oil from the kernel inside the nut (Lin, 2002).

There are great differences between palm oil and palm kernel oil with respect to their physical and chemical characteristics, especially in their fatty acid content. Palm oil has a balanced fatty acid composition in which the level of saturated fatty acids is almost equal to that of the unsaturated fatty acids: palmitic acid (44-45 wt.%), oleic acid (39-40 wt.%) and linoleic acid (10-11 wt.%) and only a trace amount of linolenic acid (Lin, 2002). Due to the low content of linoleic and absence of linolenic acid, the biodiesel from palm oil has high oxidation stability (Mekhilef *et al.,* 2011), but on the other hand, it has poor cold flow properties because of the high content of saturated fatty acids (Gui *et al*, 2008). Palm kernel oil belongs to so called ‘lauric’ oils and contains mainly lauric acid (C12:0, about 48 wt.%), myristic acid (C14:0, about 16 wt.%) and oleic acid (about 15 wt.%), while no other fatty acids are present at more than 10 wt.% (Pantzaris and Basiron, 2002).

2.2.1.5 Other edible oils

Beside these four edible oils that are most commonly used, some other oils such as corn, cottonseed, coconut, peanut, linseed, sesame, almond etc. could be used as a feedstock for

biodiesel synthesis. However, all listed oils have a high production and trade price, thus it is unlikely that they will find industrial application in the production of biodiesel (USDA, 2017 and Souza *et al*., 2016).

Table 2: Oil content and yield, the fatty acid composition and other properties of edible oils (adapted from O'Brien, 2002)

Oil	Oil content (%)	Oil yield (L/ha/year)	Fatty acid (%)						Quality indices			Reference
			16:0	18:0	18:1	18:2	18:3	other	AV (mg KOH/g)	IV (g I_2/100g oil)	SV (mg KOH/g)	
Soybean	15–20	446	13.9	2.1	23.2	56.2	4.3	NG	0.2	128-143	195.3	Atabani et al. (2012); Demirbaş (2003); Karmakar et al. (2010)
Rapeseed	38–46	1190	4.6	1.6	33.0	20.4	7.4	23	1.14	108.1	197.1	Atabani et al. (2012); Demirbaş (2003)
Canola	35-45	1400	4.3	1.7	61.0	20.8	9.3	1.2	<0.5	110	189.8	Issariyakul and Dalai, (2014); Karmakar et al. (2010)
Sunflower	25–35	952	6.4	2.9	17.7	72.9	NG	NG	0.15	132.3	191.7	Atabani et al. (2012); Demirbaş (2003)
Palm	30–60	5950	42.6	4.4	40.5	10.1	0.2	1.1	1.4	48-58	208.6	Atabani et al. (2012); Demirbaş (2003); Karmakar et al. (2010)
Corn	48	172	11.8	2.0	24.8	61.3	NG	0.3	0.11	119.4	194.1	Demirbaş (2003); Ma and Hanna (1999)
Cottonseed	18–25	325	28.7	0.9	13.0	57.4	NG	NG	0.07	113.2	207.7	Atabani et al. (2012); Demirbaş (2003); Ma and Hanna (1999)
Olive	45–70	1212	5.0	1.6	74.7	17.6	NG	0.8	<2	100.2	196.8	Atabani et al. (2012); Demirbaş (2003)
Peanut	45–55	1059	11.4	2.4	48.3	32	0.9	4.0	0.2	119.6	199.8	Atabani et al. (2012); Demirbaş (2003); Ma and Hanna (1999)
Linseed	40–44	NG	5.1	2.5	18.9	18.1	55.1	NG	8.3	156.7	188.7	Atabani et al. (2012); Aransiola et al. (2014); Demirbaş (2003)
Sesame	NG	696	13.1	3.9	52.8	30.2	NG	NG	2.4–10.2	91.8	210.3	Atabani et al. (2012); Aransiola et al. (2014); Demirbaş (2003)
Coconut	63–65	2689	8.9	2.7	6.4	1.6	NG	65.9	11.6	7.5–10.5	267.6	Demirbaş (2003); Karmakar et al. (2010); Pantzaris and Basiron (2002)

AV = acid value IV = iodine value SV = saponification value NG = not given

Cotton (*Gossypium hirsutum L.*) is an important crop that yields the natural fibre used by the textile industry. Cottonseed oil is a relatively low-cost feedstock for biodiesel production as cotton seeds are considered as by-products or waste (Karmakar *et al.,* 2010). The fatty acid profile of cottonseed oil is typical of the oleic/linoleic group of vegetable oils, since these two unsaturated fatty acids make up almost 75 wt.% of the total fatty acids. Oleic makes up about 22 wt.%, palmitic around 24 wt.%, linoleic about 52 wt.% and linolenic acid content is usually less than 1 wt.% (O'Brien, 2002).

The coconut palm is the species *Cocos nucifera* and the coconut oil is derived from copra, which is the dried kernel or 'meat' of coconuts (Pantzaris and Basiron, 2002). The largest producing countries are the Philippines and Indonesia (IEA, 2016). Coconut oil belongs to the so called 'lauric' oils, together with palm kernel oil, because lauric acid (C12:0) is the major fatty acid in this oil. These oils are characterised by high levels of the shorter and medium fatty acid chain lengths (C6-C14), of about 80 wt.%, while in the non-lauric vegetable oils they are below 2 wt.%. The major fatty acids are lauric (about 48 wt.%) and myristic (about 18 wt.%), while no other fatty acids are present at more than about 8 wt.% (Pantzaris and Basiron, 2002).

Coconut oil remains solid at relatively higher temperatures than most other vegetable oils. The main drawback of using coconut oil-based biodiesel in engines is that it starts solidifying at a temperature below 22°C such that at 14°C it does not flow at all (Karmakar *et al.*, 2010).

Peanut oil (*Arachis hypogeae*) is native to South America, Mexico and Central America. The physicochemical characteristics of peanut oil biodiesel closely resemble to those of diesel fuel. Peanut oil produces approximately 1170 L biodiesel/ha, compared to 475 L for soybean oil (Karmakar *et al.*, 2010). However, the production of biodiesel from peanut oil is not economically viable as peanut oil is more valuable than soy oil in the world market.

Corn (*Zea mays*) is a crop mainly sown in so many African countries and as well as in the United States for its starch and protein content (Agriculture South Africa [AgriSA], 2017). It is not practically viable to grow this crop specifically for biodiesel production as the grade of oil produced via primary extraction is unsuitable (Karmakar *et al*., 2010). However, when corn is first used for bioethanol production, the oil can then be separated easily, making biodiesel production viable. It is one of the most important grain crops in South Africa, being produced throughout the country under diverse environments with an approximately 8.0 million tons of maize grain produced annually on an average 3.1 million ha of land. Half of the production consists of white maize, for human food consumption (AgriSA, 2017).

Linseed (*Linum usitatissimum*) originated from Mediterranean coastal countries and is cultivated in Canada, United States, Argentina and India (USDA, 2017). Linseeds are a source of high quality proteins, soluble fibre and a high content of polyunsaturated fatty acids. The main use of linseed oil is as industrial oil based on its high unsaturation, but increasingly it is consumed as food oil. The biodiesel produced from linseed oil shows a high relative density because of the presence of more than 25% of unsaturated esters with more than two double bonds (Karmakar *et al*., 2010).

2.2.2 Non-Edible oils

The production of biodiesel from edible crops is contentious and is known as the 'food versus fuel' debate, whereby it contributes negatively to food security (USDA, 2017). There is the sociological question of whether to use oil as food or for fuel production, and there are concerns that large-scale production of biodiesel from edible oils may unbalance the global food supply and demand market (REN21, 2017 and USDA, 2017). In addition, the crops grown for biodiesel compete for limited fertile land with food crops. All of these factors increase the cost of food, which mostly affects the poorest populations of a society. The increase in raw material prices has also a negative impact on the sustainability of biodiesel production (Hotti and Hebbal, 2015).

From an environmental perspective, the intensive production of oil crops for biofuels leads to the degradation of the soil and deforestation (Hotti and Hebbal, 2015).

Therefore, non-edible vegetable oils or second-generation feedstocks are attractive as a promising cheaper, raw material for sustainable biodiesel production. There are many plants that produce significant amounts of non-edible oils. However, most of them contain high contents of free fatty acids, which increases the biodiesel production cost (Hotti and Hebbal, 2015 and Banković-Ilić *et al.*, 2012). Some of these non-edible oils include jatropha tree (*Jatropha curcas*), karanja (*Pongamia pinnata*), castor (*Ricinus communis*), tobacco seed (Nicotiana tabacum), mahua (*Madhuca indica*), neem (*Azadirachta indica*), rubber seed (*Hevea brasiliensis*), and sea mango (*Cerbera odollam*).

The oil content and yield, fatty acid composition and other properties of non-edible oils are given in Table 3.

Jatropha tree (*Jatropha curcas*) is a tropical plant from the *Euphorbiaceae* family (Nahar and Sunny, 2014). The presence of some toxic components renders this oil unsuitable for use in cooking but makes it very attractive for fuel production. It can grow almost anywhere and

under a wide variety of climatic conditions. Jatropha is grown in marginal and waste lands, on sandy, saline and degraded soils, without the need to compete with the land for food production. It is a drought-resistant plant and due to its characteristics can be easily cultivated without intensive care and with minimal effort (Nahar and Sunny, 2014; Gui *et al.*, 2008).

Recently, according to the latest REN21 annual report (2017), jatropha is considered one of the most promising potential oil sources for biodiesel production in South-East Asia, Central and South America, India and Africa. Jatropha oil content varies depending on the types of species, climatic conditions and mainly on the altitude where it is grown (Nahar and Sunny, 2014; Karmakar *et al*., 2010), but seeds contain about 40-60 wt.% and kernels 46-58 wt.% of oil (Banković-Ilić *et al.,* 2012; Kumar and Sharma, 2011). Jatropha produces oil rich in oleic (42 wt.%) and linoleic (35 wt.%) acid and smaller amounts of palmitic (14 wt.%) and stearic acid (6 wt.%), but fatty acid composition could be altered to some extent through interspecific hybridisation (Kumar and Sharma, 2011).

Karanja (*Pongamia pinnata*) is a fast-growing tree from to the *Legumnosae* family, has the potential for high oil seed production and has the ability to grow on marginal land. These properties support the suitability of this plant for large-scale vegetable oil production required by a sustainable biodiesel industry (Meenakshi, 2014 and Balat *et al.*, 2011).

Pongamia Pinnata is native to the Indian subcontinent and South-East Asia and has been successfully introduced to humid tropical regions of the world as well as parts of Australia, New Zealand, China and the USA (USDA, 2017 and Meenakshi, 2014). It is one of the few nitrogen-fixing trees and can be cultivated on land that has been exhausted of nutrients, helping to improve the soil quality so that the exhausted land can be reused for agricultural purposes (Souza *et al*., 2017).

The pongamia tree produces seeds with significant oil content, but the oil has many toxic substances that do not allow its use as cooking oil. The seed oil content ranges between 30 and 40 wt.% (Meenakshi, 2014 and Atabani *et al*., 2013) and the predominant fatty acid in the oil is oleic acid (51.8 wt.%), followed by linoleic acid (17.7 wt.%), palmitic acid (10.2 wt.%), stearic acid (7.0 wt.%), and linolenic acid (3.6 wt.%) (Meenakshi, 2014; Balat *et al.*, 2011).

Castor plant (*Ricinus communis*) belongs to the *Eurphorbiaceae* family and is a non-edible oilseed crop that is easily grown, and is resistant to drought. The tree is native to India, China, Brazil, some countries of the former Soviet Union, and Thailand. India produces about 60% of the world castor oil production (USDA, 2017). Castor seed has a high oil content of 46-55 wt.% (Rengasamy *et al*., 2014). Castor oil has a unique composition with approximately 89.5 wt.%

ricinoleic acid which is also known as castor oil acid. Ricinoleic acid is an unsaturated fatty acid which is soluble in most organic solvents (Rengasamy *et al*., 2014; Gui *et al.*, 2008).

Due to its composition, castor oil is the only oil completely soluble in alcohol and does not require heat and the consequent energy requirement of other vegetable oils to transform it into fuel (Kumar and Sharma, 2011). The viscosity of castor oil is up to seven times higher than that of other vegetable oils (Banković-Ilić *et al.,* 2012), but despite that, the kinematic viscosity of transesterified castor oil is comparable to other vegetable oils, making it suitable as a biodiesel blend (Rengasamy *et al*., 2014; Kumar and Sharma, 2011).

Tobacco (*Nicotiana tabacum L*.) seed oil is a by-product of tobacco leaf production that contains significant amounts of oil (35-49 wt.%). It is cultivated in more than 100 countries worldwide such as Macedonia, Turkey, and South Serbia and is widespread in North and South America (USDA, 2017).

The oil is non-edible, but physical, chemical and thermal properties are comparable with other vegetable oils, therefore it has the potential to be considered as a new feedstock for biodiesel production.

Mahua (*Madhuca indica*) is a tropical tree from the *Sapotaceae* family found largely in the central and northern plains and forests of India (USDA, 2017). The kernel constitutes about 70 wt.% of the seed and contains 50 wt.% oil with a relatively high percentage of saturated fatty acids such as palmitic (17.8 wt.%) and stearic (14.0 wt.%) acids (Kumar and Sharma, 2011). The remaining fatty acids are mainly distributed among unsaturated components such as oleic (46.3 wt.%) and linoleic (17.9 wt.%) acids. The relatively high percentage of saturated fatty acids (35.8 wt.%) found in mahua oil results in relatively poor low-temperature properties (Kumar and Sharma, 2011).

The mahua oil generally contains about 20% of free fatty acids, requiring more sophisticated technologies to convert it into biodiesel (Kumar and Sharma, 2011).

Neem (*Azadirachta indica*) tree belongs to the *Meliaceae* family, can grow in almost all types of soil including clay, saline, alkaline, dry and stony soils, and can tolerate extreme conditions like temperatures of 45°C and rainfall as low as 250 mm (Atabani *et al.,* 2013). The Neem tree is native to India, Pakistan, Sri Lanka, Burma, Malaysia, Indonesia, Japan, and the tropical regions of Australia. Almost the whole tree is usable for various purposes such as medicines, pesticides and organic fertilizer (Banković-Ilić *et al.*, 2012).

The seed of the fruit contains 20-30 wt.% and kernels 25-45 wt.% of oil (Atabani *et al*., 2013), generally with high amounts of free fatty acids, similar to mahua oil, which affect the process of biodiesel production.

Rubber tree (*Hevea brasiliensistree*) belongs to the family *Euphorbiaceae* and originates from the Amazon rain forest (Brazil). The tree is the primary source of natural rubber and produces 99% of world's natural rubber (USDA, 2017). The oil content of the seeds ranges from 50 to 60 wt.% and of the kernel from 40 to 50 wt.% of oil, which may contain up to 17 wt.% FFA (Atabani *et al.*, 2013). The oil is high in unsaturated constituents such as linoleic (39.6 wt.%), oleic (24.6 wt.%), and linolenic (16.3 wt.%) acids, and other fatty acids found in rubber seed oil include saturated species such as palmitic (10.2 wt.%) and stearic (8.7 wt.%) acids (Kumar and Sharma, 2011).

Sea mango (*Cerbera odollam*) is a tree belonging to the poisonous *Apocynaceae* family. It is well-known as a 'suicide tree' because of its highly poisonous nature and toxic content in the seed which is transferred into the oil after the extraction process. However, the toxin can be easily separated out from the extracted oil by decantation (Kumar and Sharma, 2011). The oil content from *Cerbera odollam* seeds is 54%. The fatty acid composition of *Cerbera odollam* oil is mainly oleic (48.1 wt.%), followed by palmitic (30.3 wt.%), linoleic (17.8 wt.%) and stearic (3.8 wt.%) (Atabani *et al.,* 2013), and the free fatty acid content in *Cerbera odollam* oil is significantly higher than in the majority of non-edible oils.

Table 3: Oil content and yield, the fatty acid composition and other properties of non-edible oils (adapted from Atabani *et al*., 2013)

Oil	Oil content (%)	Oil yield (L/ha/year)	Fatty acid (%)						Quality indices			Reference
			16:0	18:0	18:1	18:2	18:3	other	AV (mg KOH/g)	IV (g I_2/100g oil)	SV (mg KOH/g)	
Jatropha curcas	Seed: 40–60 Kernel: 46–58	1892	12.7–17.0	5.5–9.7	39.1–44.7	32.1–41.6	0.2	NG	1.2–45	82–98	193–208	Atabani et al. (2013); Balat (2011); Karmakar et al. (2010)
Karanja (Pongamia pinnata)	Seed: 25–50 Kernel: 30–50	225–2250	3.7–7.9	2.4–8.9	44.5–71.3	10.8–18.3	NG	1.1–3.5	2.53–20	81–90	185–195	Atabani et al. (2013); Karmakar et al. (2010); Srivastava and Prasad (2000)
Castor (Ricinus communis)	46–55	1188	1.1	3.1	4.9	1.3	NG	89.6	3.0	83–86	191.1	Atabani et al. (2013); Demirbaş (2003); Karmakar et al. (2010)
Tobacco seed (Nicotiana tabacum)	Seed: 36–41 Kernel: 17	2825	10.9	3.3	14.5	69.5	0.7	0.8	NG	125–154	191.5	Atabani et al. (2013); Singh et al. (2010)
Mahua (Madhuca indica)	Seed: 35–50 Kernel: 50	NG	16.0–28.2	14.0–25.1	41.0–51.0	8.9–17.9	NG	0.0–3.3	NG	58–70	190.5	Atabani et al. (2013); Srivastava and Prasad (2000)
Neem (Azadirachta indica)	Seed: 20–30 Kernel: 25–45	2670	13.6–16.2	14.4–24.1	49.1–61.9	2.3–15.8	0.8–3.4	0.2–0.26	32.6	65–80	209.7	Atabani et al. (2013); Aransiola et al. (2014); Srivastava and Prasad (2000)
Rubber seed (Hevea brasiliensis)	Seed: 50–60 Kernel: 40–50	NG	10.2	8.7	24.6	39.6	16.3	NG	1.7–42	133.9–142.5	183.9–226	Aransiola et al. (2014); Demirbaş (2003)
Sea mango (Cerbera odollam)	Seed: 54 Kernel: 6.4	NG	24.9–30.3	3.8–5.8	48.1–52.8	13.6–17.8	0.08	2.7	12.8	–	NG	Atabani et al. (2013); Kansedo and Lee (2012)

AV = acid value IV = iodine value SV = saponification value NG = not given

2.2.3 Waste cooking oils

To address issue linked to food security and economic challenges associated with the use of edible oils as feedstocks for biodiesel production (described in Section 2.2), the use of waste cooking oils has attracted attention, especially because of its relative lower price compared to pure oils as feedstock for biodiesel (Souza *et al*., 2016). However, it does have drawbacks in terms of energy security (Talebian Kiakalaieh *et al*., 2013). Some waste cooking oil is used for soap production (Chhetri *et al*., 2008).

The fatty acid composition and other properties of waste vegetable oils from different sources are given in Table 4.

Huge quantities of waste cooking oils are available throughout the world, especially in developed countries. For instance, according the IEA report (2016), an estimated potential amount of waste cooking oil collected in Europe was about 0.7-1 million tons during the year 2015; in the United States about 10 million tons; and in China 4.5 million tons.

Waste cooking oils are mainly collected from restaurants, hotels, other large food processing and service facilities, and households. Most of these oils are used for deep frying, after which they are no longer suitable for human consumption and their disposal is regulated (Souza *et al*., 2016).

The quality of the biodiesel produced from waste cooking oil is variable and largely dependent on the physicochemical properties of the feedstock. Heat treatment (i.e. cooking/frying) of vegetable oils at high temperatures (160-200°C) causes major physical and chemical changes. Some common physical changes observed are an increase in the viscosity and the specific heat, a change in colour and the surface tension, and an increase in the tendency to foam. Chemical changes are the consequence of thermolytic, oxidative and hydrolytic reactions that take place during the heating of oil at high temperature (Maddikeri *et al.*, 2012).

Oxidative reactions result in the formation of hydroperoxides, which can be converted into many other compounds such as aldehydes, ketones, hydrocarbons, alcohols, acids and esters (Kulkarni and Dalai, 2006; Maddikeri *et al*., 2012). As a result of all these reactions, waste vegetable oil contains variable quantities of undesirable compounds, primarily solid impurities, FFA (0.7 to 41.8 wt.%) and moisture (0.01 to 55.38 wt.%) (Çanakçi, 2007).

To produce biodiesel from waste vegetable oils, pretreatment is often required prior to transesterification. The separation of suspended solids from waste cooking oil can be effectively carried out by filtration or centrifugation and the removal of soluble salts by water

washing (Demirbas *et al*., 2016; Maddikeri *et al*., 2012), which unfortunately increases the energy consumption throughout the process as well as the water usage (Salim *et al.*, 2013; Perlak *et al*., 2005).

Pretreatment of waste cooking oil using steps such as neutralisation to avoid soap formation, adsorption of impurities by activated alumina or silica gel, drying, and deacidification can significantly improve the yield and quality of biodiesel, but increases the process costs (Souza *et al*., 2016).

Table 4: The fatty acid composition and other properties of different waste cooking oils (adapted from Gupta *et al.*, 2015)

Oil	Fatty acid (%)							Quality indices			Reference
	16:0	16:1	18:0	18:1	18:2	18:3	other	AV (mg KOH/g)	IV (g I_2/100g oil)	SV (mg KOH/g)	
Waste cooking oil from different local sources	8.5	NG	3.1	21.2	55.2	5.9	4.2	3.6	83	207	Yaakob *et al.* (2013)
	7.64	0.07	8.6	18.3	62.1	1.7	1.4	NG	NG	NG	Srilatha *et al.* (2012)
	11.58	0.11	4.2	24.8	53.5	5.6	3.7	7.6	NG	NG	Yan *et al*. (2009)
	5.18	0.51	2.1	59.7	19.3	6.8	6.3	NG	NG	NG	Chhetri *et al.* (2008)
	6.8	NG	3.1	33.7	56.4	NG	NG	2.24	NG	204.6	Gupta *et al.* (2015)
	26.5	NG	21.3	10.9	1.7	NG	NG	NG	NG	NG	Talebian-Kiakalaieh *et al*. (2013)
	39.3	0.18	2.3	46.3	11.9	NG	NG	5.0	NG	183.5	Lam and Lee (2010)
	20.4	4.6	4.8	52.9	13.5	0.8	2.0	2.1	NG	NG	Leung and Guo (2006)
	32.4	NG	3.8	42.5	15.3	5.9	NG	0.98	NG	183.4	Dehkordi and Ghasemi (2012)
	29.6	NG	3.7	48.6	18.0	trace	NG	1.04	NG	NG	Viola *et al.* (2012)

AV = acid value IV = iodine value SV = saponification value NG = not given

2.3 Comparison of ethanol and methanol as raw materials for biodiesel production

2.3.1 Environmental impacts

Typically, methanol is used as one of the reactants in the transesterification process, but is a non-renewable source obtainable from the Fischer-Tropsch process. Methanol is more volatile and is more toxic than ethanol. Ethanol can be obtained from fermentation of renewable sources such as agricultural wastes. It has a higher molecular weight (46 g/mole) than methanol (32 g/mole), which improves the cold flow properties of the resulting ester (Kumar and Singh, 2016; Helwani *et al*., 2009).

It has been reported that comparable yields of biodiesel can be obtained via the transesterification of oil using either ethanol or methanol as the transesterification agent. For example, Kim *et al*. (2010) reported almost 90% yield of biodiesel with $SnCl_2$ as a catalyst, using fixed high molar ratios of ethanol to oil (120:1).

Dorado *et al.* (2002) reported a high biodiesel yield working in a pressurised vessel with a lower alcohol to oil ratio (3:1). 80% and 76% biodiesel yields were obtained using heterogeneous catalysed transesterification of soybean oil with methanol and ethanol respectively, under the same reaction conditions in respect with the temperature, oil/alcohol molar ratio and catalyst loading except for the reaction times (Dorado *et al.,* 2002). Methanolysis was more rapid than ethanolysis, taking 30 and 50 min respectively (Dorado *et al*., 2002).

A comparative environmental evaluation was performed by Tangviroon and Ariyaskul (2014), using life cycle analysis (LCA) concepts to understand the contributions of different biodiesel production processes and alcohol feedstocks to the environmental load. The results are briefly discussed in the following paragraphs and depicted in Table 5.

Tanviroon and Ariyaskul (2014) found that approximately 12 to 18% less feedstock was required for biodiesel production from ethanol, and a greater yield was obtained. Larger feedstock usage equates to more chemical use and discharge.

Table 5: Comparison of different types of biodiesel feedstock produced using methanol/ethanol: reaction conditions and biodiesel yield

Biodiesel production using methanol			
Feedstock	**Reaction Conditions**	**Biodiesel Yield**	**References**
Waste cooking oil	Methanol oil molar ratio: 39/1 Temperature: 60°C H_2SO_4 as catalyst Reaction time: 4h	99%	Canakci (2007)
Mahua oil	Methanol oil molar ratio: 0.8/1 Temperature: 60°C KOH as catalyst Reaction time: 1h	98%	Ghadge and Raheman (2008)
Jatropha oil	Methanol oil molar ratio: 5/1 Temperature: 60°C KOH as catalyst Reaction time: 30min	98%	Tiwari *et al.* (2007)
Soybean oil	Methanol oil molar ratio: 39/1 Temperature: 60°C MgO as catalyst Reaction time: 20min	91%	Di Serio *et al.* (2007)
Palm oil	Methanol oil molar ratio: 6/1 Temperature: 65°C KOH as catalyst Reaction time: 90min	82%	Darnoko and Cheryan (2000)
Sunflower oil	Methanol oil molar ratio: 6/1 Temperature: 40°C $CaCO_3$ as catalyst Reaction time: 15min	65%	Pimentel and Patzek (2005)
Animal fat	Methanol oil molar ratio: 6/1 Temperature: 70°C $NaOCH_3$ as catalyst Reaction time: 2h	60%	Ma *et al*. (1998)
Biodiesel production using ethanol			
Feedstock	**Reaction Conditions**	**Biodiesel Yield**	**References**
Brassica carinata oils	Ethanol oil molar ratio: 50/1 Temperature: 35°C KOH as catalyst Reaction time: 1h	96%	Dorado *et al.* (2002)
Soybean oil	Ethanol oil molar ratio: 20/1 Temperature: 30°C SO_4-ZrO_2 as catalyst Reaction time: 1h	96%	Kouzu *et al*. (2007)
Waste cooking oil	Ethanol oil molar ratio: 30/1 Temperature: 159°C NaOH as catalyst Reaction time:1h	95%	Zhang *et al.* (2003)
Microalgal oil	Ethanol oil molar ratio: 56/1 Temperature: 30°C H_2SO_4 as catalyst; Reaction time: 4h	92%	Miao and Wu (2006); Tan and Lee (2011)
Palm oil	Ethanol oil molar ratio: 10/1 Temperature: 65°C Novozymes as catalyst Reaction time: 6h	88%	Oliveira *et al.* (2001)
Canola oil	Ethanol oil molar ratio: 10/1 Temperature: 60°C $Cs_2HPW_{12}O_{40}$ as catalyst Reaction time: 5h	80%	Warabi *et al.* (2004)

The LCA is a technique used to assess the potential environmental impacts associated with a product or service throughout its life cycle. The potential environmental impact can be measured using various parameters (Figure 3).

Many of the environmental indicators such as terrestrial ecotoxicity potential, marine aquatic ecotoxicity potential, fresh water ecotoxicity potential, human toxicity potential, eutrophication potential, and photochemical oxidation potential (Figure 3) used in the LCA were therefore lower for ethanol than methanol-based biodiesel production.

This was offset by the abiotic depletion potential (ADP), so that overall, the use of methanol for biodiesel production resulted in a slightly lower theoretical environmental impact than ethanol. The ADP and acidification potential of biodiesel from ethanol was calculated to be 44.1% and 48.5% higher respectively. This was related to the different separation processes, and the fact that 40% more heat was required to produce ethanol-based biodiesel. In contrast to the findings of Tangviroon and Ariyaskul (2014), Kiss and Boskovic (2012) reported that methanol-based biodiesel production has a lower global warming impact than the ethanol-based method (0.75 compared to 1.92 kg CO_2 per kg of biodiesel produced). However, they reported that the use of ethanol resulted in lower cumulative fossil energy requirements (19.34 compared to 36.91 MJ of energy used per kg of biodiesel produced). In addition, their investigations confirmed that the global warming impact of fatty acid ethyl esters could be reduced by using ethanol produced from other sources than corn (e.g. grass, sugar cane or sugar beets).

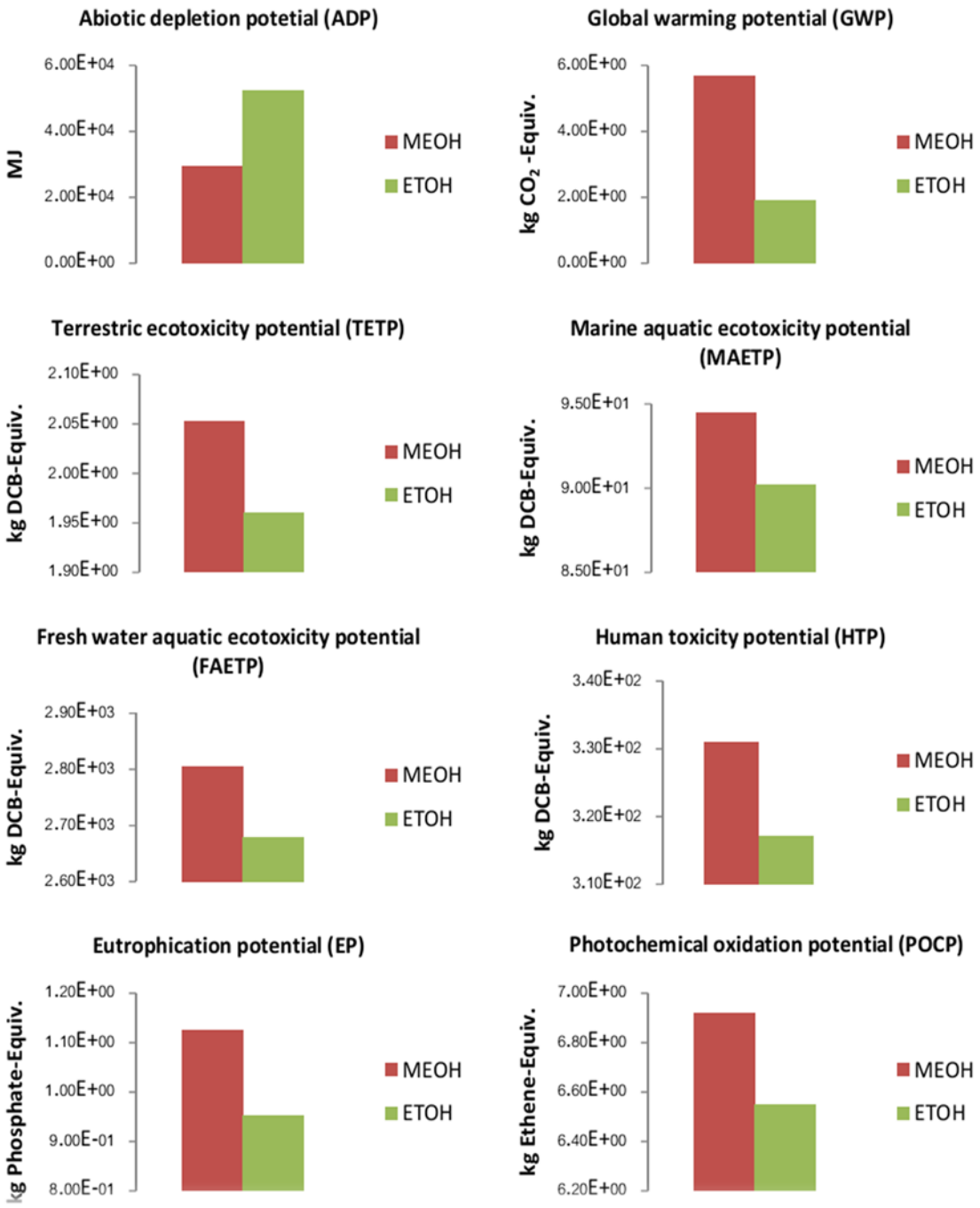

Figure 3: Comparative life cycle assessment (LCA) / Results per impact categories for methanol and ethanol (adapted from Tangviroon and Ariyaskul, 2014).

2.3.2 Comparison of economic factors

Methanol and ethanol are variants of alcohol, and they have different properties and uses. Methanol is a poisonous chemical derived through synthetic processes, while commercial ethanol is produced by factory fermentation of food crops, which makes methanol relatively cheaper than ethanol (Kang *et al*., 2014).

Ethanol used in the transesterification reaction for biodiesel production is mostly prepared from food crops, which can threaten food security (Kiss, 2010; Gutierrez *et al.*, 2009; and Farrell *et al.*, 2006).

From the Organisation for Economic Cooperation and Development annual report (OECD, 2017) liquid biofuels such as bioethanol and biodiesel, which are derived from agricultural crops, compete with fossil fuels on energy markets. As biofuel volumes produced remain small compared to the global market of petroleum fuels, oil prices are an important driver of the prices of biofuels and of their agricultural feedstocks. Agricultural crops grown for energy production also compete with food crops for resources (IEA, 2017).

For instance, a given plot of land can be used to grow maize for ethanol or for food. Farmers will sell their harvest to an ethanol or biodiesel processor if the price received is higher than what they could obtain from other sources such as food processing. Therefore, when the value of biofuel feedstocks is high, prices for other agricultural crops tend to rise. For this reason, the Food and Agriculture Organisation (FAO, 2017) as well as the International Energy Agency (IEA, 2017) have confirmed that producing second generation biofuels from non-food crops, such as wood or grasses, will not necessarily eliminate the competition between food and fuel.

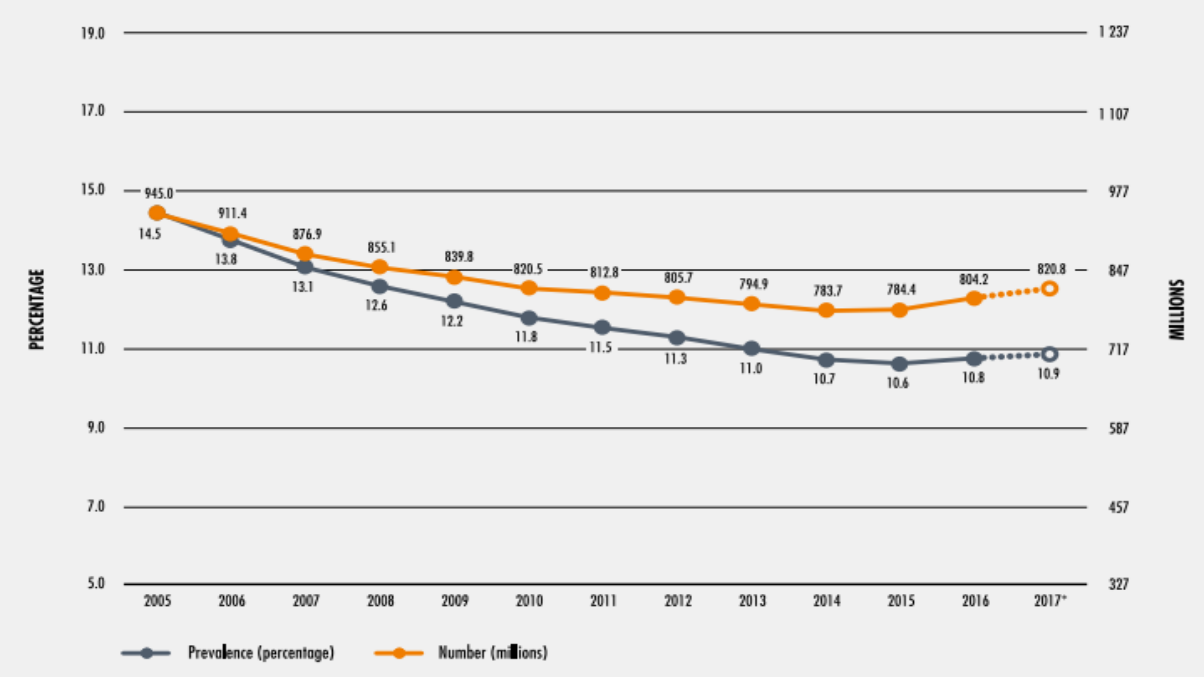

Figure 4: The state of food security and nutrition in the world (FAO, 2017)

Rapid growth in biofuel production will continue to influence food prices and this in turn will have an impact on food security (Food and Agriculture Organisation [FAO], 2017 and OECD, 2017). The FAO (2017) estimated that some 850 million people around the world will be

undernourished by 2018 with an increase from 777 million in 2015 to 815 million in 2016 (Figure 4).

Hence, the production of bioethanol and biodiesel from food sources will adversely impact on food security. While some countries will benefit from higher prices, for the least-developed countries the net food import bill is expected to increase in the livestock and dairy sectors due to price hikes in cereal and vegetable oils, which are also feedstocks for biofuel production (FAO, 2017). Furthermore, the meat import bill is set to reach a record $176 billion this year (2018), up 22 per cent from 2016, and the FAO Butter Price Index has risen 41 per cent so far in 2017 (FAO, 2017).

2.4 Bioethanol production

Bioethanol can be produced from several different biomass feedstocks: sucrose rich feedstocks (e.g. sugar-cane), starchy materials (e.g. corn grain), and lignocellulosic biomass. This last category, including biomass such as corn stover (leaves, stalks and cobs left on the field after harvest) and wheat straw, woody residues from forest thinning and paper, is promising especially in those countries with limited land availability. Residues are often widely available and do not compete with food crops for land (Kang *et al*., 2014; Sun and Cheng, 2002).

2.4.1 Lignocellulosic biomass

Lignocellulosic biomass is typically non-edible plant material, including dedicated crops of wood and grass, and agri-forest residues. Lignocellulosic materials are mainly composed of cellulose, hemicellulose, and lignin as well as small amounts of pectin, proteins, extractives (i.e. nitrogenous material, chlorophyll and waxes) and ash (Kang *et al*., 2014; Kumar *et al*., 2009). The composition of the biomass constituents can vary greatly among various sources (Table 6).

Accurate measurements of the biomass constituents, mainly lignin and carbohydrates, are of prime importance because they assist process designs for the maximum recovery of energy and products from the raw materials. Since 1900, researchers have developed several methods to measure the lignin and carbohydrate content of lignocellulosic biomass (Kang *et al.,* 2014).

Globally recognised Organisations, such as the American Society for Testing and Materials (ASTM), Technical Association of the Pulp and Paper Industry (TAPPI) and National

Renewable energy and Laboratory (NREL) have developed methods to determine the chemical composition of biomass (Kumar *et al*., 2009).

Table 6: Composition of some common sources of biomass (Sun and Cheng, 2002)

Lignocellulosic materials	Cellulose (%)	Hemicellulose (%)	Lignin (%)
Coastal bermudagrass	25	35.7	6.4
Corn cobs	45	35	15
Cotton seed hairs	80-95	5-20	0
Grasses	25-40	35-50	10-30
Hardwood steam	40-55	24-40	18-25
Leaves	15-20	80-85	0
News paper	40-55	25-40	18-30
Nut shells	25-30	25-30	30-40
Paper	85-99	0	0-15
Primary wastewater solids	8-15	NA	24-29
Softwoods stems	45-50	25-35	25-35
Solid cattle manure	1.6-4.7	1.4-3.3	2.7-5.7
Sorted refuse	60	20	20
Swine waste	6.0	28	NA
Switchgrass	45	31.4	12.0
Waste papers from chemical pulps	60-70	10-20	5-10
Wheat straw	30	50	15

NA: not applicable

Besides ethanol, several other products can be obtained following the hydrolysis of the carbohydrates in the lignocellulosic materials. For instance, xylan/xylose contained in hemicelluloses can be thermally transformed into furans (2-furfuraldeyde, hydroxymethil furfural), short chain organic acids (formic, acetic, and propionic acids), and other compounds such as hydroxy-1-propanone and hydroxy-1-butanone (Bozell and Petersen, 2010; Güllü, 2010). In addition, levulinic acid could be formed by the degradation of hydroxymethil furfural (Demirbas *et al*., 2016). Another product prepared either by fermentation or by catalytic hydrogenation of xylose is xylitol (Bozell and Petersen, 2010). Furthermore, through the chemical reduction of glucose it is possible to obtain several products, such as sorbitol (Bozell and Petersen, 2010). The residual lignin can be an intermediate product to be used for the synthesis of phenol, benzene, toluene, xylene, and other aromatics. Similarly to furfural, lignin could react to form some polymeric materials (i.e. polyurethanes) (Demirbas *et al*., 2016).

Lignocellulosic biomass is a potential source of several bio-based products. Currently, the products made from bioresources represent only a minor fraction of the chemical industry production (Capolupo and Farco, 2016). However, the interest in the bio-based products has increased because of the rapidly rising barrel costs and increasing concerns about the depletion of fossil resources (USDA, 2017; IEA, 2016; Capolupo and Farco, 2016).

The goal of the biorefinery approach is the generation of energy and chemicals from different biomass feedstocks, through the combination of different technologies, such as that described by FitzPatrick *et al*. (2010) and depicted in Figure 5.

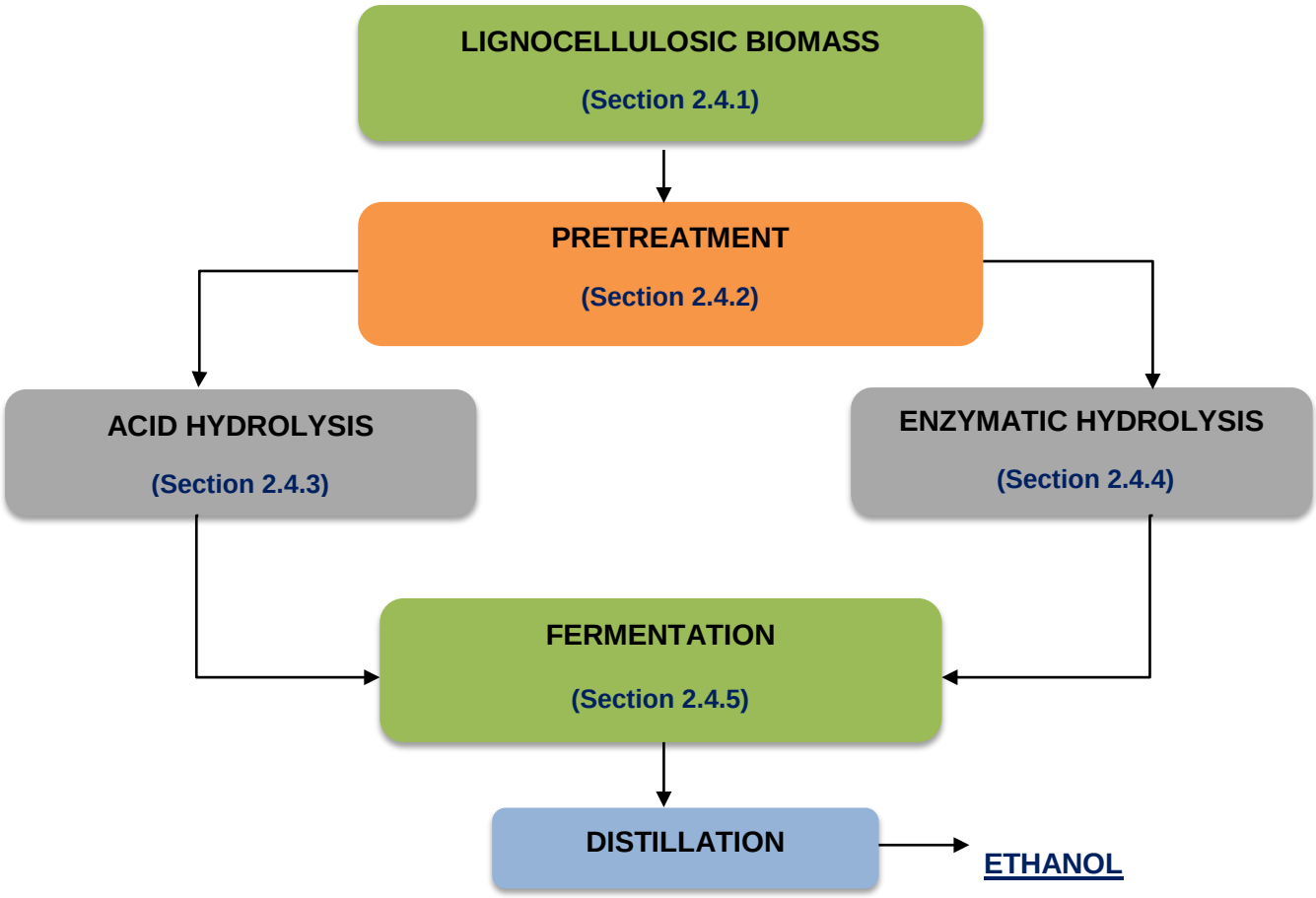

Figure 5: Process for ethanol production from lignocellulosic biomass (adapted from FitzPatrick *et al*., 2010)

2.4.2 Pretreatment

Pretreatment methods can be classified into different categories: physical (operating by grinding or milling the sample), physiochemical processes such as steam explosion and ammonia fibre explosion (AFEX), chemical (acid, alkaline or organosolv), biological processes with the use of several fungi, electrical (which some authors include within the physical pretreatment category), or a combination of these. The advantages and disadvantages of the different pretreatment techniques are summarised in Table 7 (Kumar *et al*., 2009).

A pretreatment step is necessary for the both acid and enzymatic hydrolysis processes. It can remove the lignin layer so that the hydrolytic enzymes can easily access the biopolymers. The

pretreatment is a critical step in cellulosic bioethanol technology because it affects the quality and the cost of the carbohydrate-containing streams (Jonsson and Martin, 2016).

Pretreatment is necessary to break down the crystalline structure of the lignocellulose material, isolating the cellulose from the lignin in the cell walls for hydrolysis. Pretreatment is carried out to increase the surface area and accessibility of the plant fibre to enzymes and thus, achieve high sugar yield for ethanol fermentation (Jonsson and Martin, 2016; Balat *et al*., 2008). The feedstock is subjected to steam whose temperature and treatment time may increase the cellulose surface area, as the fibrous feedstock is converted to a muddy texture with little conversion of the cellulose to glucose. This process is referred to as pretreatment of the feedstock. Chemical pretreatment generally refers to the addition of a diluted acid, mainly diluted sulphuric acid, to improve the cellulose separation from lignin and other impurities that might inhibit the extraction of fermentable sugars (Jonsson and Martin, 2016). However, the feedstock becomes acidic and the pH is adjusted by the addition of alkaline (often NaOH) to 6, which is the optimal pH range for celluloses. Higher pH is acceptable if alkalophilic cellulose is used. Overall, the final yield of the enzymatic process depends on the combination of several factors such as the biomass composition, the type of pretreatment used, and the dosage and the efficiency of the hydrolytic enzymes (Capolupo and Faraco, 2016; Zabed *et al.,* 2014).

Table 7: Methods for biomass lignocellulosic pre-treatment (Kumar *et al.*, 2009)

	Method	Operating conditions	Advantages	Disadvantages
Physical	Chipping Grinding Milling	Room temperature; Energy input <30 KW per ton biomass	Reduces cellulose crystallinity	Power consumption higher than inherent biomass energy
Physico-chemical	Steam pre-treatment	160-260°C (0.69-4.83 MPa) for 5-15 min	Causes lignin transformation; cost-effective for hardwoods and agricultural residues	Generation of inhibitory compounds; less effective for softwoods
	AFEX (Ammonia fibre explosion method)	90°C for 30 min. 1-2 kg ammonia / kg dry biomass	Increases accessible surface area; removes lignin and hemicellulose	Does not modify lignin or hydrolyse hemicellulose
	CO_2 explosion	4 kg CO_2 / kg fibre at 5.62 Mpa 160 bar for 90 min at 50°C under supercritical carbon dioxide	Does not produce inhibitors for downstream processes	Not suitable for biomass with high lignin content (such as woods and nut shells); does not modify lignin or hydrolyse hemicellulose
	Ozonolysis	Room temperature	Reduces lignin; does not produce toxic residues	Expensive because of ozone required
	Wet oxidation	148-200°C for 30 min	Efficient removal of lignin; low formation of inhibitors; low energy demands	High cost of oxygen and alkaline catalyst
Chemical	Acid hydrolysis: dilute-acid pre-treatment	Type I: T>160°C; Continuous-flow process for low solid loading (5-10 wt.%; Type II: T<160°C, batch process for high solid loadings (10-40 wt.%)	Hydrolyses hemicellulose to xylose and other sugars; alters lignin structure	Equipment corrosion; formation of toxic substances
	Alkaline hydrolysis	Low temperature; For soybean straw: ammonia liquor (10 wt.%) for 24 h at room temperature	Removes hemicellulose and lignin; Increases accessible surface area	Residual salts in biomass
	Organosolv	150-200°C with or without addition of catalysts (oxalic, salicylic, acetylsalicylic acid)	Hydrolyses lignin and hemicelluloses	High costs due to the solvent recovery
Biological		Several fungi (brown, white and soft-rot fungi)	Degrades lignin and hemicelluloses; low energy requirements	Slow hydrolysis rate

2.4.3 Acid hydrolysis

The main advantage of acid hydrolysis is that acids can penetrate lignin without any preliminary pre-treatment of biomass, thus breaking down the cellulose and hemicellulose polymers to form individual sugar molecules. Several types of acids, concentrated or dilute, can be used, such as sulphurous, sulphuric, hydrochloric, hydrofluoric, phosphoric, nitric and formic acid (Ziolkowska, 2013).

Sulphuric and hydrochloric acids are most commonly used for hydrolysis of lignocellulosic biomass (Zabed *et al.*, 2014). The concentration used in the concentrated acid hydrolysis process is in the range of 10-30%. The process occurs at low temperatures, producing high hydrolysis yields of cellulose (i.e. 90% of theoretical glucose yield). However, this process requires large amounts of acids, causing corrosion of equipment (Ziolkowska, 2013).

The main advantage of the dilute hydrolysis process is the low amount of acid required (2-5%). However, this process is carried out at high temperatures to achieve acceptable rates of cellulose conversion. The high temperature increases the rates of hemicellulose sugar decomposition, thus causing the formation of toxic compounds such as furfural and 5-hydroxymethyl-furfural (HMF). These compounds inhibit yeast cells and the subsequent fermentation stage, causing a lower ethanol production rate; in addition, these compounds lead to the reduction of fermentable sugars, and high temperatures increase corrosion of the equipment (Ziolkowska, 2013 and Kootstra *et al.*, 2009).

Though the acid hydrolysis is a faster reaction, it does have some disadvantages (Koostra *et al.,* 2009):

a) Lower conversion of cellulose to glucose because process is more equilibrium driven;

b) Sugar degradation to substances which can be detrimental to fermentation occurs;

c) Mineral acid treatment makes possible utilisation of the other lignocellulosic constituents more difficult; and

d) Non-selectivity of mineral acids to lignocellulosic material.

2.4.4 Enzymatic hydrolysis

The use of enzymes in the hydrolysis of cellulose is more advantageous than use of chemicals because enzymes are highly specific and can work under mild process conditions (Ting *et al.*, 2009).

Despite these advantages, the use of cellulases in industrial applications is still limited by several factors: (i) the costs of enzyme isolation and purification are high (accounting for up to 50% of the cost of hydrolysis); (ii) enzymes are inhibited if acid hydrolysis is used; and (iii) the specific activity of cellulases is low compared to the corresponding starch degrading enzymes. In consequence, to obtain satisfactory process yields, the enzyme dosage and the hydrolysis time must be increased and the loading of solids decreased (Kumar *et al*., 2009; Viikari *et al*., 2007). One typical index used to evaluate the hydrolytic performances of the cellulases is the conversion rate, for example g glucose/L/h. Berlin et al. (2007) reported conversion rates for softwood substrates (5 wt.% solids loading) in the range 0.3-1.2 g/L/h.

Most cellulose microfibrils contain two crystalline allomorphs, cellulose I_a and I_b, in which the chains are packed slightly differently. The chain conformation in both forms is similar, a flat ribbon with a 180° twist between successive glucosyl residues. This chain conformation is stabilised by two hydrogen bonds parallel to the glycosidic linkage, one from O-3 to the ring oxygen of the preceding glucose unit and the other from O-2 to O-6 of the next glucose unit (Demain *et al*., 2005).

At the surface of higher plants, the microfibrils contain cellulose chains that do not conform to either I_a or I_b allomorphs. Differences in hydrogen bonding mean that the surface chains have some freedom to move out of the flat-ribbon conformation. The lack of intra-molecular hydrogen bonding in the surface chains also means that they can form more hydrogen bonds to water or adjacent polysaccharides (Demain *et al*., 2005).

These crystals (I_a and I_b) are sometimes so tight that neither water nor enzymes can penetrate them; only exoglucanase, a subgroup of cellulases that attacks the terminal glycosidic bond, is effective in degrading cellulose (Jonsson and Martin, 2016; Ziolkowska, 2013).

In addition to crystallinity, the chemical compounds surrounding the cellulose in plants, e.g. lignin, also limit the diffusion of the enzyme into the reaction sites and play an important role in determining the rate of hydrolysis (Ziolkowska, 2013).

Sometimes, wood chips are pre-treated with acid to strip hemicellulose and lignin before they are treated with an enzyme or a mixture of enzymes. In general, 20 to 70% yield of glucose can be expected after 24 hours (Kumar *et al.*, 2009).

Ting and his research team (2009) have observed that the mechanism of enzymatic hydrolysis of cellulose involves three simultaneous processes (Ting *et al*., 2009):

a) Chemical and physical changes in the cellulose solid phase via endogluconase (EG or endo-1,4-D-glucan glucanohydrolase) enzyme activity. The chemical stage includes changes in the degree of polymerization, while the physical changes comprise modifications in the accessible surface area;

b) Primary hydrolysis via cellobiohydrolase (or CBH or 1,4-D-glucan cellobiohydrolase) enzyme activity. This process is slow and involves the release of soluble intermediates from the cellulose surface.

Generally, cellulases consist of three major enzymes: endo-1,4-D-glucan glucanohydrolase, exoglucanases and β-glucosidase (or BGL). These enzymes act in perfect synergism and tight regulation under natural conditions and break the cellulose polymer. Endoglucanases act randomly along the chain length, thereby producing new sites to be attacked by exoglucanases (or CBH) (Finore *et al.,* 2012).

Exoglucanases hydrolyse cellulose polymers from the terminal reducing or non-reducing ends, producing mainly cellobioses. The cellobioses liberated are acted upon by β-glucosidases which convert them to glucose (Finore *et al.,* 2012). However, the proportion of β-glucosidase is meagre in most of the commercial cellulases, and this causes not only accumulation of cellobioses but also feed-back inhibition of the cellulase enzyme complex. Hence, supplementation of β-glucosidases in the enzymatic cocktails is suggested (Finore *et al.,* 2012 and Ting *et al*., 2009). Also, industrial-level scale up of the process is not efficient as the current sources of commercial cellulases do not contain all the three components in optimal ratios and specific activities (Finore *et al.*, 2012 and Ting *et al*., 2009).

For example, in *Trichoderma reseei*, the proportion of these enzymes is EG (18%), CBH (72%) and BGL (<1%) (Finore *et al.,* 2012).

Therefore, augmenting enzymatic mixtures with β-glucosidases or using microbes with desirable proportions of β-glucosidases will cause an increase in sugar yields (Capolupo and Faraco, 2016; Kumar and Singh, 2016; Haankuku *et al.*, 2015; Finore *et al.,* 2012 and Ting *et al*., 2009). Supplementation with β-glucosidases effects the further hydrolysis of the soluble fractions to lower molecular weight intermediates, and ultimately to glucose. In order to meet future challenges, innovative bioprocesses for the production of new generations of enzymes are needed (Capolupo and Faraco, 2016; Kumar and Singh, 2016).

As already described, conventional cellulases work within a range of temperatures around 50°C and they are typically inactivated at temperatures above 60-70°C due to disruption of

their three-dimensional structures, followed by irreversible denaturation, which is defined as the loss of the primary structure (*Viikari et al*., 2007).

Since the hydrolysis is believed to be the key process, optimisation of this step is essential to be able to improve the efficiency of the whole fermentation process. Different factors influence the efficiency of the hydrolysis of lignocellulosic material, including both pretreatment conditions and process conditions. The factors can be separated in two groups: substrate-related and enzyme-related (Olsson *et al*., 2006). The factors related to the substrate include the structural properties within the substrate, e.g. cellulose degree of polymerisation and cellulose crystallinity (Sassber *et al*., 2006).

The hydrolysis conditions, e.g. temperature, pH, mixing and enzyme concentration are also highly important factors for enzyme activity (Kumar and Singh, 2016). However, results from different studies indicated that these factors alone do not impact the efficiency of the hydrolysis. Presumably it is a combination of these factors together with factors such as surface area and particle size (Elumalai and Thangavelu, 2010).

Surface area is a critical factor for the hydrolysis, since the accessibility of the substrate to the cellulases is a fundamental parameter. Pretreatment methods are used to increase this area. An increased surface area can also possibly be achieved by reducing the feedstock particle size (Kumar and Singh, 2016). Another size factor is porosity. Studies have shown that the size of the enzymes in relation to the pore size is of importance. As mentioned earlier, cellulases have a synergistic effect and pore size large enough for capturing the three enzymes at the same time would therefore improve the efficiency of the enzymatic hydrolysis (Kumar and Singh, 2016).

Lignin is another parameter that plays an important role in the efficiency of the enzymatic hydrolysis process. It acts both as a physical barrier covering cellulose from cellulase attack, and as an enzyme binding material, which results in non-productive binding. This will require the addition of a hydrophobic compound or surfactant that competes with cellulases for the adsorption sites on lignin to hinder the unproductive binding, and thus enhance the enzymatic hydrolysis and subsequently improve the fermentation efficiency (Kumar and Singh, 2016; Chandra *et al., 2*007).

Another factor that affects the enzymatic hydrolysis is the hemicellulose content. In the same way as lignin, it acts as a barrier against cellulases, and decreases the enzymatic digestibility of lignocellulose (Elumalai and Thangavelu, 2010). Hemicellulose removal will increase the pore size of the lignocellulosic material and thereby result in improvement of enzymatic

hydrolysis. However, the monomeric sugars from hemicellulose could also be fermented to achieve a higher ethanol yield (Kumar and Singh, 2016).

Solid concentration in the material supplied to the process is also an important parameter. However, high substrate concentrations that are too high can cause substrate inhibition and thereby result in reduced efficiency (Sun and Cheng, 2002). The severity of substrate inhibition depends on the ratio between enzyme and substrate. Adding more enzymes, up to a certain level, will increase the efficiency of the hydrolysis, but it is not cost-effective. Normally, cellulase in the concentration of 5 to 35 FPU/g substrate is used for hydrolysis (Taherzadeh and Karimi, 2007).

A common concentration is 10 FPU/g substrate, since this can provide an efficient hydrolysis with reasonable residence time (48-72 h) and at an acceptable cost (Sun and Cheng, 2002). Enzymes are expensive, and one way to reduce the cost is to reuse the cellulases. Cellulase recycling could improve both the efficiency of the hydrolysis and cut down the enzyme cost. However, separation of enzymes from the hydrolysate can be difficult since it is mixed with different solids, mainly lignin, and due to the enzymes dissolving in the broth (Taherzadeh and Karimi, 2007).

Other hydrolysis conditions apart from enzyme concentration are temperature and pH. A temperature of 45-50°C together with a pH of 4.5-5 are typical optimum conditions for cellulases (Kumar and Singh, 2016; Elumalai and Thangavelu, 2010). However, residence time can impact the optimum conditions, and studies have found optimums that differ from the commonly used conditions by having prolonged residence time (Saha *et al.,* 2005).

Another important enzyme property that influences the hydrolysis process is the enzyme activity, shown for selected commercial cellobiases in Table 8. The activity is generally measured in filter paper units (FPU), which represents the amount of enzyme that forms 1 μmol of reducing sugars/min during the hydrolysis reaction of filter paper [specifically Whatman filter paper (Little Chalfont, UK), and/or in cellobiase units (CBU). This is the amount of enzyme which forms 2 μmol of glucose/min from cellobiose bioprocesses (Demain *et al*., 2005).

Since the hydrolysis is believed to be the key process, optimisation of this step is essential to improve the efficiency of the whole fermentation process. Different factors influence the efficiency of the hydrolysis of lignocellulosic material, including both pretreatment conditions and process conditions. The factors can be separated in two groups: substrate-related and enzyme-related (Olsson *et al*., 2006).

The factors related to the substrate include the structural properties within the substrate, e.g. cellulose degree of polymerisation and cellulose crystallinity (Sassber *et al*., 2006).

The hydrolysis conditions, e.g. temperature, pH, mixing and enzyme concentration are also highly important factors for enzyme activity (Kumar and Singh, 2016). However, results from different studies indicated that these factors alone do not impact the efficiency of the hydrolysis. Presumably it is a combination of these factors, together with factors such as surface area and particle size (Elumalai and Thangavelu, 2010).

Surface area is a critical factor for the hydrolysis, since the accessibility of the substrate to the cellulases is a fundamental parameter. Pretreatment methods are used to increase this area. An increased surface area can also possibly be achieved by reducing the feedstock particle size (Kumar and Singh, 2016). Another size factor is the porosity. Studies have shown that the size of the enzymes in relation to the pore size is important. As mentioned earlier, cellulases have a synergistic effect and pore size large enough for capturing the three enzymes at the same time would therefore improve the efficiency of the enzymatic hydrolysis (Kumar and Singh, 2016).

Lignin is another parameter that plays an important role in the efficiency of the enzymatic hydrolysis process. It acts both as a physical barrier covering cellulose from cellulase attack and as an enzyme binding material, resulting in non-productive binding. This will require the addition of a hydrophobic compound or surfactant that competes with cellulases for the adsorption sites on lignin to hinder the unproductive binding, and thus enhance the enzymatic hydrolysis and subsequently improve the fermentation efficiency (Kumar and Singh, 2016; Chandra *et al., 2*007).

Another factor that affects the enzymatic hydrolysis is the hemicellulose content. In the same way as lignin, it acts as a barrier against cellulases and decreases the enzymatic digestibility of lignocellulose (Elumalai and Thangavelu, 2010). Hemicellulose removal will increase the pore size of the lignocellulosic material and thereby result in improvement of enzymatic hydrolysis. However, the monomeric sugars from hemicellulose could also be fermented to achieve a higher ethanol yield (Kumar and Singh, 2016).

Solid concentration in the material supplied to the process is also an important parameter. However, substrate concentrations that are too high can cause substrate inhibition and thereby result in reduced efficiency (Sun and Cheng, 2002). The severity of substrate inhibition depends on the ratio between enzyme and substrate. Adding more enzymes, up to a certain level, it will increase the efficiency of the hydrolysis, but it is not cost-effective.

Other hydrolysis conditions apart from enzyme concentration are temperature and pH. A temperature of 45-50°C together with a pH of 4.5-5 is typically optimum conditions for cellulases (Kumar and Singh, 2016; Elumalai and Thangavelu, 2010). Although, residence time can impact the optimum conditions and studies have found optimums that differ from the common used conditions by having prolonged residence time (Saha *et al.,* 2005).

Table 8: Common commercial cellobiases and their activities

Commercial mixture	*FPU (U/ml)*	Cellobiase *(CBU/ml)*	Source
Bio-feed beta L	<5	12	*Trichoderma longibrachiatum Trichoderma reesei*
Cellubrix (Celluclast)	56	136	*Trichoderma. longibrachiatum Asperlligus niger*
Cellulase 2000L	10	nd	*Trichoderma longibrachiatum Trichoderma reesei*
Cellulyve 50L	24	nd	*Trichoderma longibrachiatum Trichoderma reesei*
Energex L	<5	19	*Trichoderma longibrachiatum Trichoderma reesei*
GC220	116	215	*Trichoderma longibrachiatum Trichoderma reesei*
GC440	<5	70	*Trichoderma longibrachiatum Trichoderma reesei*
GC880	<5	86	*Trichoderma longibrachiatum Trichoderma reesei*
Novozymes 188	<5	1.116	*Asperlligus niger*
Rohament CL	51	28	*Trichoderma longibrachiatum Trichoderma reesei*
Spezyme CP	49	nd	*Trichoderma longibrachiatum Trichoderma reesei*
Ultraflo L	<5	20	*Trichoderma longibrachiatum Trichoderma reesei*
Viscozyme L	<5	23	*Trichoderma longibrachiatum Trichoderma reesei*
Viscostar 150L	33	111	*Trichoderma longibrachiatum Trichoderma reesei*

ND = not determined

2.4.5 Fermentation process

The fermentation process can be simply defined as a chemical process by which molecules such as glucose are broken down anaerobically in the presence of microorganisms (Kumar and Singh, 2016).

Theoretically, the conversion of glucose to ethanol is 0.51 g ethanol (EtOH)/g glucose. However, the fermenting efficiency of the yeast is generally assumed to be 90% and therefore results in a maximum conversion of 0.46 g EtOH/g glucose (Öhgren *et al*., 2007). When the glucose yield is high, *S. cerevisiae* has the ability to produce ethanol also under aerobic

conditions (Brandberg, 2005). One drawback is that it cannot ferment pentoses, which are of interest when using lignocellulosic biomass. Studies have therefore been performed to genetically modify *S. cerevisiae* into both a pentose and glucose fermenting yeast. Other microorganisms have the potential to ferment pentoses and another way to ferment lignocellulosic material is therefore to use different yeasts and to separate the two processes; glucose fermentation and pentose fermentation (Galbe and Zacchi, 2002).

The efficiency of the fermenting process depends on several factors: choice of microorganism, raw material, pretreatment method, hydrolysis method and environmental factors such as pH, temperature, substrate and ethanol concentration. Common conditions for fermentation with *S. cerevisiae* are normally pH 5.0 and a temperature of maximum 37°C (Ohgren *et al*., 2007). The performance of the process is affected by different inhibitors generated from the upstream process steps. The hydrolysate contains, together with fermentable sugars, inhibitors which restrict the fermenting microorganisms, and thus decrease the ethanol yield. Recirculation of the process water increases these compounds further (Ohgren *et al*., 2007).

Hydrolysis and fermentation can be separated (separate hydrolysis and fermentation (SHF)) or combined (simultaneous saccharification and fermentation (SSF)), each with different advantages and disadvantages (Kumar and Singh, 2016; Elumalai and Thangavelu, 2010; Galbe and Zacchi, 2002).

Major advantages of SSF technology

- The end-product inhibition is reduced because of the rapid conversion of glucose into ethanol by yeasts (Viikari *et al*., 2007);
- The number of process steps is reduced (Elumalai and Thangavelu, 2010);
- The presence of ethanol minimises microbial contamination (Viikari *et al*., 2007).

Disadvantages of SSF technology

- Difficulty of recirculating and reusing the yeast due to the presence of the solid residues from hydrolysis (Kumar and Singh, 2016);
- High solids loadings are usually required to obtain high ethanol levels in the fermentation broths (high gravity fermentation) (Sassner *et al*., 2006);
- The reaction time is very short, while the requirement for sterile conditions is lower since glucose is rapidly converted to ethanol (Elumalai and Thangavelu, 2010).

Major advantages of SHF technology

- The major advantage of this method is that it is possible to carry out the cellulose hydrolysis and fermentation under their optimum conditions. The optimum temperature for cellulase enzymes lies between 45 and 50°C depending on the cellulase producing microorganism (Olsson *et al*., 2006 and Saha *et al*., 2005);
- The two processes (hydrolysis and fermentation) can be performed under their own individually optimal conditions (Althuri and Banerjee, 2017);
- It is possible to run the fermentation process in a continuous mode with cell recycling. This is possible because lignin residue removal can occur before fermentation (this removal is much more problematic if lignin is mixed together with the yeast) (Althuri and Banerjee, 2017).

Disadvantages of SHF technology

- The major drawback of SHF is that an end product, i.e. glucose and cellobiose, released in cellulose hydrolysis strongly inhibits the cellulase efficiency (Saha and Cotta, 2006). Hence, to achieve a reasonable ethanol yield, lower loadings of solids and higher enzyme additions are generally required (Balat, 2011);
- Another disadvantage of SHF is the risk of contamination. Due to the relatively long residence time for the hydrolysis process (1-4 days), there is a risk of microbial contamination of the sugar solution (Taherzadeh and Karimi, 2007).

The optimum temperature for SSF by using *T. reesei* cellulase *and S. cerevisiae* was reported to be around 38°C, which is a compromise between the optimal temperatures for hydrolysis and fermentation (Tenborg *et al*., 2001). Hydrolysis of cellulose is a rate-limiting step in SSF, hence several thermotolerant bacteria and yeasts, e.g. *Candida acidothermophilum* and *Kluyveromyces marxianus* have been proposed for use in SSF to raise the temperature close to the optimum for enzymatic hydrolysis (Hong *et al*., 2007; Ballesteros *et al*., 2004; Hari Krishna *et al.*, 2001). This is a very delicate operation that will adversely affect the efficiency of all processes within the SSF system for ethanol production.

Saccharomyces cerevisiae and *Kluyveromyces marxianus* strains on the same substrate were investigated by Kadar *et al.* (2004), who concluded that there was no significant difference observed between *S. cerevisiae* and *K. marxianus* when the results of SSF were compared. The ethanol yields were in the range of 0.31-0.34 g/g for both strains, which clearly indicates that there was no much difference in ethanol yield using the SSF technology with different yeast strains.

Several researchers have attempted to evaluate these two fermentation technologies in terms of ethanol production from a wide different source of feedstock as well as divers yeast strains. For instance, Ohgren *et al.* (2006) performed SSF on steam-pretreated corn stover at 5, 7.5 and 10% water-insoluble solids (WIS) with 2 g/L hexose fermenting Saccharomyces cerevisiae. SSF at 10% WIS resulted in an ethanol yield of 74%, based on the glucose content in the raw material, and an ethanol concentration of 25 g/L. While Linde *et al*. (2007) carried out SSF on sulphuric acid (H_2SO_4) and steam pretreated barley straw. Three concentrations of WIS (5, 7.5 and 10 wt.%), and three enzyme loadings (5, 10 and 20 FPU/g cellulose) of Celluclast 1.5L complemented with Novozymes 188 were investigated in terms of ethanol yield. The highest ethanol yield, 82% of the theoretical yield based on the glucose content in barley straw, was obtained after SSF with 5 wt.% WIS at an enzyme loading of 20 FPU/g cellulose together with 5 g/L ordinary cultivated yeast. Furthermore, Olofsson *et al*. (2008) investigated different substrates and their ethanol yield along with the organism used in their review on SSF. For SSF using *S. cerevisiae*, the ethanol yield was reported around 60-90% for lignocellulosic biomass such as corn cob, corn stover, wheat straw and rice straw.

Dahnum *et al.* (2015) investigated the production of ethanol from fruit bunch using dry yeast to obtain at 40 FPU optimum enzyme concentrations; 4.74% of ethanol was produced in 72 h fermentation by SHF process and 6.05% of ethanol in 24 h by SSF process. From this study, the SSF method was considered a better process than SHF due to rapid ethanol production and the highest concentration of produced ethanol.

Althuri and Banerjee (2017) explored the possibilities of enhanced ethanol productivity using *Saccharomyces cerevisiae* through a central composite design (CCD)-based response surface methodology (RSM), employed to infer the optimum conditions to conduct SSF and SHF. At optimal conditions, they found that SSF resulted in higher ethanol productivity (1.396 g/L/h) after 30 h at lower cellulase loading (80 U/g) than SHF (0.929 g/L/h) after 27.33 h at higher cellulase loading (132.9 U/g), suggestive of the advantage of SSF (41.9 g/L) over SHF (25.40 g/L) under CCD-RSM systems.

To summarise, from all these findings from previous researchers, it is quite difficult to categorise the SSF technology as being more advantageous than SHF technology or the other way around, since the ethanol yield is very much a dependant variable of the reaction conditions and of the feedstock and yeast strains used for ethanol production with the appropriate fermentation model.

2.5 Catalysts employed for biodiesel production

There are many catalysts used for biodiesel production and they are classified depending on their mode of action and reaction phases, which can be homogeneous, heterogeneous or enzymatic (Demirbas, 2016).

2.5.1 Homogeneous catalysed processes

Homogeneous catalysts can be basic, acidic or enzymatic. Basic catalysts include alkalis such as sodium or potassium hydroxide, alkoxides such as sodium and potassium meth-oxides, and carbonates. Basic catalysts show high activity in transesterification. Alkoxides such as $NaOCH_3$ give high yields (>98%) in a short time (30 min) at low temperature and pressure (Dorado *et al*., 2002; Zhang *et al.,* 2003). Metallic hydroxides such as sodium and potassium hydroxides are frequently used as catalysts due to lower cost but have lower activity than alkoxides. Homogeneous acid catalysts include sulphuric, hydrochloric or sulphonic acids (Fadhil, 2013 and Singh *et al*., 2006).

In homogeneous-catalysed transesterification, FFAs can react with the base catalyst to form soap, making the removal of the catalyst after reaction technically difficult. In addition, it requires large volumes of water to separate and clean the products. This adds to the cost and generates large volumes of wastewater, which increases the environmental burden of the process, to prevent soap formation; feedstock pretreatment is required to limit the impurities entering the reactor (Thangaraj *et al*., 2014; Ma *et al*., 1998).

In addition, the end products, which comprise the desired esters along with glycerol, FFAs, unreacted triglycerides, diglycerides, monoglycerides, soap, alcohols and catalyst, must be refined to meet fuel standards. This refining process increases production costs and time. It is also technically difficult, potentially leading to a loss in the yield of the biodiesel product, hence, less than 0.06 wt.% water and 0.5 wt. % FFAs are required in the homogeneous-catalysed transesterification reaction to ensure an adequate yield (Lorero *et al.,* 2005).

Transesterification with an acid catalyst is the preferred process method for a triglyceride feedstock containing high levels of FFAs because the acid catalyst can simultaneously transesterify the triglyceride and esterify the FFAs to produce the desired alkyl esters (i.e. biodiesel). Sulphuric acid is typically used in transesterification of triglyceride and alkyl esterification of the FFAs to produce the alkyl esters. Other acids such as HCl, BF_3, H_3PO_4, and organic sulphonic acid have also been employed. When sulphuric acid is used, the catalyst concentration is typically 1-5 wt. %. This reaction gives a high product yield (92%) when using a high alcohol to oil molar ratio (30:1), within a reaction period of 3–20 hours. Processing time can be reduced by increasing the reaction temperature. For example, in the

butanolysis of soybean oil with 1 wt. % sulphuric acid, 3 hours was required to complete the reaction at 117°C whereas 20 hours was required at 77°C and the yield of biodiesel ranged between 84 and 90% (Lotero *et al*., 2005).

Another option to reduce reaction time and deal with high FFA content in the reactant is to employ a two-step catalysed process. In this process, the FFAs in the feed are first esterified by acid catalysis to produce alkyl esters. This step prevents soap formation during the second step. The transesterification of the unreacted triglyceride with an alkali catalyst to obtain alkyl esters was used by Wang *et al*. (2014) to produce 97% biodiesel. In their work, the first step involved esterification of FFAs at 95°C for 4 hours using 2 wt. % ferric sulphate with a methanol to oil molar ratio of 10:1. The subsequent step was transesterification of the triglycerides with an alkali catalyst, 1 wt.% potassium hydroxide, using a 6:1 molar ratio of methanol to oil at 65°C for 1 hour. Although acid-catalysed transesterification can handle feedstock with a high FFA content (25%), the reaction is very sensitive to water content. Even 0.1% of water in the feed can result in a significant reduction (62%) of product yield. In addition, the separation of product and catalyst is required, which costs time and money (Kusdiana and Saka, 2004).

2.5.2 Enzymatic catalysed processes

Many studies have focused on using the enzyme lipase as a catalyst for biodiesel production. As reviewed by Fukuda (2001), enzyme-catalysed biodiesel synthesis can overcome the problems of impurities that plague alkali/acid catalysed transesterification. FFAs in the raw materials can be converted to esters, and water has no influence on the reaction. In lipase catalysis, the recovery of glycerol is easy, and a relatively high yield of ester (96%) is produced. Lipases from bacteria and fungi are the most commonly used for transesterification, and optimal parameters for the use of a specific lipase depend on the origin as well as the formulation of the lipase. In general, the best enzymes can reach conversions above 90%, while reaction temperatures vary between 30 and 50°C. Reaction time also varies greatly from 8h for immobilised *Pseudomonas cepacia* lipases transesterifying jatropha oil with ethanol to a very long reaction time of 20 h for the same free enzyme transesterifying soybean oil with methanol. Thus, the biodiesel yield, reaction time and loss of enzyme activity over time are influenced not only by the origin of the lipase, but also by water activity, reaction temperature, choice of alcohol, and alcohol to oil molar ratio. In addition, free enzyme activity may differ from that of immobilised enzymes, and the type of immobilisation also needs to be considered. To elucidate these points, a closer look at the reaction mechanism and kinetics is necessary (Fauzi and Amin, 2013).

The enzymatic transesterification has certain advantages over the chemical catalysis of transesterification: As for the enzymatic transesterification, it is less intensive, it does allow easy recovery of glycerol and furthermore, the transesterification process of glycerides with higher FFA content can proceed without any soap formation, hence making the biodiesel and glycerol purification much easier.

Limitations of the enzyme catalysed reactions include the high cost of enzymes, lengthy reaction time, and the large volumes of water and organic solvents needed in the reaction mixture (Fauzi and Amin, 2013; Wang *et al*., 2008 and Fukuda *et al*., 2001).

Bajaj *et al.* (2010) investigated the use of various biocatalysts for the transesterification of soybean oil, and biodiesel yields of between 80 and 86% were obtained using lipases from *Candida antartica, Thermomyces lanuginosus* (under supercritical methanol), *Photobacterium lipolyticum* (at high methanol concentration), and *Thermomyces lanuginosus* (immobilised enzyme at a temperature between 34 and 37°C for 24 h with a methanol-to-oil molar ratio of 4:1).

2.5.3 Heterogeneous catalysed processes

To avoid the separation challenges of final products involved in a homogeneous catalytic system, researchers have explored the use of heterogeneous catalysts. The use of heterogeneous catalysts promotes the development of a process that can eliminate the additional running costs associated with the separation and purification stages; in addition, the use of heterogeneous catalysts does not produce soap through FFA neutralisation (Xie and Fan, 2014; Di Serio *et al*., 2007).

To reduce the cost of the purification process, heterogeneous solid catalysts such as metal oxides, zeolites, hydrotalcites, and γ-alumina have been used (Table 3); these catalysts can be easily separated from the reaction mixture and reused while keeping their catalytic activity (Alhassan *et al*., 2015; Kawashima *et al*., 2008).

Di Serio *et al*. (2007) studied the transesterification of soybean oil by both basic and acidic heterogeneous catalysis. The investigation was performed at 180°C with 2 g soybean oil, 0.88 g methanol and 0.1 g catalyst (Table 3). The acidic catalysts, titanium oxide supported on silica (TS) and vanadyl phosphate (VOP) were used. An average yield of 70% was obtained for VOP, but strong deactivation occurred when the catalyst was reused. The TS catalyst was more stable when reused, but only 40% yield was observed (Di Serio *et al*., 2007). The basic catalysts, hydrotalcites (CHT) and magnesium oxide (MgO) were used, with yields of 92% and

75% respectively. The yield decreased to 78% with MgO and 69% with CHT when the catalysts were reused. However, soap formation occurred when the feedstock contained FFAs. The presence of water also promoted hydrolysis of triglycerides to FFAs, enhancing the saponification process. Although the separation of heterogeneous catalysts is easier than that of homogeneous catalysts, the problem associated with impurities in the feedstock still persists. The use of heterogeneous catalysts for biodiesel production from different feedstocks has been well researched and shows promising results in terms of performance when compared to the use of homogeneous catalysts as shown in Table 9 (Amani *et al*., 2014).

Oxides of alkaline earth metals such as beryllium, magnesium, calcium, strontium and barium have been investigated as potential heterogeneous catalysts for the synthesis of biodiesel (Teo *et al*., 2014; Hu *et al*., 2011 and Ngamcharussrivvichai *et al*., 2009).

Table 9: Comparison of different catalysts used for biodiesel production

Type	Advantages	Disadvantages	Biodiesel Yield	References
Homogeneous Catalysts	Basic catalysts: favourable kinetics; high activity; high yield in short time; 4000 times faster reaction than acid catalysed transesterification; Acid catalysts: used for both esterification and transesterification simultaneously; preferred for low grade oils; insensitive to FFA and water.	Separation and waste problems after reaction; saponification; emulsion formation; catalyst reuse not possible; limited to batch type of reactors; Basic catalysts: sensitive to the presence of FFA and water; high production costs compared with heterogeneous type; Acid catalysts: Corrosive, slow reaction rate; higher molar ratio of methanol to oil; higher temperature.	85-99%	Ma *et al*., (1998); Demirbas (2003); Lotero *et al*., (2005); Atadashi *et al*. (2011); Fauzi and Amin, (2013) ; Corach *et al*., (2016).
Enzymatic Catalysts	Very selective; low reaction temperature; insensitive to water; easy separation; higher yield; can be implemented as homogeneous/heterogeneous catalysts.	Expensive; are inhibited in the presence of methanol; require additional supportive solvents as medium.	75-92%	Fukuda *et al*., (2001); Kose *et al*., (2002); Xie and Ma (2009) ; Shahir *et al*., (2014).
Heterogeneous Catalysts	Environmentally benign; noncorrosive; recyclable; easy separation of products; higher selectivity; longer catalyst life; Acid heterogeneous catalyse both esterification and transesterification simultaneously, insensitive to FFA and water; comparatively cheap; can be used in continuous fixed bed reactors.	Moderate conversion; Mass transfer limitation; Basic catalyst: low FFA; anhydrous conditions and pretreatment is required for high FFA feedstock; high alcohol to oil ratio required; high temperature and pressure required; Acidic catalysts: low microporosity; high cost compared with basic types; low reusability; high energy consumption for separation via centrifugation	65-97%	Canacki (2007); Kawashima *et al*. (2008); Di Serio *et al*., (2008); Montero *et al.,* (2010) ; Xie and Fan (2014) ; Alhassan *et al*., (2015).

2.5.4 Heterogeneous catalyst synthesis methods

Catalyst preparation aims at bringing the best from the catalyst in terms of activity, selectivity and stability. These can be related to the physical and chemical properties of the catalyst, which in turn can be related to the variable parameters inherent in the preparation method (Di Serio *et al*., 2008).

The development of systematic studies for the synthesis of oxide nanoparticles is a current challenge and, essentially, the corresponding preparation methods may be grouped in two main streams based upon the liquid-solid and gas-solid nature of the transformations (Montero *et al*., 2009). Liquid-solid transformations are possibly the most broadly used. Several specific methods have been developed, among which the following are currently broadly in use:

a) **The sol-gel method:** This method prepares metal oxides via hydrolysis of precursors, usually alkoxides in alcoholic solution, resulting in the corresponding oxo-hydroxide. Condensation of molecules by giving off water leads to the formation of a network of the metal hydroxide: hydroxyl-species undergo polymerisation by condensation and form a dense porous gel. Appropriate drying and calcinations lead to ultrafine porous oxides (Montero *et al*., 2009 and Wen *et al.*, 2010). There are four distinct steps in the sol-gel technique:
   i. Formation of the gel;
   ii. Aging to allow fine tuning of gel properties;
   iii. Drying to remove solvent from the gel; and
   iv. Calcination to permanently change the physical and chemical properties of the solid.

Using the Utamapanya method as a typical example of sol-gel synthesis, a solution of magnesium methylate in methanol/toluene is slowly hydrolysed with water overnight at room temperature. A white sol that slowly transforms to a clear gel is formed during the process. The gel is then fed to an autoclave and N_2 gas is introduced at 1.8 bars. The autoclave is heated to 265°C and then vented to evacuate the solvent. This process minimises sintering and damage to the pore structures due to vapour-liquid interface within the capillaries in the gel network and results in surface tension. It is suggested that the presence of hydrophobic solvent reduces tension at the gas-liquid-pore wall (Utamapanya *et al*., 1991).

Verziu *et al*. (2008) synthesised unsupported MgO nano-catalyst using three different methods where one of the methods was adapted from the method mentioned above. Instead of drying in an oven, they dried in vacuum. The method produced interconnected MgO domains about 2 nm with parallel (110) planes with lattice spacing of 1.45Å.

b) **Ultrasonic method:** Sonochemistry is the research area in which molecules undergo a chemical reaction due to the application of powerful ultrasound radiation (20 kHz-10 MHz). The ultrasonic method, compared with the other methods, which have been used for CaO, MgO and other oxide metal nanostructured materials, is very fast and does not need high temperatures during reaction, and it can produce higher yield with smaller particles (Aslani *et al*., 2009).

c) **Combustion process:** The most conventional method for CaO and especially for MgO is via the thermal decomposition of their respective salts. However, the resulting oxide particles yield relatively large, non-uniform particle sizes and a low specific surface area, which are not preferable for most applications (Buzby *et al*., 2007).

Yanga *et al*. (2010) used H_2/O_2 while Rao *et al*. (2008) used urea as fuel. A schematic block flow diagram is shown in the figure 6.

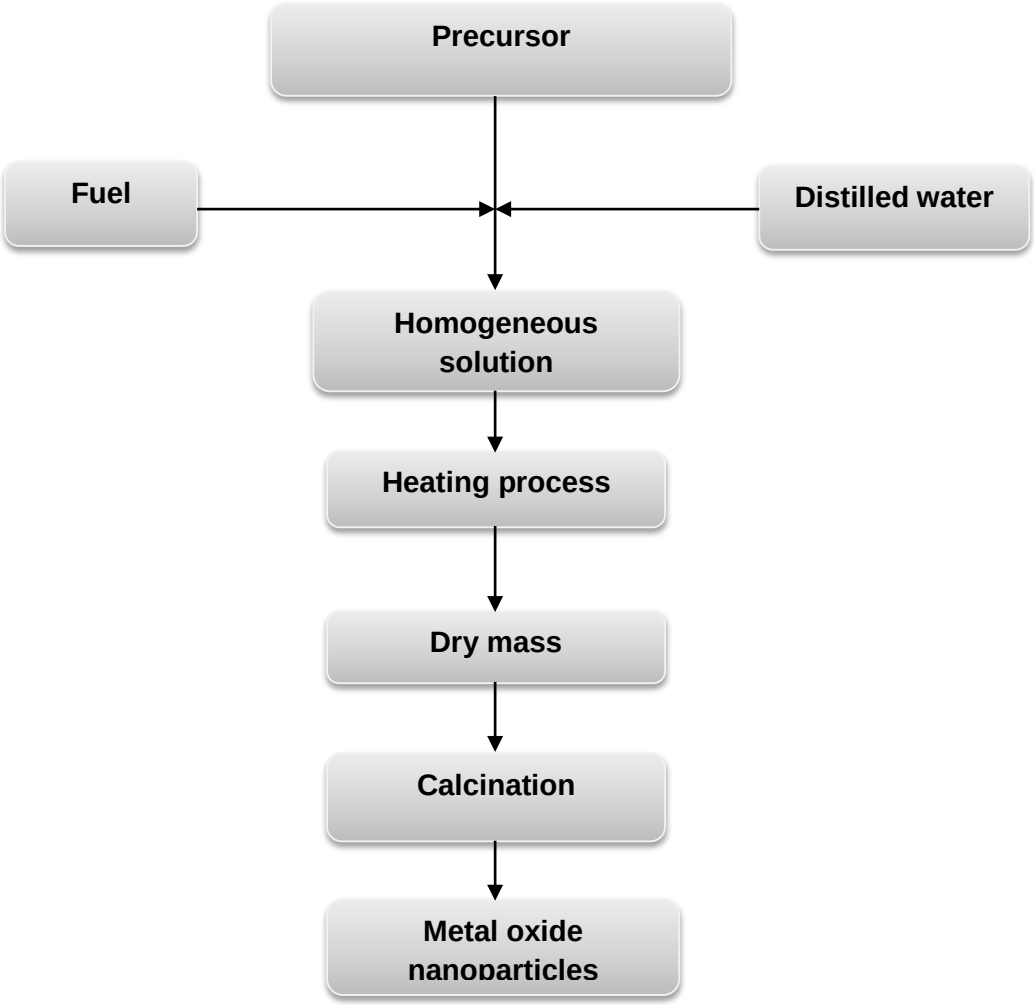

Figure 6: Preparation steps for metal oxide nanoparticles using the combustion method (Buzby *et al*., 2007)

d) **Co-precipitation methods:** This involves dissolving a salt precursor (mainly chloride or nitrate) in water (or other solvent) to precipitate the oxo-hydroxide form with the help of a

base. Very often, control of size and chemical homogeneity in the case of mixed-metal oxides is difficult to achieve. However, the use of surfactants, and high-gravity reactive precipitation, appear as novel and viable alternatives to optimize the resulting solid morphological characteristics (Taufiq-Yap and Lee, 2013; Buzby *et al*., 2007; D'Souza *et al*., 2007).

e) **Impregnation method:** This technique consists of depositing an active phase on porous support in contact with a solution containing a dissolved precursor. Incipient wetness impregnation is the most common method to prepare a supported catalyst, in which the solids' pores are filled with the solution without any excess of moisture. Parameters such as temperature, drying time and the rate of addition of impregnating solution require careful attention for successful synthesis reproducibility (Taufiq-Yap and Lee, 2013; Montero *et al*., 2010).

   Albuquerque *et al.* (2008) prepared a series of CaO catalysts supported on mesoporous silica using an impregnation method, and Wen *et al*. (2010) prepared KF/CaO nanocatalyst by using impregnation method. The same experiments were repeated on a series of different feedstock by Wang *et al.* (2014) achieving a maximum biodiesel yield of 98% with soybean oil. These supported CaO catalysts, thermally activated at 1073 K, can give rise to FAME (fatty acid methyl esters) yield higher than 90 %, after 2 h of reaction, when a methanol/oil molar ratio of 12:1 and 1.3 wt. % of the catalyst with a 16 wt. % CaO were employed.

f) **Hydrothermal method:** In this case, metal complexes are decomposed thermo-chemically either by boiling in an inert atmosphere or using an autoclave. A suitable surfactant agent is usually added to the reaction media to control particle size growth and limit agglomeration. Kumari *et al*. (2009) as well as Ding *et al*. (2001) used NaOH as a catalyst and produced with a particle size distribution between 30-200 nm and an average surface area of 150 and 160 m^2/g respectively.

g) **Gas-solid transformation methods:** With broad use in the context of ultrafine oxide powder synthesis is restricted to chemical vapor deposition (CVD) and pulsed laser deposition (PLD) (Xie and Fan, 2014; Feldman *et al*., 2008).

   There are many CVD processes used for the formation of nanoparticles among which we can highlight the classical (thermally activated/pyrolytic), metalorganic, plasma-assisted, and photo CVD methodologies. The advantages of this methodology consist of producing uniform, pure and reproduce nanoparticles and films although requires a careful initial setting up of the experimental parameters (D'Souza *et al.*, 2007).

Multiple-pulsed laser deposition heats a target sample (4000 K) and leads to instantaneous evaporation, ionisation, and decomposition, with subsequent mixing of desired atoms. The gaseous entities formed absorb radiation energy from subsequent pulses and acquire kinetic energy perpendicularly to the target to be deposited in a substrate generally heated to allow crystalline growth (Xie and Fan, 2014; Buzby et al., 2007).

Irrespective of the preparation method use to obtain ultrafine nano-oxides, the studies of nanoparticle preparation yield compelling evidence concerning the fact that crystallisation does not follow a traditional nucleation and growth mechanism (Mather and Martinez, 2007).

Although subject to further assessment, it appears that the simple idea that a small primary size would prime nucleation as the key step of crystallisation seems essentially correct and holds certain general validity, at least in solid-solid crystallisation mechanisms (e.g.heating of oxo-hydroxides to form oxides). The primacy of one of them has been postulated to be a function of the oxide chemical nature and temperature (Buzby *et al*., 2007).

2.5.5 Nano-magnetic catalysed processes

The use of nano-magnetic catalysts is a promising alternative in the transesterification process because the magnetic separation generally avoids loss of catalyst and increases its reusability in comparison to filtration or centrifugation separation (Corach *et al*., 2016 and Lu *et al*., 2007).

In addition to a large specific surface area and high catalytic activity, nano-magnetic catalysts have been applied widely in the fields of photocatalysis (Beydoun *et al*., 2000), biocatalysis (Gao *et al*., 2003) and phase-transfer catalysis (Wen *et al*., 2008), but not yet in the production of biodiesel through the transesterification process.

However, magnetic particles have been used to immobilise catalysts for transesterification.

Ying and Chen (2007) stabilised the cells of lipase-producing *Bacillus subtilis* on the net of a hydrophobic carrier with Fe_3O_4 magnetic particles for the transesterification of waste cooking oils with methanol, and Xie and Ma (2009) immobilised lipase on Fe_3O_4 nanoparticles for biodiesel production. In these instances, the magnetic particles did not possess catalytic properties; they merely acted as immobilisation matrices to enhance catalyst recovery.

Previous studies have also identified MgO as a promising heterogeneous catalyst for the transesterification of soybean and vegetable oils into biodiesel (Amani *et al*., 2014).

2.5.6 Heterogeneous magnetic catalysis for the transesterification of oils extracted from edible oil wastewater sludge: rationale and novelty

In this study, a nano-magnetic solid base catalyst was synthesised and used for transesterification. This particular catalyst was prepared from dolomite which is considered to be an alkaline gangue in the cupriferous mineral process industry. Minerals must be beneficiated to increase the metal content. Depending on their nature (sulphide, oxides or mixed), or on the initial metal purity in the ore, pyrometallurgy (use of heat to extract the metal) or hydrometallurgy (use of a selective solvent to leachate the metal) processes will be chosen (Thyse *et al*., 2017).

As for the hydrometallurgy process, being the most suitable for low grade ores (Subramanian *et al.*, 2017) froth flotation is the essential concentration operation, after the ore has been reduced into an appropriate size for valuable mineral liberation from the unwanted material. This is a process of separating the gangue from the valuable mineral containing the particular metal to be extracted (Thyse *et al*., 2017).

In this process, it is highly important to use some reagents for effective separation (Yao and Gong, 2016). The gangue can be acidic (mainly containing silica and quartz) in the case of sulphide ores, or it can be alkaline (mainly dolomite and calcite) in the case of oxide and mixed ores (Chen and Tao, 2004).

Dolomite, the most important material in the tailings outlet stream from froth flotation cells, is a carbonaceous material containing mainly calcium and magnesium (Chen and Tao, 2004; Thyse *et al*., 2017). It is used as a raw material to synthesise the catalyst to be employed for biodiesel production. The selection of a catalyst for any process depends on a number of parameters which include cost, availability, activity, selectivity and stability (Chen *et al.,* 2014; Hu *et al*., 2011; Montero *et al*., 2010). The aim of the catalyst preparation under investigation is to meet these criteria.

MgO and CaO have been shown to have high catalytic activity (Amani *et al*., 2014), good robustness and favourable resistance to acid (Wen *et al.*, 2010). Due to their nano-particulate nature, this catalyst should also provide a large catalytic surface area.

It has been found that these oxides do not require magnetic cations to become ferromagnetic, and a novel type of magnetism, tentatively called interface magnetism, has been recognised. It has been theoretically and experimentally confirmed that under certain conditions

magnetism arises in the absence of transition metal elements, a phenomenon that confers potential ferromagnetic properties to MgO and CaO (Guilen *et al.*, 2006; Elfimov *et al.*, 2002).

It is proposed that production of heterogeneous magnetic catalysts from MgO and CaO will enable more efficient mass transfer than conventional heterogeneous catalysts, thereby reducing catalyst loading, improving the biodiesel yield, and ultimately reducing biodiesel production costs.

2.6 Biodiesel properties

The quality of biodiesel can be described in two groups (Hoekman *et al*., 2012):

a) The general physicochemical properties, for example, density, viscosity, flash point, % sulphur, carbon residue, % sulphate, cetane number, and acid number; and
b) The composition and purity of fatty esters such as methanol (ethanol), free glycerol, total glycerol, water, and esters contents, among others. The evaluation of biodiesel quality is achieved through the determination of the chemical composition and physical properties of fuel. In fact, some contaminants and other minor components are the major issues in the quality of biodiesel.

The implementation of biodiesel production processes based on native raw material, which should be optimised to obtain a low production cost biodiesel that would make it competitive while fulfilling international specifications of quality in order to be used as a diesel engine is a major challenge (Dincer and Zamfirescu, 2014).

Therefore, several indicators (water presence, acid index, methanol content, triglycerides, etc.) are studied to know the mechanic and environmental efficiency, as well as the impurities (glycerides, glycerol, free fatty acids, and catalysed waste) are investigated as they bring adverse consequences to the engine performance, for example, soot deposits in the injectors. The mass calorific power of biodiesel is 13% lower than diesel and around 8% per volume unit; however, it is not exactly revealed in the loss of power because biodiesel has a slightly higher density than diesel (Dincer and Zamfirescu, 2014; Knothe and Steidley, 2007).

In South Africa (study field of this project), the legislation SANS1598 specifies the quality requirements of the produced biodiesel and related petroleum fuels, and it corresponds with the American Union ASTM (Table 10). The requirements and trial methods for pure biodiesel applied in diesel engines have been established (South Africa DoE, 2016).

Biodiesel is an alternative fuel that can be used in diesel engine neat, or blended with diesel. The physiochemical properties of fuel are important in design of fuel systems because compression ignition engine run on diesel, biodiesel or biodiesel blend.

Table 10: ASTM Biodiesel Standard D 6751* (ASTM, 2016)

Properties	Test Method	Limits	Units
Flash point (closed cup method)	D 93	130.0 min	°C
Water and sediment content	D 2709	0.050 max	% volume
Kinematic viscosity	D 445	1.9 – 6.0	mm^2/s
Sulphated ash content	D 874	0.020 max	% mass
Sulphur content	D 5453	0.0015 max (S15) 0.05 max (S500)	% mass
Copper strip corrosion test	D 130	No. 3 max	ppm
Cetane number	D 613	47 min	NA
Cloud point	D 2500	Report	°C
Carbon residue	D 4530	0.050 max	% mass
Acid number	D 664	0.50 max	mg KOH/g
Free glycerin content	D 6584	0.020	% mass
Total glycerin content	D 6584	0.240	% mass
Phosphorus content	D 4951	0.001 max	% mass
Sodium/Potassium content	UOP 391	5 max. combined	ppm
Distillation temperature (Atmospheric equivalent temperature method (90% recovered)	D 1160	360 max.	°C

NA: Not applicable *The limits are for Grade S15 and Grade S500 biodiesel, with S15 and S500 referring to maximum sulphur (in ppm)

2.6.1 Viscosity and density

The kinematic viscosity is equal to the dynamic viscosity divided by density. It is a basic design specification for the fuel injectors used in diesel engines. Viscosity that is too high will not allow the injectors to perform properly (Sandford *et al*., 2009). Viscosity typically decreases as the temperature of a liquid increases. The viscosity of the produced biodiesel was measured using a viscometer. The density of biodiesel decreases with temperature, therefore the density of biodiesel as a function of temperature can be an important factor in biodiesel commerce. The specific gravity of biodiesel is between 0.86 and 0.90. It can be determined using a hydrometer (Chinnusamy *et al*., 2009).

Esteban *et al.* (2012) studied the temperature dependency of density and kinematic viscosity of several commonly used vegetable oils, diesel fuel and pure biodiesel. This research showed that the analysed vegetable oils require preheating to 120ºC minimally to match the studied physical properties of automotive diesel and biodiesel fuels. Aworanti with his team (2012) studied the binary and ternary blends of biodiesel and the effect of temperature on their kinematic viscosity and density. They used binary and ternary blends of soybean biodiesel that was prepared from soybean biodiesel with soybean oil and petroleum diesel fuel respectively. The results showed that the viscosities and densities of both the binary and ternary blends decrease with increasing temperature (Aworanti *et al.*, 2012)

2.6.2 The 3/27 conversion test

According to the Utah Biodiesel Blog (Warnqvist, 2005), the 3/27 conversion test method of biodiesel can be used to readily determine whether a good conversion of triglycerides into biodiesel has been obtained. The test works on the principle of biodiesel being soluble in ethanol, triglycerides and diglycerides but not in monoglycerides. 3 ml of biodiesel are dissolved in 27 ml of ethanol. If the biodiesel dissolves in ethanol, then a good conversion of triglycerides has been obtained. If the mixture of ethanol and biodiesel still contains traces of oil, then the biodiesel still contains unreacted triglycerides.

2.6.3 High heating value (HHV)

The heating value (HHV) of a fuel is the thermal energy released per unit quantity of fuel when the fuel is burned completely, and the products of combustion are cooled back to the initial temperature of the combustible mixtures (Canakci, 2007 and Olkiewicz *et al*., 2012).

Sivaramakrishnan and Ravikumar (2011) studied the higher heating values (HHVs) of vegetable oils and their biodiesels. The HHVs measured and correlated using linear least square regression analysis. An equation was developed relating HHV and thermal properties. The higher heating values compare well with the measured higher heating values.

The HHV is an important property which characterises the energy content of fuels such as solid, liquid and gaseous fuels, as well as the flash point of the produced fuel, in order to establish the delay between ignition and the moment pressurised fuel drop feeds into the engine cylinder for energy generation (Hoekman *et al*., 2012).

2.6.4 Flash point

The flash point of biodiesel is used as the mechanism to limit the level of unreacted alcohol remaining in the finished fuel. The flash point is important in connection with legal requirements, and for the safety precautions involved in fuel handling and storage. It is normally specified to meet fire regulation (Prugh, 2007).

The flash point of pure biodiesel is considered higher than prescribed limits but can decrease rapidly with increase residual alcohol. As these two aspects are strictly correlated, flash point is used as a regulation for categorizing the transport and storage of fuels with different thresholds from region to region, so aligning the standards would possibly require a corresponding alignment of regulation (Amit, 2009).

CHAPTER THREE: RESEARCH DESIGN AND PROCESS METHODOLOGY

The oil extracted from the oilseed wastewater sludge (OWS) was analysed at the Food Technology Station (Cape Peninsula University of Technology) using gas chromatography-flame ionisation detection (GC-FID) (***Section 3.1***).

The residue left after oil extraction was used to produce bioethanol, and the hydrolysates were analysed for sugars and ethanol using high performance liquid chromatography (HPLC) and gas chromatography-mass spectrometry (GC-MS) at the Biocatalysis and Technical Biology Research Group (BTB) and the Food Technology station at the Cape Peninsula University of Technology (CPUT) (***Section 3.2***).

The catalysts were synthesised in the laboratory at the Department of Chemical Engineering situated on the Bellville campus of CPUT. The synthesised catalysts were characterised at the Spectroscopy Unit at the University of the Western Cape using energy dispersive X-ray spectroscopy (EDX), scanning electron microscopy (SEM) and transmission electron microscopy (TEM), while BET (Brunauer–Emmett–Teller) analyses of the surface area of the catalysts were carried out the Department of Chemical Engineering at the University of Cape Town (UCT) (***Section 3.3***).

The biodiesel was synthesised in the laboratory of the Department of Chemical Engineering laboratory situated on the Bellville campus of CPUT. Evaluation of the biodiesel properties and performance (using an internal combustion (IC) engine) were conducted in the Thermodynamics Laboratory at the Department of Mechanical Engineering at CPUT (***Section 3.4***).

3.1 Oil extraction from oilseed industry wastewater sludge

The OWS was pretreated, and oil containing monounsaturated fats was extracted from pretreated OWS using the Soxhlet apparatus E-816 method described by the Association of Official Analytical Chemists (AOAC, 2005) and Dufreche *et al*. (2007).

3.1.1 Materials

The following materials were used: analytical grade ethanol (>99.8%, Sigma-Aldrich, St Louis, USA), anhydrous hexane (95%, Sigma-Aldrich), sodium chloride (anhydrous ≥99%, Sigma-Aldrich), distilled water, and OWS collected from an industrial wastewater treatment plant at a facility producing predominantly canola oil.

3.1.2 Experimental protocol

3.1.2.1 Pretreatment of oilseed industry wastewater sludge

Pretreatment (Figure 7) was performed in triplicate. For each replicate, 100 g of OWS was mixed, soaked in 250 mL of NaCl 1M to improve the oil quality in the demulsification of the mixture of oil and water. The moisture then was removed in a tray dryer. Samples were weighed before and after drying to determine the moisture content.

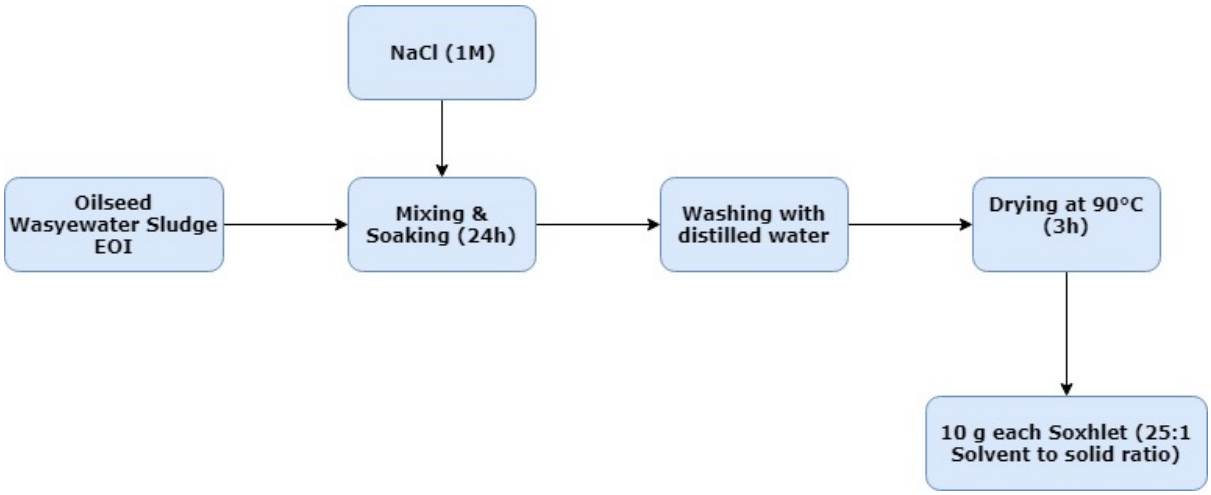

Figure 7: Integrated process flow diagram for pretreatment before oil extraction

3.1.2.2 Oil extraction from pre-treated oilseed industry wastewater sludge

Oil was extracted from the pre-treated OWS using in a Soxhlet apparatus E-816 for 145 min at the boiling points of the solvents tested (78°C and 67-69°C, for ethanol and n-hexane respectively). Subsequently, the solvent was evaporated under reduced pressure and the mass of extracted material was determined by weighing using an analytical scale (Mettler Toledo model). Extraction times of 60, 120 and 180 minutes were used. For each, the oil-solvent solution was recovered in a flask, the solvent evaporated under reduced pressure and the extracted oil quantified. This experiment was carried out in an attempt to determine the near-optimum extraction time with ethanol and *n*-hexane.

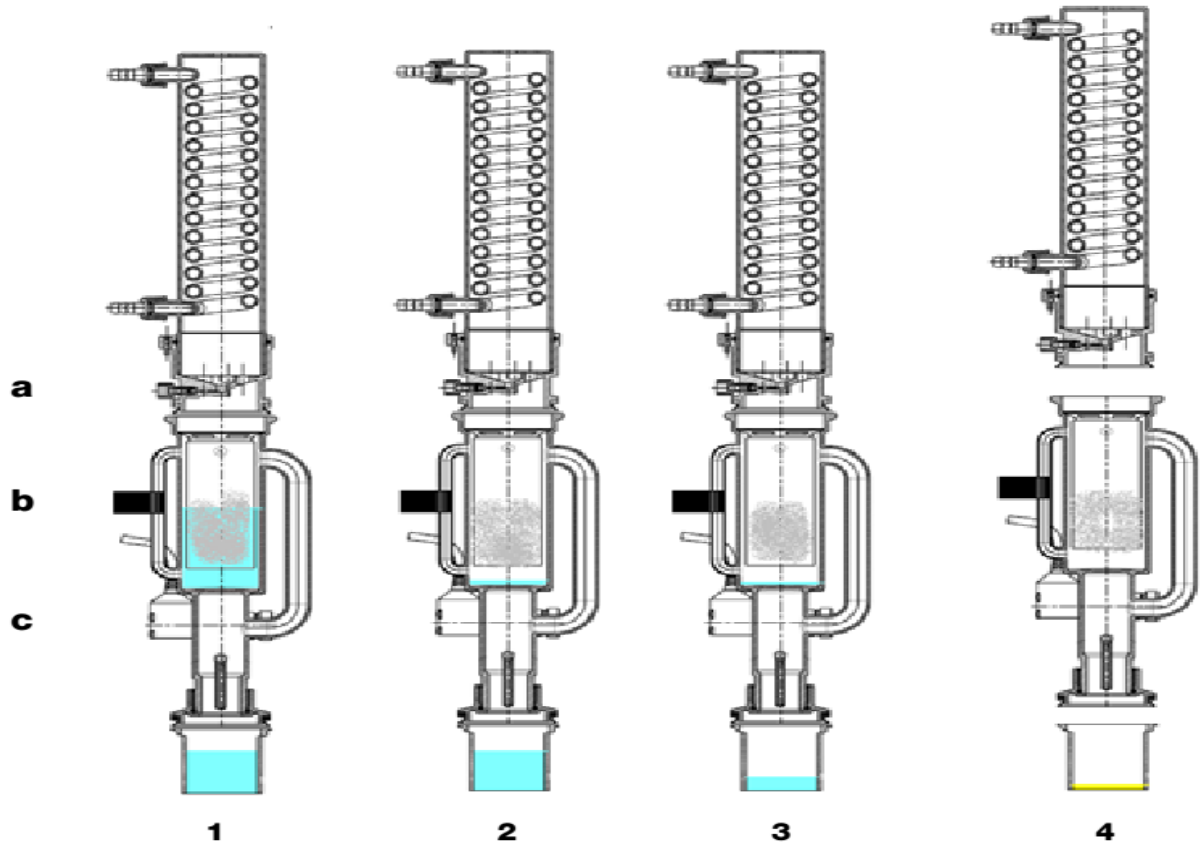

Figure 8: Schematic diagram of a Soxhlet extraction (a: Tank valve, b: Level sensor, c: Valve unit)

(1) Extraction: the extraction chamber is filled up with condensed solvent. As soon as the solvent reaches the optical sensor, the chamber is emptied by opening the valve unit; (2) Rinse: the valve unit is always open, which allows the condensed solvent to rinse the sample; (3) Drying: the solvent is evaporated and collected in the water-cooled tank at the back of the instrument, which allows it to be reused for further extractions; (4) After completion of the extraction, the beakers containing the extract were removed and dried to constant weight.

3.1.3 Analysis of oil extracted from the oilseed industry wastewater sludge

The quality of biodiesel is reliant on the monounsaturated (MU) fats used in transesterification. The quality and quantity of MU fats in the extracted oil were determined using an Agilent (Santa Clara, California, USA) 6980A GC-FID instrument. The column used was a HP88 (60 m x 150 µm, 0.250 µm) manufactured by Agilent Technologies (Santa Clara, California, USA). Nitrogen was used as the carrier gas. Both the injector and the detector temperatures were kept constant at 250°C. The injection volume of sample was 1 µl with a split ratio of 50:1. The oven temperature program started at 50°C hold for 2 minutes, increased by 5°C/minute to

160°C, and thereafter increased by 2.9°C/minute to 250°C hold for 15 minutes. The total run time was 65 min.

3.2 Bioethanol production

A portion of the solid residue remaining after oil extraction from the OWS (ROE) was pre-treated by washing and drying (Section 3.2.2.1) to give a dried pre-treated substrate (DPS). Both the ROE and DPS were hydrolysed with different concentrations of acid or enzymes (Section 3.2.2.2), and the sugar yields were compared with the yields from non-hydrolysed controls. The hydrolysates were then fermented to produce bioethanol (Section 3.2.2.3) and then distilled (Section 3.2.2.4).

3.2.1 Materials

The following materials were used: sulphuric acid (99.9%, Sigma-Aldrich), sodium hydroxide (anhydrous pellets ≥98%, Sigma-Aldrich), industrial *Saccharomyces cerevisiae* MH-100 strain (obtained from Prof WH van Zyl, Department of Microbiology, Stellenbosch University, South Africa), cellulase from *Trichoderma reesei* ATCC 26921 (Celluclast® Sigma-Aldrich), distilled water, analytical grade ethanol (>99.8%, Sigma-Aldrich), DPS.

3.2.2 Experimental methods

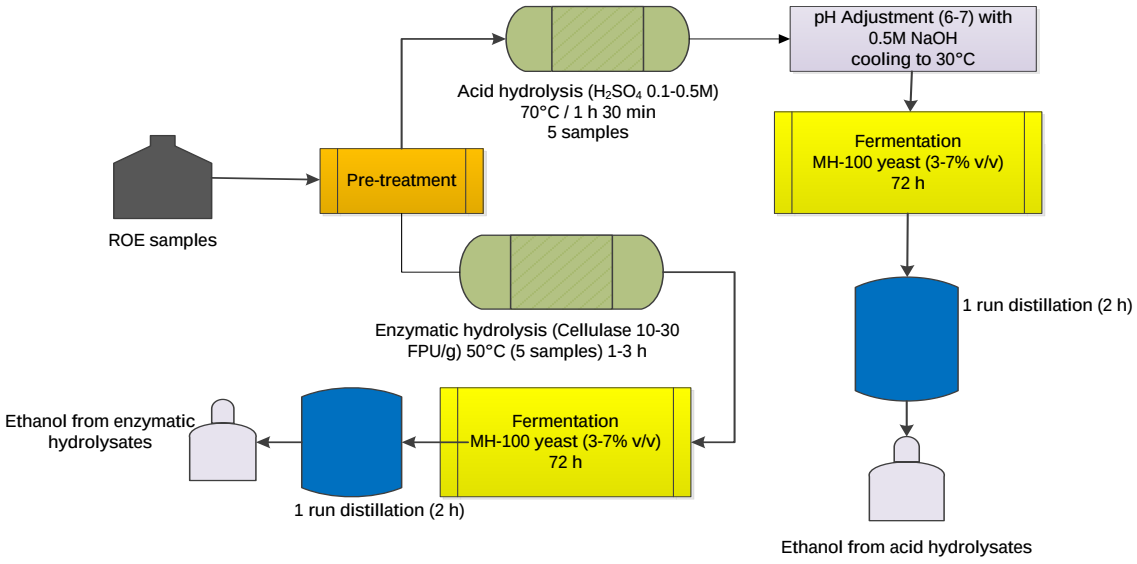

Figure 9: Process flow diagram for bioethanol production from wastewater sludge residue after oil extraction (ROE: residues after oil extraction)

3.2.2.1 Pre-treatment of substrate for bioethanol production

The ROE was washed in hot water at a maximum temperature of 75°C and the residue was collected using a plastic sieve of 0.5 mm aperture and dried at 80°C for 24 hours. The DPS sample was kept in a desiccator for 24 h to prevent chemical decomposition before being used.

3.2.2.2 Hydrolysis

The ROE and/or DPS samples were split equally into two different hydrolysis streams (acidic and enzymatic). The resulting hydrolysates were used as substrates in the fermentation process. Fermentable sugars were quantified using HPLC (Section 3.2.4).

- **Acidic Hydrolysis**

Dilute sulphuric acid at 5 different concentrations (0.1; 0.2; 0.3; 0.4 and 0.5 M) was employed for the hydrolysis of 50 g DPS and/or ROE at a constant temperature (70°C) and reaction time (1h 30min). Based on the acid concentration range (each in duplicate), 5 hydrolysate samples (20% w/w each) were filtered using a vacuum filtration set-up with filter paper (1 μm aperture). The pH was adjusted to 6.5 during the fermentation process.

- **Enzymatic hydrolysis**

The DPS and/or ROE was hydrolysed for 24 h at 50°C using one of two different types of commercial cellulase: Onozuka RS® (Section 4.2.2) at 5 different activities (Table 11) and Cellulclast® (Section 4.2.3). Each hydrolysis reaction was performed in triplicate in 250 ml Erlenmeyer flasks containing 10 g DPS and 200 ml of distilled water. A magnetic stirrer was employed for mixing at 100 rpm for 4 h. The pH was measured every hour using a pH probe and meter, and the value was adjusted within the range (4.76-4.84) by addition of 4M HCl and/or 8M NaOH during the hydrolysis process. The hydrolysate samples generated were filtered using a vacuum filtration set-up with filter paper (1 μm aperture).

This particular hydrolysis process was evaluated with cellulase as enzyme at five different activities for a period of 8 h every run, as described in Table 11. Each run was performed in triplicate.

Table 11: Enzymatic hydrolysis conditions of DPS samples

Company	Enzyme formulation	Enzyme activity and loading (FPU/g)	Duration (h)	Run
Novozymes	**Onozuka RS**	10	8	1
			16	2
			24	3
		15	8	4
			16	5
			24	6
		20	8	7
			16	8
			24	9
		25	8	10
			16	11
			24	12

3.2.3 Fermentation of hydrolysates produced

3.2.3.1 Inoculum preparation and fermentation

Freeze-dried *S. cerevisiae* MH-1000 cultures in skim milk cryoprotectant were rehydrated with sterile water and plated out on tryptic soy agar (TSA (casein peptone, 17 g/L; dipotassium hydrogen phosphate, 2.5 g/L; glucose, 2.5 g/L; sodium chloride, 5 g/L; soya protein, 3 g/L; 15 g/L bacteriological agar, pH 7.3±0.2)) and incubated at 25°C for 72 hrs.

For the pre-culture, a loopful of *S. cerevisiae* MH-100 was inoculated into 20 ml tryptic soy broth (TSB) in a 50 mL Erlenmeyer flask with and incubated aerobically at 30°C at 160 rpm for 48 hours. The yeast cell optical density (OD) was measured at 600 nm (OD600) using a RayLeigh UV-9200 spectrophotometer (sterile TSB was used as a blank). The pre-culture was diluted with sterile TSB to an OD600 of 0.5, which is approximately 1.5 x 10^8 colony-forming units (CFU)/mL. The fermentation was carried out by inoculating 500 mL reactors consisting of Schott bottles containing 50% v/v (media volume/flask volume) with 5% v/v inoculum (pre-culture/media volume). An outlet glass tube was centred in the plastic Schott bottle cap to allow release of carbon dioxide during the fermentation process. The bottles were incubated at 30°C for 72 hours. The bottles were placed on an orbital shaker at 160 rpm for the first 8 hours, after which the speed was reduced to 100 rpm. The fermentation was performed under

three different yeast loadings ($1.5*10^5$, $2*10^5$ and $2.5*10^5$ CFU/mL), which was a variable in order to investigate its influence on the yield of ethanol produced, and the results obtained were compared to those generated without yeast addition (as control).

3.2.3.2 Distillation

The raw product obtained after fermentation (fermentate) was directly distilled using a simple apparatus (Figure 10). The fermentate was transferred into a 500 ml round-bottomed flask containing three boiling chips and boiled. The distillate was collected in a receiving vessel (100 ml graduated measuring cylinder) at the rate of about 1 drop per second. The temperature was recorded after every 2 ml of the distillate was collected. The distillation was allowed to continue until 50 ml of distillate has been obtained. The density of the distillate was calculated by weighing a 10 ml aliquot and the ethanol was determined by HPLC (Section 3.2.5). The distillation step was performed in duplicate.

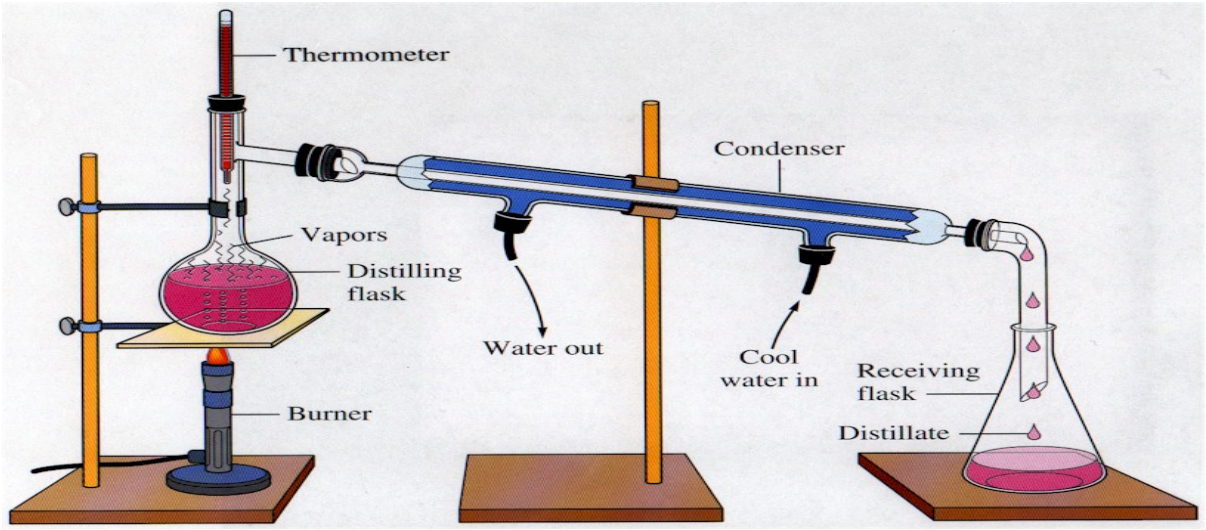

Figure 10: Distillation set-up (adapted from Kumar and Singh, 2016)

3.2.4 Sugar and ethanol analyses

Samples were analysed by high performance liquid chromatography (HPLC) according to the method by Welz *et al*. (2011). A Merck La-Chrom instrument with a La-Chrom® D-7400 ultraviolet detector set at 210 nm and an Agilent™ refractive index detector were employed for the detection of sugars and alcohols respectively. Sample components were separated using a Phenomenex Rezex RHM-monosaccharide H + (8% cross-linkage) column and a 1 mM H_2SO_4 solution at pH 2.52 (mobile phase). Sample acquisition time and flow rate were set at 60 min and 0.550 $mLmin^{-1}$ respectively. Gas chromatography-mass spectrometry (GC-MS)

was used to measure the amount of ethanol produced; the column used was an HP88, (100 m x 150 µm, 0.250 µm). Nitrogen was used as carrier gas. Both the injector and the detector temperatures were kept constant at 25°C. The injection volume of sample was 1 µl with a split ratio of 50:1.

3.3 Catalyst preparation

3.3.1 Materials

Ethylene glycol, ferric sulphate, sodium borohydride and nitric acid used in this study were obtained from Sigma Aldrich Co. A simulation was done based the current composition of mineral processing waste in the cupriferous ore, and the oil used for catalyst testing in the production of biodiesel was extracted from the edible oil wastewater sludge. All other chemicals were obtained commercially, and no additional purification was done on materials.

3.3.2 Standard operating procedure

10 g of the gangue sample was dissolved with warm (60°C) 100 cm^3 of 1 mol/L nitric acid into a 500 cm^3 beaker. The mixture was then filtrated into an evaporative basin until crystals formed, and this was stored in a tube; the mass was then recorded. Secondly, 9 g from the crystals obtained was dissolved in minimum amount of water and then it was added to 25 ml of ethylene glycol, being mixed by mechanical mixer. 2 g of NaOH was dissolved in 25 ml of purified water, added drop by drop, as the mixing took place.

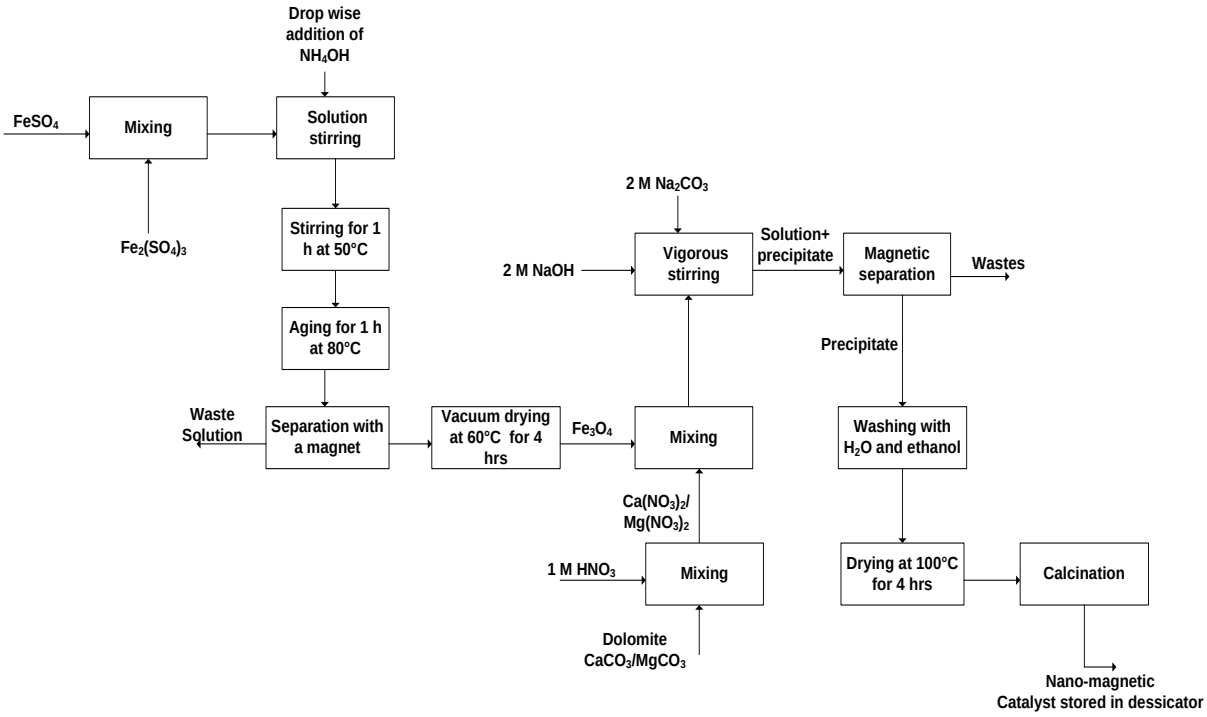

Figure 11: Co-precipitation method for catalyst (CMCO) preparation

The produced mixture was mixed for 2 h so that a clear white gel was obtained. The white gel was kept still for 2 h for the reaction to complete. Then being washed with water four times, NaOH was excreted and pH was adjusted at about 10. After that, the gel was heated up to 80°C for 2 h so that the water could be vaporised, and the gel concentrated. The concentrated gel was placed in a desiccator for one hour to dry completely. The resulting dry gel was milled in the form of a white powder. The produced powder was put in the cruse and into the oven which was gradually heated up to 800°C, and kept there for an hour for decarbonisation.

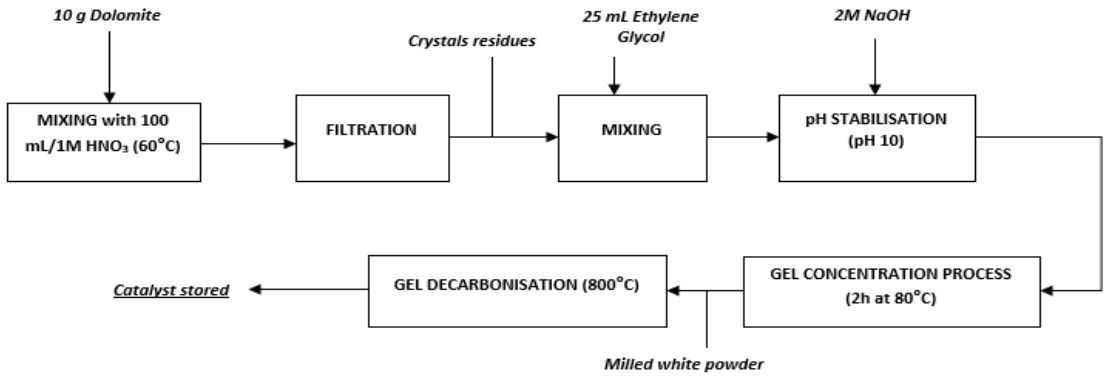

Figure 12: Sol-gel method for catalyst (CMSG) preparation

Additionally, the zero valent iron nanoparticles (ZVINPs) were prepared using the sulphate method (Sun *et al*., 2007) by metering equal volumes of 0.5M sodium borohydride at 0.15 L/min into 0.28M ferrous sulphate according to the following stoichiometry:

$$2Fe^{2+}_{(aq)} + BH_4^-{}_{(aq)} + 3H_2O_{(l)} \rightarrow 2FeO_{(s)} + H_2BO_3^-{}_{(aq)} + 4H^+_{(aq)} + 2H_{2(g)} \quad (2)$$

All parameters were kept constant during the experiments except for the ratio of dolomite and ZVINPs which was 2:1, 3:1 and 4:1 and 80/20 respectively. Afterwards, their catalytic properties were tested to produce biodiesel under the same conditions during the transesterification reaction. All experiments were done in triplicate.

3.3.3 Catalyst characterisation and testing

The morphology and particle size of the catalyst were assessed by X-ray diffraction (XRD) (STADI-P, STOE model, Darmstadt, Germany). An Auriga (Carl Zeiss model, Jena, Germany) high-resolution scanning electron microscope (HRSEM) was used with a resolution of 1.5 nm to provide detailed high-resolution images by rastering a focussed electron beam across the surface of the sample. These images were magnified using another Auriga TF 20 high-resolution transmission electron microscope (Carl Zeiss model, Jena, Germany) with a resolution of 0.25 nm for 45 minutes to 2 hours for sample mapping and imaging. Furthermore, an Aztec series (Hitachi High-Technologies, Tokyo, Japan) TM 4000 energy dispersive X-ray analyser with a 30 mm^2 detector) was employed to provide the elemental identification and quantitative composition of the prepared catalyst. Catalyst surface areas were studied using a VF-Sorb 2400CE BET(Brunauer-Emmett-Teller) surface area analyser (Beijing, China).

The performance of the catalyst was evaluated via the production of biodiesel from edible oil wastewater sludges for different catalyst dosages (3, 5 and 8 wt.%) and ethanol-oil ratios (3:1, 6:1 and 9:1) respectively. The particle surface area was confirmed using BET analysis.

In the current study, the magnetic susceptibility of the catalysts was calculated based on the Gouw's principle (Frisch and Pizarek, 2008) and data was collected using a simple mass balance; two measurements were taken, m_0 (the initial mass reading) and m_f (the final mass reading after lowering the sample into the magnetic field). In the current study, the magnetic field was provided by a lightweight neodymium magnet assembly. It had a mass of 75 g with an air gap between the magnets of 2 cm and a magnetic field of approximately 0.22 T (Tesla). The force is thus given by:

$$\vec{F} = \Delta m\vec{g} = \left(m_f - m_0\right)\vec{g} \quad \text{(Eq.3)}$$

where *g* is the acceleration due to gravity (about 9.81 m/s^2). An expression for the force applied by the magnet on the catalyst was then derived: its magnetic permeability μ is given by:

$$\mu = \mu_0(1 + x) \quad \text{(Eq.4)}$$

where μ_0 is the permeability of free space or the magnetic constant ($4\pi \times 10^{-7}$ N/A^2), and χ is the magnetic susceptibility. Then, the difference in magnetic potential energy per unit volume between the catalyst of magnetic permeability μ and the displaced medium (in the current study, it was air, which has the permeability of free space) is shown below:

$$\Delta\left(\frac{U}{V}\right) = \left(\frac{H^2}{2\mu_0}\right)_{\text{air}} - \left(\frac{H^2}{2\mu}\right)_{\text{sample}} = \frac{H^2}{2\mu_0} - \frac{H^2}{2\mu_0(1+\chi)}$$

$$\Delta\left(\frac{U}{V}\right) = \frac{\chi H^2}{2\mu_0(1+\chi)} \quad \text{(Eq.5)}$$

Eq.5 was further simplified assuming the fact that the magnetic susceptibility is significantly smaller than 1 (Frisch and Pizarek, 2008). Subsequently, the value χ becomes negligible. Hence, to make the approximation to get:

$$\Delta\left(\frac{U}{V}\right) = \frac{\chi H^2}{2\mu_0} \quad \text{(Eq.6)}$$

For this study, it was important to consider a gradient in the field along the *z*-direction (upwards direction), as there is in the case of this experiment. But an assumption had to be made that the magnetic susceptibility is constant throughout the sample (Frisch and Pizarek, 2008). The force per unit volume *f* experienced by the catalyst was then given by:

$$f = -\frac{\partial U}{\partial Z} = -\frac{\chi}{2\mu_0}\frac{\partial}{\partial Z}(H^2) \quad \text{(Eq.7)}$$

From Eq.7, the integral over the length (with a constant cross-sectional area *A*), was used to find the total force on the sample by the magnetic field. Here, the top and the bottom *z*-values of the sample are simply denoted as “top” and “bottom”.

$$F = \int_{bottom}^{top} f A dz = \frac{\chi A}{2\mu_0}(H_{bottom}^2 - H_{top}^2) \quad \text{(Eq.8)}$$

where *A* is the cross-sectional area of the sample and *H* is a measure of magnetic field at the top and bottom of the sample respectively.

H_{top} and H_{bottom} are the measured magnetic fields at the top and bottom of the catalyst in the apparatus. If the length of the sample is sufficiently long, H_{top} may be treated as zero and H_{bottom} may be generalised to simply *H*. Thus, Eq.8 was simplified to:

$$F \simeq \frac{\chi A}{2\mu_0} H^2 \qquad \text{(Eq.9)}$$

Now, if Eq.3 and Eq.9 are equated, the final equation for the magnetic susceptibility will be:

$$\chi = \frac{2\mu_0 \Delta m g}{AH^2} \qquad \text{(Eq.10)}$$

3.3.4 Separation process

Two separation techniques were used, the electrostatic separation method for separating the biodiesel produced from glycerol and the magnetic separation/filtration for the catalyst that had to be regenerated from the process.

This separation process was carried out using an LG electronic neon transformer, 8 kV and 25 mA in a 1L sample biodiesel produced, for a period of 15 to 20 minutes.

The magnetic separation used was adapted from Rossi *et al.* (2014), and involved a magnetic field/force which was used to capture and withhold the particles (which in this study, were the catalyst) against the drag force of the surrounding fluid.

The biodiesel was washed with water and then collected and tested for the conversion of triglycerides and for further chromatographic analyses. The catalyst was then recovered for reuse by washing with anhydrous ethanol and drying overnight at 105°C.

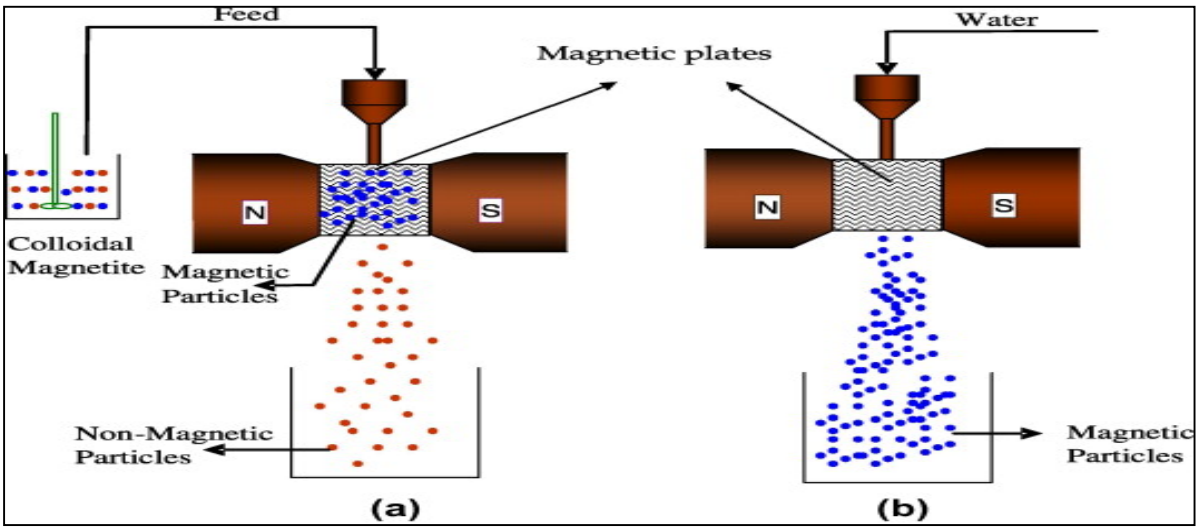

Figure 13: Working principle of magnetic separation (Adapted from Rossi *et al*., 2014)

3.4 Biodiesel production

Transesterification reaction was carried out in a three-necked glass reactor/beaker with a magnetic stirrer. The catalyst was dispersed in the bioethanol under continuous stirring.

The extracted oil containing monounsaturated fats from the wastewater sludge was then added to the mixture and heated by the water bath to 60°C. The ethanol to oil molar ratio together with the catalyst loading were the variables investigated until the optimum conditions for better yield were reached. The yield of biodiesel was compared with the reaction time for each feedstock used (Farooq *et al*., 2013; Hu *et al*., 2011).

3.4.1 Materials

Monounsaturated oil (*obtained from objective 1*), nanomagnetic catalyst (*obtained from objective 2*), bioethanol (*obtained from objective 3*) and distilled water.

3.4.2 Experimental set-up

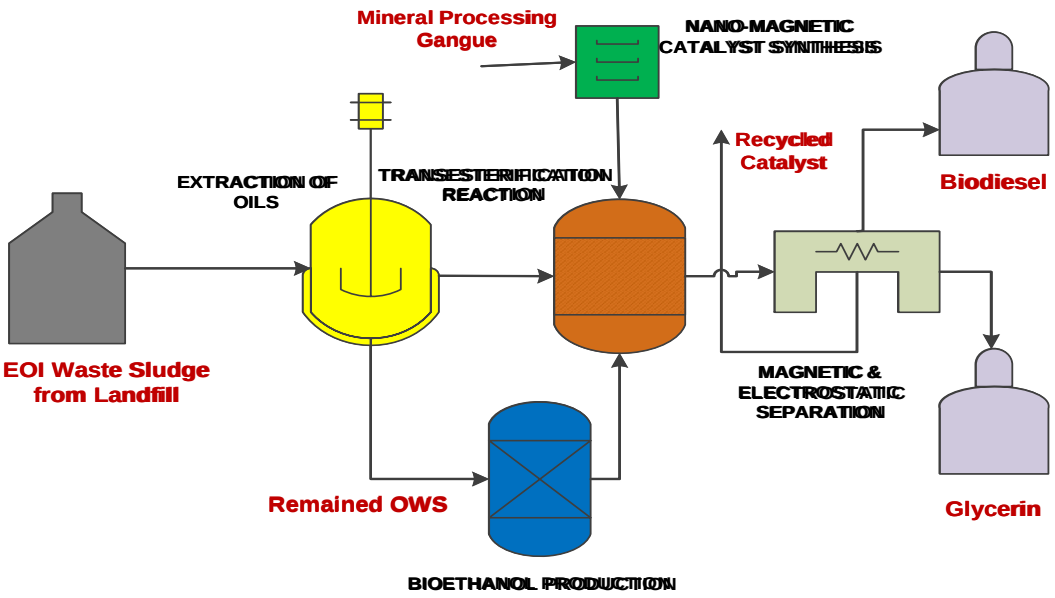

Figure 14: Biodiesel production by transesterification of edible oil wastewater sludge

3.4.3 Product analysis

In order to determine the quality of the biodiesel, the product was tested in accordance with the methods specified by the American Society for Testing and Materials and the European normalisation (ASTM, 2016). Determinations of the parameters given in Table 4 were outsourced to a suitable accredited laboratory:

a) Higher heating value (HHV)

It is the measure of energy content in a fuel. The HHV of the biodiesel produced was measured in a bomb calorimeter (Model 1341 Plain Jacket Calorimeter, Parr Instruments Company, Moline, US) at the Thermodynamic Labs, Mechanical Engineering department (CPUT). According to the ASTM D2015 standard method, the oxygen bomb was set at 3 Mpa pressure, and the calorimeter bomb was fired automatically after the jacket and the bucket temperature equilibrated to the acceptable accuracy of each other as per the manufacturer recommendations, and based on the required ASTM D2015 standards (ASTM, 2016).

b) Viscosity and density

The determination of kinematics viscosity was carried out in a digital viscometer with stand and probe (Model BROOKFIELD LVDV-I Prime C-Digital, Middleboro, US) by first inserting and centring the spindle in the test material until the (≈50 ml) level of the fluid was at the immersion groove in the spindle shaft attached to the viscometer, and then heating the samples to 40°C for 30 min in a viscosity tube while recording the flow rate. To make the viscosity measurement, the desired speed setting was selected (ASTM D2270). The time required for stabilisation, which mainly depends on the speed at which the viscometer is running and the characteristics of the sample fluid, was allowed to stabilise before taking the readings. For maximum accuracy, readings below 10% were avoided. The kinematics viscosity (ν) was then calculated according to Eq. 1, to confirm the measured value, in case the calibration was not done properly. This equation was adapted from Sandford *et al*. (2009). The viscosity indexes all fuels tested was determined using the VI-ASTM D2270 standard (ASTM, 2016).

c) Flash point

The flash point of biodiesel was measured by a flash point tester which consisted of 80 ml closed copper cup, heater, and a source that provided continuous sparks. The source consisted of a battery connected to a small engine, coil, and spark plug. The engine was used to fractionate the current to electrical pulses. A coil was used to amplify the electrical pulses, and spark plug was used to create sparks inside the cup. The biodiesel sample was heated, and the vapour accumulated inside the cup; at the moment that the vapour was sufficient to ignite, a flash light was noticed, and the temperature measured.

In this study, the flash point of biodiesel was measured by a flash point tester (Model Pensky-Martens-PM5, Rigana Manufacturing, Westmead, South Africa). The Pensky-Martens flash point tester is a flammability tester for each type of measuring task in its product line. Tests according to 4 standardised methods in the temperature range of -30 °C to 400 °C are possible to cover a wide range of applications.

3.5 Quality assessment of biodiesel (Thermodynamic study and GHGs evaluation)

The biodiesel produced from edible oil wastewater sludge was evaluated in terms of its performance in an internal combustion engine (IC engine) to check mainly the thermal and mechanical efficiency of this particular fuel and suggest at what extent in volumetric ratio to

blend it with commercial diesel, in order to optimise the effectiveness of the engine while improving the environmental aspect by reducing GHGs emissions, as compared to normal diesel.

A stationary and computerised Plint & Partners TTE95/5604 (Berkshire, Reading, England) 4 stroke, 5.2 kW (Figure 15), water cooled, single cylinder diesel engine was used to evaluate the performance of diesel EOWSS-biodiesel (biodiesel obtained from edible oil wastewater sludges), PCO-biodiesel (biodiesel obtained from pure canola oil using the conventional transesterification process) and C-diesel (diesel obtained from the local petrol station).The efficiency of an internal combustion engine depends on where and when in the cycle the heat is released (Ganesan, 2003).

In an ideal Otto cycle (four-stroke cycle) this means that heat release must occur at a constant volume. This however is not possible as combustion takes a finite time. (Srivinivasaan, 2001). The same procedure was applied to the commercial diesel sample and each trial on the IC engine was conducted in duplicate to compute the thermal and mechanical efficiency.

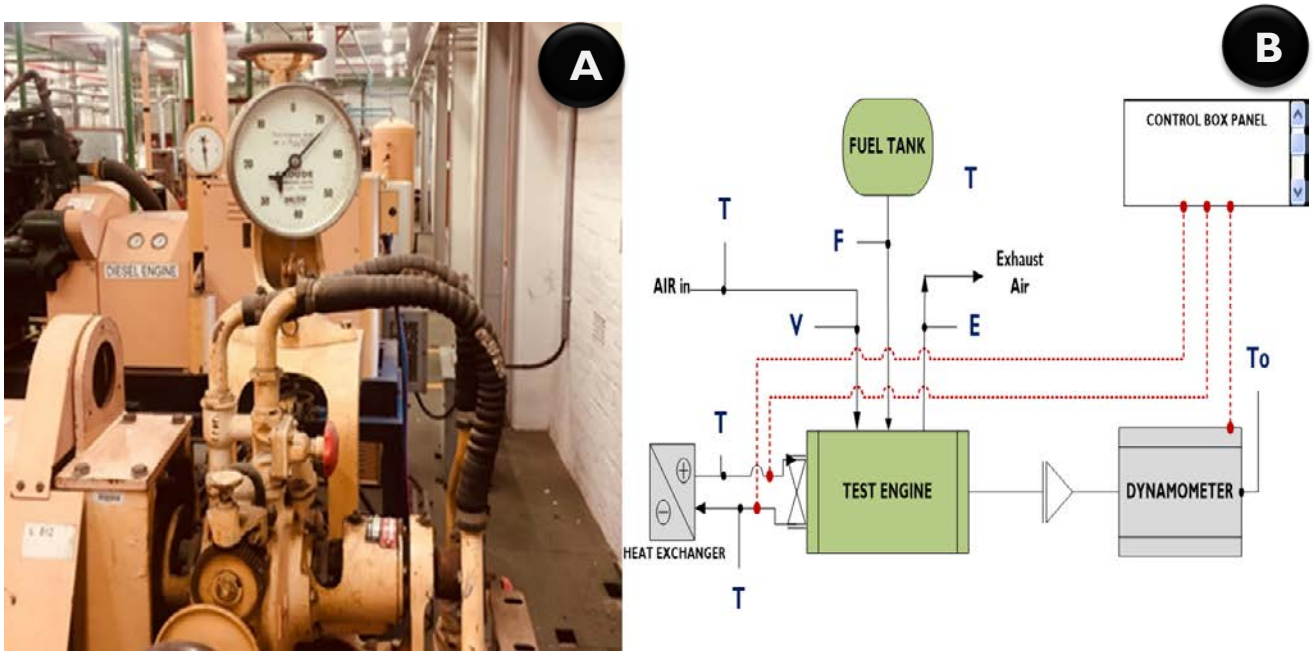

Figure 15: **(A)** Picture of the diesel engine used for these experiment; **(B)** Schematic diagram of experimental setup (T: Temperature; V: Velocity; Emissions (CO, NOx); F: Flow rate; To: Torque)

3.6 Statistical analysis

The obtained results were tabulated and statistically analysed. The statistical analysis of the data was done using Microsoft Office Excel. The equations were fitted using two parameters:

a) The coefficient of determination R^2 gives the proportion of the variance of one variable that is predictable from the other variable;

b) The standard deviation (SD), which is a measure of the dispersion of the calculated data from the experimental data obtained.

3.7 Waste generation and disposal method

Besides glycerol as by-product that can be considered as a potential raw material for biogas production, other waste was minimal and stored in specific labelled containers. Afterwards, the catalyst was recycled and reused for future experiments. Waste was disposed of using a commercial company and according to City of Cape Town by-laws for landfill disposal.

CHAPTER FOUR: RESULTS AND DISCUSSION

4.1 Extraction of oil and characterisation

The objectives described in this thesis are related to one another as shown in Figure 15. At the beginning of each section of this chapter, the same figure is included with the process under discussion highlighted in red. The first objective was to extract the monounsaturated component from OWS using the Soxhlet technique.

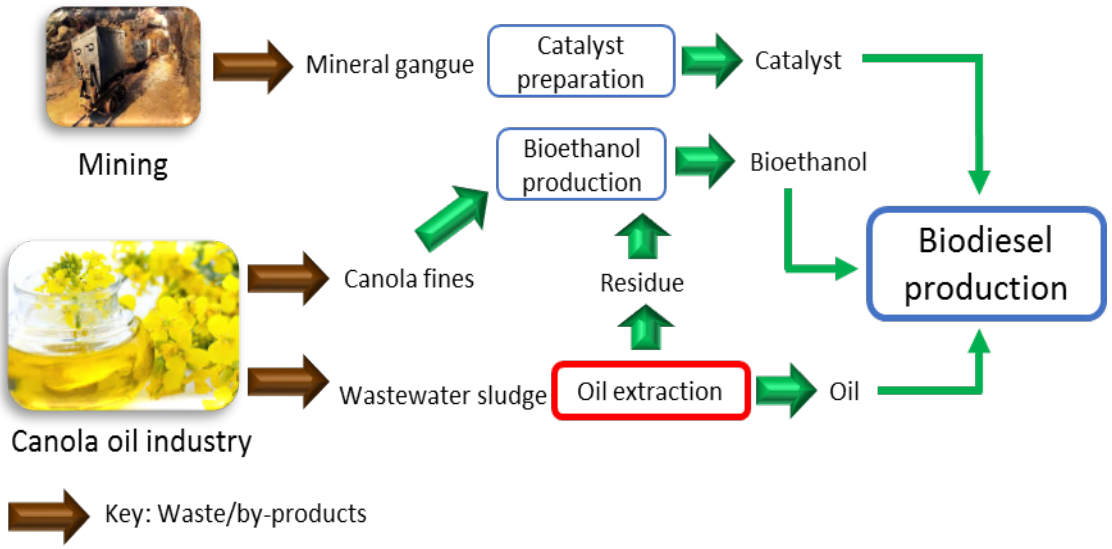

Figure 16: Flow diagram showing the relationship of oil extraction to the other primary study objectives (Objective 1:Extraction of oil)

There are different methods used for oil extraction from solid material. Popular techniques, including their respective advantages and drawbacks, are given in Table 11. In this study, Soxhlet extraction was employed.

During the extraction process, relevant solvent properties including the vaporisation temperature, boiling point, oil solubility, viscosity, specific gravity, polarity, reactivity, purity and stability to heat, light and water should be scrupulously examined. As the solvent is recycled, it must withstand repeated cycles of heating, vaporisation and cooling. Stability is also required to prevent contamination of the substrate and oil with potentially hazardous decomposition products (Glensvig and Pors, 2006). Due to the hazardous nature of hexane, alternative solvents have been tested. For example, Ferreira-Dias *et al*. (2003) evaluated how feasible it is to replace *n*-hexane as solvent, with ethanol for the oil extraction process from *Quercus suber* fruits.

Table 12: Summary of popular oil extraction techniques

Oil extraction methods	Advantages	Disadvantages	References
Cold pressing	No degradation of oil characteristics	Low oil recovery	Terata *et al*., 2010; Ogunsina *et al*, 2014
Heat pressing	High oil recovery	Problematic temperature control; removal of some important oil properties	Zhu *et al*., 2013; Toda *et al*., 2016
Expeller pressing	Small amount of solvent used; not capital-intensive	Low oil yield recovery; pre-press stage has to be applied	Zhu *et al*., 2013; Ogunsina *et al*., 2014
Supercritical fluid	Very good selectivity in comparison to classic organic solvents; convenient critical temperature of 31°C	High cost equipment; skilled operational requirements	Sajfatara *et al*., 2010; Zhu *et al*., 2013
Ultrasound assisted	Environmentally friendly; lower energy	Loss of efficiency during the cavitation process, if ultrasound energy decreases	Upadhyay *et al*., 2012; Shao, 2013
Steam distillation	Simple temperature control; preservation of botanical oils	High cost equipment; skilled operational requirements	Tamini et al., 2008; Ogunsina *et al*., 2014
Soxhlet	Mechanically gentle process yet quite efficient; elemental sulphur removal simultaneously (activated Cu)	Use of hazardous solvent; long extraction time	Shao et Shen, 2012; Ogunsina *et al.*, 2014

In this study, two different types of solvents were used, namely *n*-hexane and ethanol. Of the three Soxhlet steps, the times for extraction rinsing were the same for both, but the drying stage was shorter for *n*-hexane (Table 13) because it is more volatile than ethanol (vapour pressure of 17.6 kPa in comparison to 7.3 kPa for ethanol at 20°C) (Granero *et al*., 2014; Toda *et al.*, 2016). While *n*-hexane might be characterised by a high stability and a low vaporisation temperature, ethanol can be considered more environmentally friendly then *n*-hexane based on their respective solvent performances and health and safety concerns (Capello, 2007; Ellerman *et al*., 2013).

The extraction was performed using three different solvents to solid ratios (15:1 / 20:1 / 25:1) for each solvent, in order to identify which of these was optimal for the process. The extraction,

rinsing and drying times were based on literature values, and were not varied (Ferreira-Dias *et al*., 2003; Zhu *et al.*, 2013).

Table 13: Duration of steps and solvent to solid ratios applied for oil extraction using ethanol and n-hexane

Steps	**Soxhlet with ethanol**	**Soxhlet with *n*-hexane**
Extraction (min)	180	180
Rinsing (min)	10	10
Drying (min)	20	5
Total time	**205**	**190**
Solvent to solid ratio	15:1 / 20:1 / 25:1	15:1 / 20:1 / 25:1

The most significant factor affecting solvent-based oil extraction efficiency is the type of solvent. The sample preparation technique, the duration of extraction, and general operating conditions related to the equipment and material inputs are also considered as important. For example, if samples contain water, it can prevent the dissolution process of oils into the solvent. (Gildemeister *et al., 2*003). In addition, water-soluble components such as urea or carbohydrates may be co-extracted with the fat (Toda *et al.*, 2016). In this study, the best total fat yields from OWS were obtained at solvent to solid mass ratios of 20:1 and 25:1 for *n*-hexane and ethanol respectively (depending on the degree of solubility) (bold in Table 14). The fat in the OWS extracts was also characterised: saturated fat (S Fat), monounsaturated fat (MU Fat) and poly-unsaturated fats (PU Fat) using GC-FID (Table 14).

Table 14: Fatty acid profile and composition in oil extracted from oilseed wastewater sludge with different ratios of solvents to solids

Solvent ratio (v/v)	**T fat (wt.%)**	**S Fat (wt.%)**	**MU Fat (wt.%)**	**PU Fat (wt.%)**
Ethanol (15:1)	76.19 ± 1.43	C14:0 = 0.31 ± 0.36 C16:0 = 11.63 ± 1.24 C18:0 = 5.35 ± 0.99 C20:0 = 1.82 ± 1.11 C22:0 = 0.91 ± 1.21 **Total SFat = 18.23 ± 2.09**	C16:1 = 0.18 ± 1.02 C18:1 = 43.28 ± 1.35 C20:1 = 0.90 ± 0.18 C22:1 = 0.22 ± 0.08 **Total MUFat = 44.58 ± 1.77**	C18:2n-6 = 12.47 ± 0.91 C20:3n-3 = 5.96 ± 0.05 **Total PUFat = 18.43 ± 0.56**

Results are expressed as averages ± standard deviation (*n*=3) T fat = total fat S fat = saturated fat MU fat=monounsaturated fat PU fat=polyunsaturated fat

Table 15: Fatty acid profile and composition in oil extracted from oilseed wastewater sludge with different ratios of solvents to solids (Continued…)

Solvent ratio (v/v)	T fat (wt.%)	S Fat (wt.%)	MU Fat (wt.%)	PU Fat (wt.%)
Ethanol (20:1)	81.41 ± 1.65	C14:0 = 0.89 ± 0.37 C16:0 = 10.68 ± 1.04 C18:0 = 6.01 ± 1.36 C20:0 = 1.44 ± 0.10 C22:0 = 1.12 ± 0.09 **Total SFat = 20.14 ± 0.97**	C16:1 = 0.05 ± 1.33 C18:1 = 42.85 ±1.07 C20:1 =1.19 ± 0.09 C22:1 = 0.26 ± 0.85 **Total MUFat = 44.35 ± 1.93**	C18:2n-6 = 13.11 ± C20:3n-3 = 5.96 ± **Total PUFat = 18.36 ± 1.90**
Ethanol (25:1)	84.16 ± 1.22	C14:0 = 0.41 ± 1.22 C16:0 = 11.20 ± 1.17 C18:0 = 5.71 ± 0.04 C20:0 = 1.88 ± 2.11 C22:0 = 0.83 ± 2.78 **Total SFat = 20.03 ± 3.11**	C16:1 = 0.32 ± 1.51 C18:1 = 43.28 ± 2.01 C20:1 =1.51 ± 0.07 C22:1 = 0.23 ± 0.74 **Total MUFat = 45.34 ± 0.88**	C18:2n-6 = 12.89 ± 0.20 C20:3n-3 = 5.90 ± 1.25 **Total PUFat = 18.79 ± 1.67**
***n*-hexane (15:1)**	88.12 ± 1.87	C14:0 = 0.27 ± 1.00 C16:0 = 10.21 ± 0.74 C18:0 = 4.65 ± 1.85 C20:0 = 1.02 ± 1.82 C22:0 = 0.30 ± 0.11 **Total SFat = 16.45 ± 1.56**	C16:1 = 1.89 ± 2.46 C18:1 = 43.73 ± 0.91 C20:1 =2.30 ± 1.03 C22:1 = 0.42 ± 2.81 **Total MUFat = 48.34 ± 3.06**	C18:2n-6 = 14.24 ± 1.09 C20:3n-3 = 8.18 ± 1.78 **Total PUFat = 22.42 ± 2.45**
***n*-hexane (20:1)**	92.05 ± 2.39	C14:0 = 0.32 ± 0.41 C16:0 = 10.13 ± 0.90 C18:0 = 5.66 ± 0.11 C20:0 = 1.74 ± 1.61 C22:0 = 1.26 ± 1.02 **Total SFat = 19.11 ± 1.72**	C16:1 = 1.04 ± 1.80 C18:1 = 48.35 ± 0.22 C20:1 =1.59 ± 0.09 C22:1 = 0.29 ± 1.04 **Total MUFat = 51.27 ± 1.41**	C18:2n-6 = 14.02 ± 1.55 C20:3n-3 = 5.96 ± 0.44 **Total PUFat = 19.34 ± 2.14**

Results are expressed as averages ± standard deviation (*n*=3) T fat = total fat S fat = saturated fat MU fat=monounsaturated fat PU fat=polyunsaturated fat

Table 16: Fatty acid profile and composition in oil extracted from oilseed wastewater sludge with different ratios of solvents to solids (Continued…)

Solvent ratio (v/v)	T fat (wt.%)	S Fat (wt.%)	MU Fat (wt.%)	PU Fat (wt.%)
***n*-hexane (20:1)**	92.05 ± 2.39	C14:0 = 0.32 ± 0.41 C16:0 = 10.13 ± 0.90 C18:0 = 5.66 ± 0.11 C20:0 = 1.74 ± 1.61 C22:0 = 1.26 ± 1.02 **Total SFat = 19.11 ± 1.72**	C16:1 = 1.04 ± 1.80 C18:1 = 48.35 ± 0.22 C20:1 =1.59 ± 0.09 C22:1 = 0.29 ± 1.04 **Total MUFat = 51.27 ± 1.41**	C18:2n-6 = 14.02 ± 1.55 C20:3n-3 = 5.96 ± 0.44 **Total PUFat = 19.34 ± 2.14**
***n*-hexane (25:1)**	89.36 ± 1.92	C14:0 = 0.50 ± 1.55 C16:0 = 10.77 ± 1.23 C18:0 = 5.09 ± 0.88 C20:0 = 1.52 ± 0.12 C22:0 = 0.88 ± 0.05 **Total SFat = 20.12 ± 0.85**	C16:1 = 0.96 ± 2.08 C18:1 = 49.62 ± 1.64 C20:1.09 ± 2.17 **Total MUFat = 53.71 ± 2.01**	C18:2n-6 = 13.09 ± 1.99 C20:3n-3 = 5.13 ± 0.23 **Total PUFat = 18.22 ± 1.33**

Results are expressed as averages ± standard deviation (*n*=3) T fat = total fat S fat = saturated fat MU fat=monounsaturated fat PU fat=polyunsaturated fat

An increase in ethanol to solid ratio slightly increased the oil extraction yield which led to a maximum of 92% fat content when using a solvent ratio of 20:1 (*n*-hexane/wastewater sludge), as shown in Table 14. This could have been due to the rate of the chemical reaction and diffusion coefficient at which the driving force of the process increased (Gildemeister *et al., 2*003).

With *n*-hexane, the decrease in extraction efficiency between a ratio of 20:1 and 25:1 may have been due to the formation of complexes between fatty acids and carbohydrate breakdown components at higher solvent concentrations that inhibited the extraction process (Al-Hamamre *et al*., 2012).

No clear relationship between the molecular weight of both solvents (ethanol: 46.07 $gmol^{-1}$ and *n*-hexane: 86.18 $gmol^{-1}$) and extraction efficiency was demonstrated. This suggests that the penetration of the solvent molecules into the OWS was not limited by the size of the molecule. In addition, several researchers, including Kondamudi *et al.* (2008) and Caetano *et al.* (2012) have demonstrated that the degree of polarity of a molecule is positively related to

the oil extraction efficiency in wet samples. This could explain why the oil yield obtained with *n*-hexane was higher than with ethanol (which is less polar).

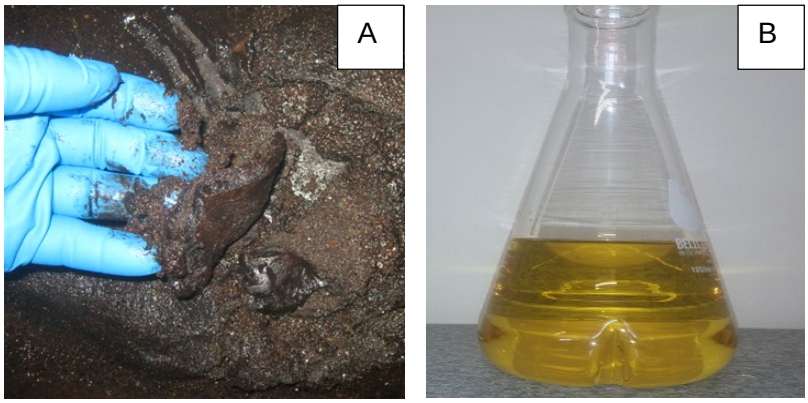

Figure 17: Oilseed wastewater sludge (A) and extracted and purified oil (B)

The composition of food grade canola oil makes it an ideal feedstock for biodiesel production; apart from the favourable fat content, it has a low cloud point, so it gels at lower temperatures than many other feedstocks (Demirbas, 2016). The specific gravity, viscosity and refractive index, as a qualitative measure of the purity of the extracted oil compared favourably with a food grade canola oil sample (Table 15). The kinematic viscosity of both the extracted oil from OWS and food grade canola oil samples (at 20°C), were within the recommended range of between 75 and 90 mm^2/s for monounsaturated fats (Tinprabatha *et al*., 2016).

The refractive index and specific gravities were very similar (0.89 g/cm^3 and 1.42 mm^2/s at 20°C) to those reported by Barrot and Andher (2015) in their study on the physico-chemical properties of several edible oils. The comparable composition to food grade canola oil provides a substantive motivation for the use of the OWS extract for biodiesel production.

Table 17: Properties of oil obtained from soxhlet and pure commercial canola oil

Properties	**Extracted oil from OWS**	**Food grade canola oil**
Specific gravity (g/cm^3)	0.95 ± 0.78	0.91 ± 0.92
Viscosity (mm^2/s) at 20°C	91.2 ± 1.01	78.4 ± 1.22
Refractive index at 20°C	1.49 ± 0.85	1.46 ± 0.77

Results are expressed as averages ± standard deviation (*n*=3)

4.2 Bioethanol production

After oil extraction the second step was to assess the feasibility of producing bioethanol from the dry pre-treated residue left after extraction of oil (DPS) from OWS (red highlighted, Figure

18). Canola fines could be used as a potential feedstock to produce bioethanol (Figure 18), but this has been well investigated previously (e.g. Agu *et al*., 2017; Iroba and Tabil, 2013).

The rationale is that bioethanol produced on-site could be used in biodiesel production as part of an integrated process.

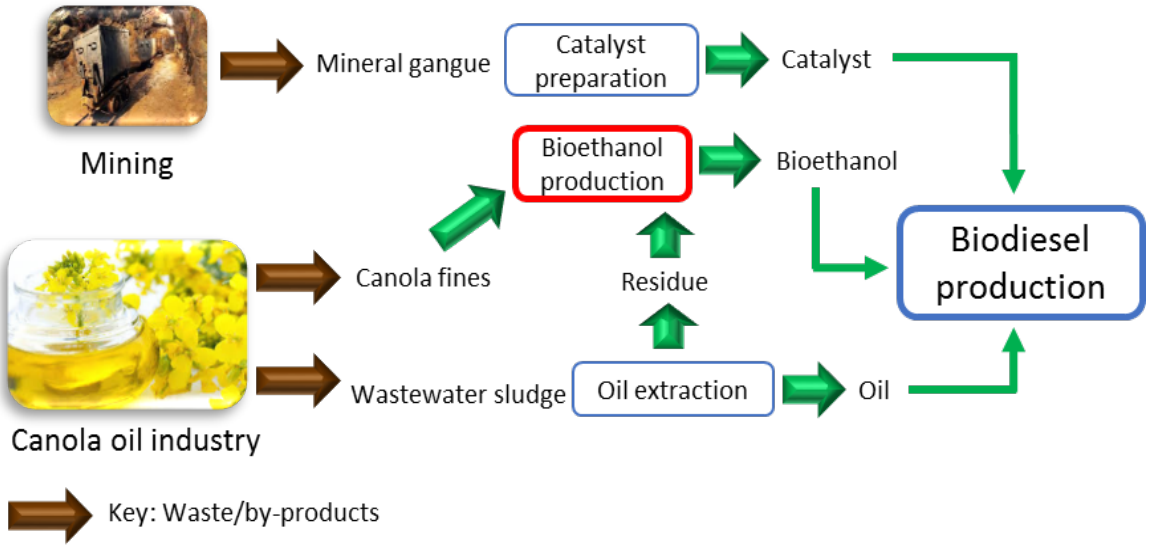

Figure 18: Flow diagram showing the relationship of bioethanol to the other primary study objectives (Objective 2: bioethanol production)

4.2.1 Pre-treatment and hydrolysis of oilseed wastewater sludge

Lignin from fines generated during crushing and expelling of oilseeds may enter the wastewater, but lignin may be broken down during downstream processes. Measurements of lignin in different wastewater streams was beyond the scope of this feasibility study. No conventional pretreatment to break down lignin was carried out. In a screening study, it was found that the pretreatment that was conducted (washing in hot water, filtering and drying) did not significantly change the sugar yields of the acid or enzyme hydrolysates (Table 16).

Table 18: Sugar concentrations in selected (maximum concentrations) hydrolysates from pre-treated and non-pre-treated residues of oilseed wastewater sludge after oil extraction

	Non-pre-treated (ROE)		**Pre-treated (DPS)**	
Hydrolytic agent	**0.4M H_2SO_4**	**25 FPU enzyme**	**0.4M H_2SO_4**	**25 FPU enzyme**
Cellobiose (mg/L)	621.7±0.56	1121.7±0.44	633.1±0.99	1258.8±0.08
Glucose (mg/L)	699.3±1.45	1009.2±0.76	641.8±1.11	1599.5±0.25
Xylose (mg/L)	638.2±0.12	988.1±0.09	829.3±0.23	1008.4±1.32
Fructose (mg/L)	231.6±0.17	565.4±1.03	397.4±0.51	477.6±0.61

Results are expressed as averages ± standard deviation (*n*=3)

4.2.2 Hydrolysis process

- **Acid hydrolysis**

This hydrolysis process was conducted on the DPS at different dilute sulphuric acid concentrations, at the same temperature, and reaction times of 1 h and 2 h (Section 3.2.2.2). The change in acid concentration was investigated to improve fermentable sugar recovery. It was found that the concentration of glucose (Figure 19A), cellobiose (Figure 19B), fructose (Figure 19C) and xylose (Figure 19D) generally increased with each increase in acid concentration from 0.1 M to 0.3 or 0.4 M, then decreased thereafter. This may have been because hydrolysis at each concentration was carried out at the same temperature, but hydrolysis at lower acid concentrations (0.4 - 1 M) is more efficient at higher temperatures (up to 70°C) than highly concentrated acid hydrolysis (≥1.2 M), which operates at relatively low temperatures (below 40°C) (Weib and Alt, 2017; Kumar *et al.*, 2015; Iroba and Tabil, 2013). The highest concentrations of glucose (874 mg/L (0.4 M H_2SO_4)) and cellobiose (781 mg/L (0.3 M H_2SO_4)) were measured after 2 h hydrolysis, while the highest concentrations of xylose (994 mg/L (0.5M H_2SO_4)) and fructose (0.4M H_2SO_4) were measured after 1 h hydrolysis (Figure 19). These differences may have been due to preferential microbial degradation of released sugars, as these experiments were not conducted in a sterile environment.

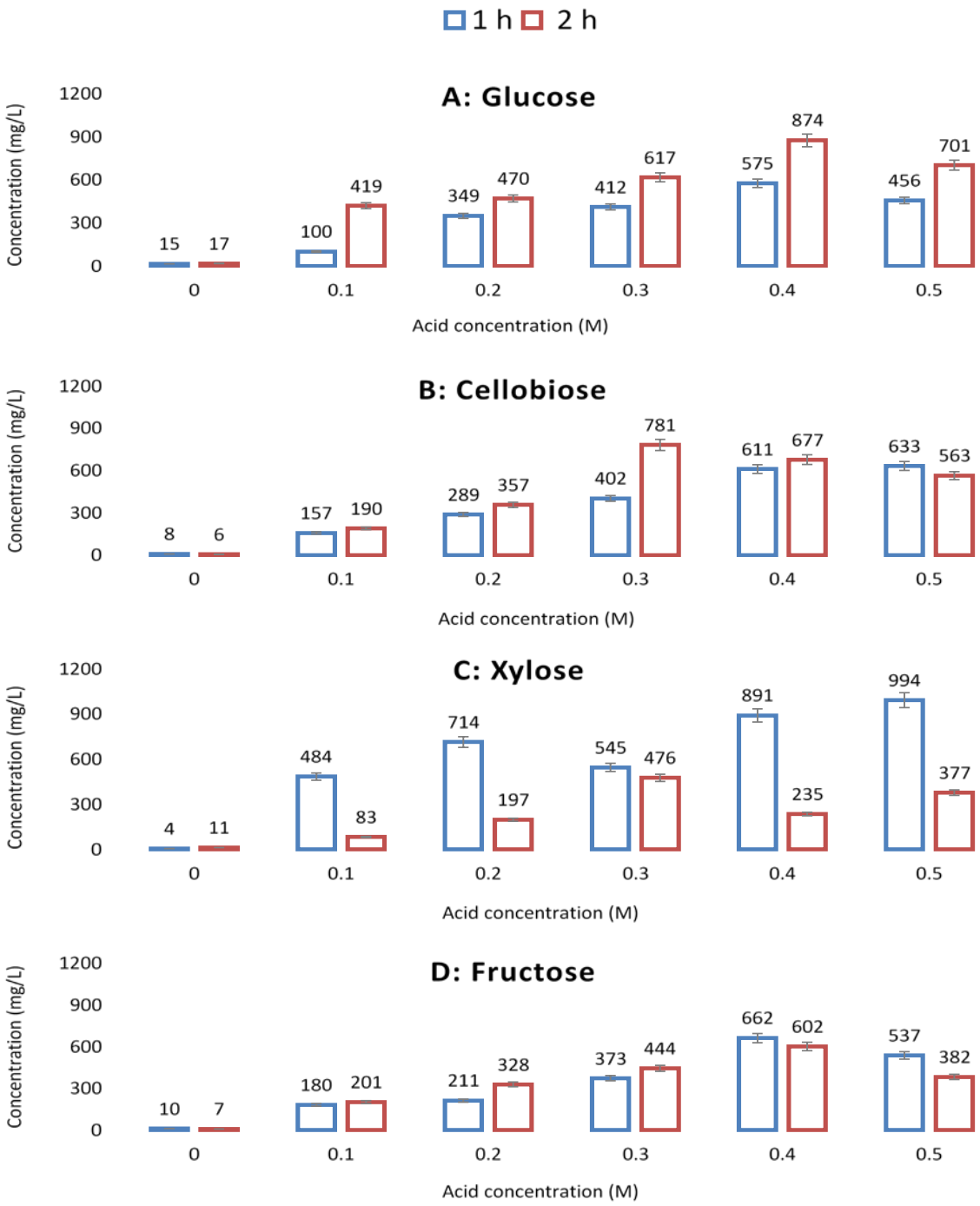

Figure 19: Comparison of selected sugar concentrations (A: Glucose / B: Cellobiose / C: Fructose / D: Xylose) from dried pre-treated substrate hydrolysed with different concentrations of sulphuric acid for 1 and 2 h hydrolysis process at different H_2SO_4 concentration. Error bars represent the standard deviation from the mean (n = 3)

Generally, results of research on the dilute acid hydrolysis of different lignocellulosic materials have defined optimal process conditions: temperature 60-150°C, sulphuric acid concentration

0.5-1M, and reaction time from 10 min to 30 h (Lavarack *et al*., 2002, Hon *et al*., 2001 and Garotte *et al*., 2001). It was concluded that acid hydrolysis of ROE to generate sugar for bioethanol production would not be viable due to the low sugar yield obtained.

- **Enzymatic hydrolysis**

As per the process methodology described in Section 3.2.2.2, enzymatic hydrolysis was performed to investigate the impact of enzyme loadings on the enzymatic conversion of ROE into fermentable sugars. The temperature during this process was 50°C and the pH set to 4.8. These criteria were adapted from literature in order to be within the optimal activity ranges of the enzymes (Gellerstedt *et. al.*, 2009). Studies determining hydrolysis rates under different enzyme loadings provide maximum insight into hydrolysis patterns with different raw materials (Gao *et al.,*2013; Lehtio *et al.*, 2003). The maximum concentrations of glucose (2773 mg/L), cellobiose (2403 mg/L), xylose (1088 mg/L) and fructose (1085 mg/L) were all found after 1 h hydrolysis (Figure 20 A-D). With the exception of xylose, where the maximum concentration was obtained at an enzyme loading of 25 FPU/g cellulose, the optimal enzyme loading was 20 FPU/g cellulose. The substrate was not pre-sterilised, and the concentrations of all sugars decreased at all enzyme loadings, either between 1-2 h or between 2-3 h (Figure 20). This strongly suggested biotic and/or biotic degradation of sugars within the test flasks as described by Tan and Lee (2014). This may have been confounded by enzyme substrate inhibition with time.

Although a low yield of fermentable sugars was observed (Table 17), it was concluded that for sugar conversion, enzymatic hydrolysis was more favourable than acid hydrolysis of this particular substrate.

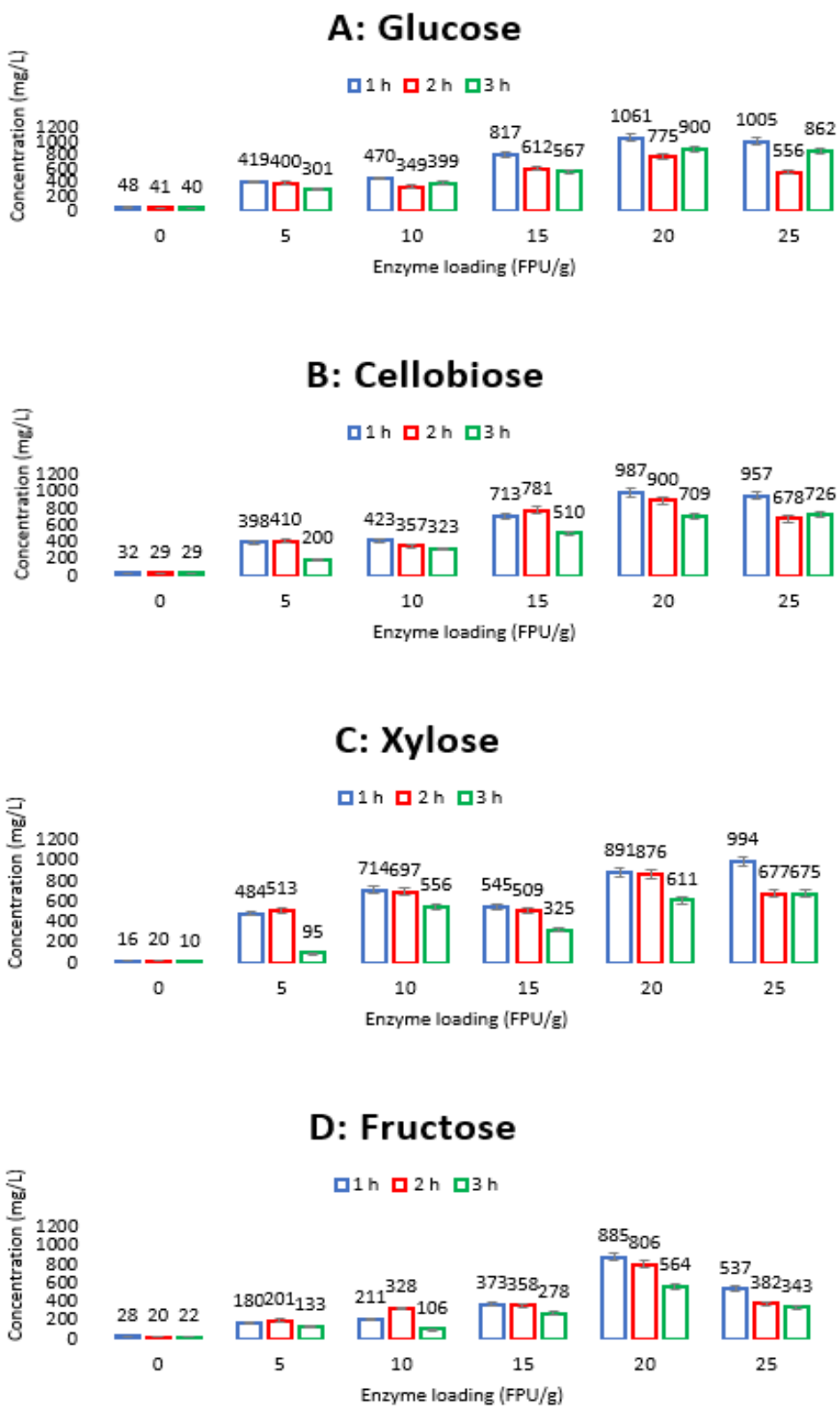

Figure 20: Comparison of selected sugar concentrations (A: Glucose / B: Cellobiose / C: Fructose / D: Xylose) from dried pre-treated substrate hydrolysed with different enzyme loading for 1, 2 and 3 h hydrolysis process at different cellulase loadings. Error bars represent the standard deviation from the mean (n = 3)

The results did not compare favourably with studies utilising lignocellulosic substrates i.e. the sugar concentrations were notably lower (Section 2.4). For instance, Lavarack *et al.* (2002) used cellulase to hydrolyse sorghum bagasse and triticale straw, and obtained xylose concentrations of 10.31 g/L of xylose, and 0.62 g/L of both cellobiose and glucose. Furthermore, Gao *et al.* (2013) investigated the conversion from sugarcane bagasse and triticale feedstock using a combination of enzymes under same conditions, and obtained 18.4 g/L and 8.99 g/L glucose respectively. This justifies the importance of feedstock evaluation for ethanol production by using different or a combination of different enzymes, through composition analyses, response to pre-treatment and digestibility of enzymes employed (Herrera *et al*., 2016 and Rajan *et al*., 2004). Typical lignocellulosic pre-treatment will yield anywhere from 10-60 g/L fermentable sugars (Robinson *et al*., 2003). This concentration is low compared to a typical starch fermentation (100-300 g/L) (Robinson *et al*., 2003). Methods exist for concentrating the sugars in the hydrolysate and are focused on the removal of the water from the feed stream. Evaporation has yielded glucose concentrations of 170 g/L (Herrera *et al*., 2016). The main issue with concentrating of sugars in the hydrolysate can be the presence of toxins that could also be concentrated, making fermentation that much more difficult (Robinson *et al*., 2003). Apart from the composition of the ROE, another possible reason for the low sugar yield could be due to the lack of stirring mechanism during the treatment which could imply that might have deposited in the vessel, hence forming a wet cake and hindering enzyme penetration.

Table 19: Comparison of results with literature values

Main raw materials	Process conditions	Average (maximum) sugar concentrations (g/L)	References
Grasses/Tropical legumes	Reaction temperature: 50°C Reaction time: 2 h 0.7M H_2SO_4	Cellobiose: 55 Glucose: 71 Xylose: 32 Fructose: 16	Kagan *et al.* (2014)
Maize silage/Cereal grains	Reaction temperature: 75°C Reaction time: 4 h 0.5M H_2SO_4	Cellobiose: 39 Glucose: 65 Xylose: 51 Fructose: 37	Weib and Alt (2017)
Sugarcane bagasse	Reaction temperature: 90°C Reaction time: 2 h 0.5M H_2SO_4	Cellobiose: 28 Glucose: 47 Xylose: 11 Fructose: 25	Kumar *et al., 2*015
DPS (Acid hydrolysis)	Reaction temperature: 70°C Reaction time: 1.5 h 0.4M H_2SO_4	Cellobiose: 0.78 Glucose: 0.87 Xylose: 0.99 Fructose: 0.66	This study
DPS (Enzymatic hydrolysis)	Reaction temperature: 50°C Cellulase: 25 FPU/g Reaction time: 72 h	Cellobiose: 0.98 Glucose: 1.06 Xylose: 0.99 Fructose: 0.88	This study

DPS: dry pre-treated residue of ROE (residues obtained after oil extraction of oil from edible oil wastewater sludge)

To conclude, as a general rule, the conversion of the substrate increases with increase of enzyme concentration/dosage (Herrera *et al*., 2016; Tan and Lee, 2014). However, in this study the conversion was not directly proportional to the augmentation of enzyme loading (Figure 20A-D). It was observed that an increase in enzyme dosage to a maximum of 25 FPU/g only resulted in approximately 25-32% increase in all tested fermentable sugars concentrations for acid hydrolysis, and a maximum of 44% hike in concentration for enzymatic hydrolysis. Furthermore, the sugars' concentration was low when compared to previous studies (Table 17).

4.2.3 Fermentation

To obtain sufficient hydrolysates for fermentation, hydrolysis was repeated using the methods that resulted in the highest sugar yields determined during the original screening studies (Section 4.2.2). The concentrations of sugars obtained for the acid hydrolysis were not notably different (Table 18). However, due to the use of a different commercial enzyme, the sugar yields were significantly higher than those obtained during the screening studies (Table 18), particularly glucose and cellobiose, which increased more than twofold. This was still low in comparison to literature values (Table 17).

The produced acid and enzymatic hydrolysates were fermented with *Saccharomyces cerevisiae* strain MH-1000 ($1.5*10^5$, $2*10^5$, $2.5*10^5$ CFU/mL) using the same methodology.

Table 20: Highest sugar concentration comparison as per the hydrolysis reaction (acid and enzymatic) conditions

	Acid hydrolysis (0.4 M H_2SO_4, 2 h)		**Enzymatic hydrolysis (25 FPU/g, 1 h)**	
	Fermentation	**Screening study**	**Fermentation (Celluclast 1.5 FG cellulase)**	**Screening study (Onozuka RS cellulase)**
Glucose (mg/L)	873.9±1.01	874.3±0.56	986.7±1.42	2772.5±1.00
Cellobiose (mg/L)	781.4±1.24	781.8±1.11	1060.5±0.91	2403.1±1.53
Xylose (mg/L)	993.5±0.54	994.4±1.25	993.6±0.33	1088.3±0.87
Fructose (mg/L)	601.5±1.08	662.3±1.74	884.5±0.75	1084.8±0.59

Results are expressed as averages ± standard deviation (*n*=2)

Only negligible decreases in sugars were noted in the control acid and enzyme hydrolysates that were incubated with no yeast up to 72 h (Figures 21 & 22). In contrast, in the fermentates containing yeast, no glucose, cellobiose or fructose was present after 48 h fermentation (Figures 21 & 22). However, there were only negligible changes in the xylose concentrations after 72 h in the yeast fermentates. These results showed that glucose, cellobiose and fructose, but not xylose, provided growth substrates for *S. cerevisiae* MH-1000. This was expected because it has been determined that glucose and cellobiose are preferential substrates for *S. cerevisiae* MH-1000, for which a model 80% conversion of 40 g/L glucose to ethanol using SSF has been calculated (van Zyl *et al*., 2010). Further, *S. cerevisiae* cannot metabolise xylose (Sluiter *et al*., 2008 and Walker, 2009).

No ethanol was detected in the fermentates of the acid or enzymes hydrolysates after 12 h (data not shown), presumably because the yeast growth was in the lag phase (Phisalophong *et al*., 2006). A maximum of 988 mg/L and 3539 mg/L in ethanol were obtained after 48 h fermentation in the acid and enzyme hydrolysates respectively loaded with $2.0*10^5$ CFU/mL and $2.5*10^5$ yeast cells (Figures 21 & 22). It was assumed that the difference in yeast loading requirements to achieve maximum ethanol generation was because of the different substrate availability (i.e. sugar concentrations) as described by Gomar-Alba *et al.* (2015). In all instances, there was a decrease in the ethanol concentration in the fermentates between 24-48 and/or 48-72 h fermentation, suggesting biodegradation of ethanol as the hydrolysates were not sterilised (Singh *et al.,* 2013; Mohd Azhar *et al.,* 2017).

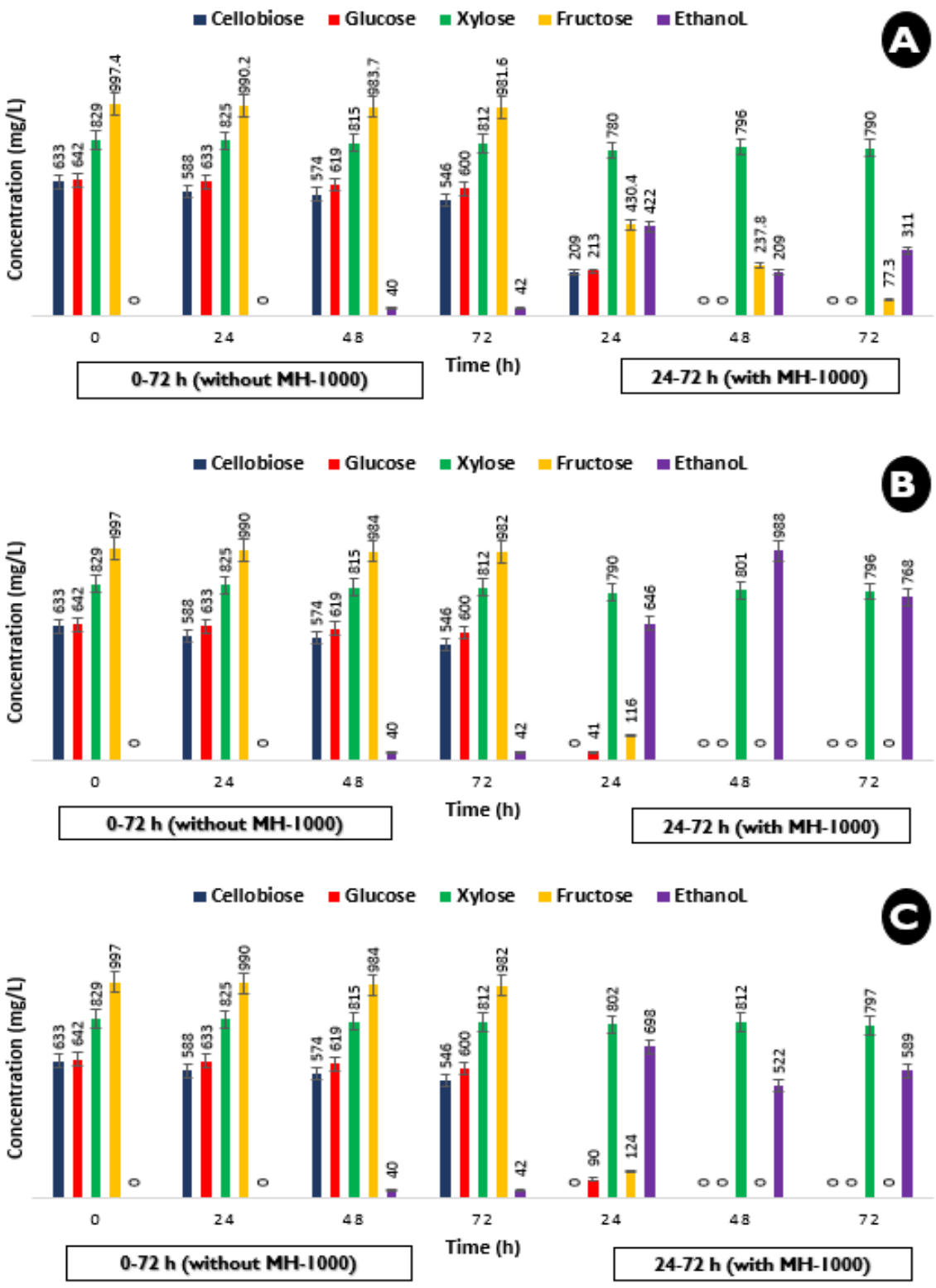

Figure 21: Fermentation results obtained from acid hydrolysates without and with MH-1000 yeast (A: $1.5*10^5$ CFU/mL yeast loading / B: $2*10^5$ CFU/mL yeast loading / C: $2.5*10^5$ CFU/mL yeast loading) for a period of 72 h. Error bars represent the standard deviation from the mean (n = 3).

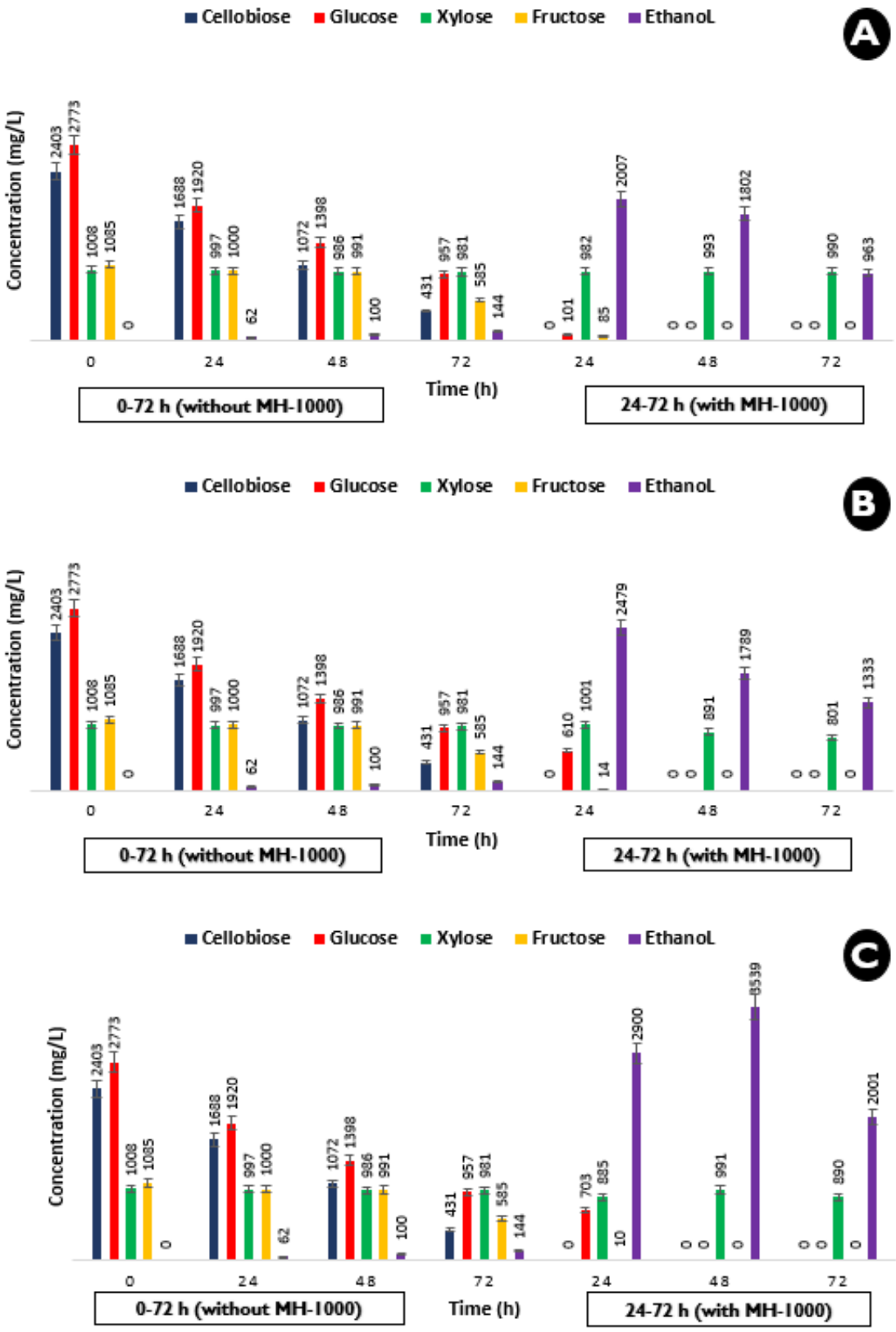

Figure 22: Fermentation results obtained from enzymatic hydrolysates without and with MH-1000 NCP yeast (A: 1.5*10^5 CFU/mL yeast loading / B: 2*10^5 CFU/mL yeast loading / C: 2.5*10^5 CFU/mL yeast loading) for a period of 72 h. Error bars represent the standard deviation from the mean (n = 3).

The final ethanol concentration was very low yield when compared with other studies. For example, Zabed *et al.* (2014) obtained an average of 68 g/L and 17.5 g/L ethanol in batch and continuous systems containing sugar juice as a substrate; Boulbaba *et al.* (2013) obtained 25% (v/v) ethanol after 72 h at 30°C from date juice containing an initial 200 g/L sugars (Table 18). It was assumed that only negligibly higher concentrations of ethanol from ROE could be achieved by optimising temperature, pH, and agitation rate (Zabed *et al.,* 2014). Firstly, the fermentation temperature of 30°C that was applied was based on literature values that should allow good growth of yeast, but not inactivate enzymes (Singh *et al.,* 2013). Secondly, the pH at which the ethanol production was conducted was adjusted to 6. This was since the rate of ethanol production is reduced by the carbon dioxide generated into the system at lower pH, which encourages the production of acid instead of alcohol (Tan and Lee, 2014; Berg, 2007). Thirdly, mass transfer limitations for fermentation can be decreased by stirring (Tan and Lee, 2014), and in this study, flasks were rotated on an orbital shaker at 100-160 rpm. Most importantly, the sugar concentrations in the hydrolysates were low (Section 4.2.2). Generally, the maximum rate of ethanol production is achieved with sugars at a concentration of 150 g/L (Liu and Shen, 2008). High ethanol productivity and yield in batch fermentation can be obtained by using higher initial sugar concentration. However, longer fermentation times are required, and the cost of recovery is higher (Zabed *et al*., 2014).

To determine whether the low ethanol concentration in the fermentate was indeed mainly due to low substrate availability, a material balance was linearly computed as a combination of stoichiometric equations for the conversion of the measured sugars into ethanol (Eq.11)., which was generated by summation of substrates' and products' stoichiometric coefficients with adequate proportionalities defined by the individual reaction rates. The fermentation efficiencies for both hydrolysates were calculated as follows:

***Glucose*: $C_6H_{12}O_{6\,(aq)} \longrightarrow 2C_2H_5OH_{\,(aq)} + 2CO_{2\,(g)}$**

***Cellobiose:* $C_{12}H_{22}O_{11\,(aq)} + H_2O_{\,(l)} \longrightarrow 4C_2H_5OH_{\,(aq)} + 4CO_{2\,(g)}$**

***Fructose:* $C_6H_{12}O_{6\,(aq)} \longrightarrow 2C_2H_5OH_{\,(aq)} + 2CO_{2\,(g)}$**

***Xylose:* $C_5H_{10}O_{5\,(aq)}$ (No conversion with MH-1000)**

Eq.11

(Average molecular weights: C: 12 g mol^{-1} / H: 1 g mol^{-1} / O: 16 g mol^{-1})

The maximum concentrations of glucose, cellobiose and fructose were converted to molar concentrations.

From acid hydrolysates:

Glucose: $\frac{0.642\ g/L}{180\ g/mol} = 3.56 * 10^{-3} mol/L$ ⟶ ***(X 2)***

Cellobiose: $\frac{0.638\ g/L}{324\ g/mol} = 1.96 * 10^{-3}\ mol/L$ ⟶ ***(X 4)***

Fructose: $\frac{0.997\ g/L}{180\ g/mol} = 5.53 * 10^{-3}\ mol/L$ ⟶ ***(X 2)***

$\boldsymbol{n_{C2H5OH} = 26.02 * 10^{-3}\ mol/L}$, Which gives a total of **1.196 g/L theoretical ethanol**

Hence, the fermentation efficiency being the ratio between the maximum actual and theoretical yield as follows:

$$\frac{\mathbf{0.988\ gL^{-1}}}{\mathbf{1.196\ gL^{-1}}} * \mathbf{100} = \mathbf{88\%}\ \boldsymbol{Efficiency}$$

From enzymatic hydrolysates:

Glucose: $\frac{2.77\ g/L}{180\ g/mol} = 15 * 10^{-3} mol/L$ ⟶ ***(X 2)***

Cellobiose: $\frac{2.40\ g/L}{324\ g/mol} = 7.4 * 10^{-3}\ mol/L$ ⟶ ***(X 4)***

Fructose: $\frac{1.08\ g/L}{324\ g/mol} = 6.02 * 10^{-3}\ mol/L$ ⟶ ***(X 2)***

$\boldsymbol{n_{C2H5OH} = 71.64 * 10^{-3}\ \frac{mol}{L}}$, Which gives a total of **3.3 g/L theoretical ethanol**

Hence, the fermentation efficiency being the ratio between the maximum actual and theoretical yield as follows:

$$\frac{\mathbf{3.5\ gL^{-1}}}{\mathbf{3.3\ gL^{-1}}} * \mathbf{100} = \mathbf{106\%}\ \boldsymbol{Efficiency}$$

The results supported the hypothesis that the low ethanol concentration obtained was due to low concentrations of starting substrate. Lower maximum fermentation efficiency was achieved with the acid enzyme hydrolysates when compared to the enzyme hydrolysates. It has been demonstrated that acid hydrolysates are subjected to make the fermentation very difficult due to the presence of some toxic components.

Furthermore, acid pre-treatment has high capex cost, is conducted under high pressure, and requires neutralisation of the hydrolysate obtained before the fermentation. It is also

characterised by slow cellulose digestion by enzymes, and non-productive binding of enzymes to lignin (Herrera *et al*., 2016 and Laopaiboon *et al.,* 2010).

The anomalous >100% fermentation efficiency of the enzyme hydrolysates may have been due to the presence of other substrates that were not measured, or release of sugars from more complex substrates during the fermentation process. Although low ethanol concentrations were obtained from both hydrolysates, the fermentation process itself was highly efficient, and comparable to previous studies (Table 19).

For instance, Yanzhi *et al.* (2017) investigated the glucose-xylose co-fermentation at high solid loadings with mixed *Saccharomyces cerevisiae* strains from green liquor ethanol-pretreated sugarcane bagasse, and they have obtained higher ethanol yield and concentration (92.80% and 23.22 g/L).

Additionally, Thomsen *et al.* (2005) reported 70% of the theoretical ethanol yield with pre-treated wheat straw and maize silage. Furthermore, the theoretical ethanol yield was calculated and improved with addition of enzymes during the fermentation (cellulases and amylase, depending on the feedstock used).

Table 21: Comparison between ethanol fermentation efficiencies between this study and previous research

Feedstock	Fermentation conditions	EtOH Conc. (g/L)	Fermentation efficiency (%)	References
Sugarcane (*Saccharum officinarnum*)	Batch SSF; Time: 96 h; Temperature: 30°C Yeast: *S. cerevisiae;* (7%v/v loading)	67.9	99%	Zabed *et al.* (2014)
Sugarcane juice	Continuous SSF; Time: 117 h; Temperature: 35°C; Yeast: *S. cerevisiae* (9%v/v loading)	17.5	88%	Zabed *et al.* (2014)
Kunta (a variety of date produced in the region of Gabès (Tunisia)	Batch SSF; Time: 72 h; Temperature: 32°C; Yeast: *S. cerevisiae* (7%v/v loading)	25	86%	Boulbaba *et al.* (2013)
Green-liquor bagasse	SSF; Time: 72 h; Temperature: 35°C; Yeast: *S. cerevisiae* (5%v/v loading)	23.2	90%	Yanzhi *et al.* (2017)
Edible oil wastewater sludge	Batch SSF; Time: 72 h; Temperature: 30°C; Yeast: *S. cerevisiae* (5%v/v loading)	3.5	88% (acid hydrolysates; >100% (enzymatic hydrolysates;	This study

4.2.4 Distillation

To increase the ethanol yield, the fermentates were distilled and the ethanol concentrations were measured in the distillates (Table 20). The main purpose behind this was to try to increase the concentration of ethanol to a suitable level for use in biodiesel generation from the oil extracted from edible oil wastewater sludge in the presence of a nano-catalyst.

The ethanol concentration of the acid and enzyme hydrolysates increased by 4 – 7-fold in a single distillation step, with a maximum concentration of 6.7 g/L ethanol from the enzymatic hydrolysates (Table 19) being achieved. This concentration was still very low when compared to the ethanol requirement for the transesterification reaction (Fukuda *et al.,* 2001; Lotero *et al*., 2005; Fadhil, 2013; Thangaraj *et al*., 2014). Nevertheless, this study demonstrated the feasibility of producing ethanol from edible oil wastewater sludge as a proof of concept.

Table 22: Increase in ethanol concentration using a single distillation step

Sample	Type of fermentation	Before distillation (g/L)	After distillation (g/L)	Fermentation conditions
Acid hydrolysates-Control (without MH-1000)	SHF	0.06±0.31	1.0±1.07	Temperature: 30°C; pH: 6; Stirring rate: 100-160 rpm
Enzymatic hydrolysates-Control (without MH-1000)	SHF	0.19±0.25	2.1±0.05	Temperature: 30°C; pH: 6; Stirring rate: 100-160 rpm
Acid hydrolysates-Optimum (with MH-1000)	SHF	0.5±0.09	3.3±0.17	Temperature: 30°C; pH: 6; Stirring rate: 100-160 rpm
Enzymatic hydrolysates-Optimum (with MH-1000)	**SHF**	**3.5±1.51**	**6.7±0.11**	Temperature: 30°C; pH: 6; Stirring rate: 100-160 rpm

Results are expressed as averages ± standard deviation (*n*=2)

4.3 Catalyst preparation

Once the oil had been extracted and the bioethanol prepared, the alkaline gangue was then used to synthesise the nano-magnetic catalyst to be employed in the transesterification as described on the figure below, and highlighted in red on the block flow diagram (Figure 23).

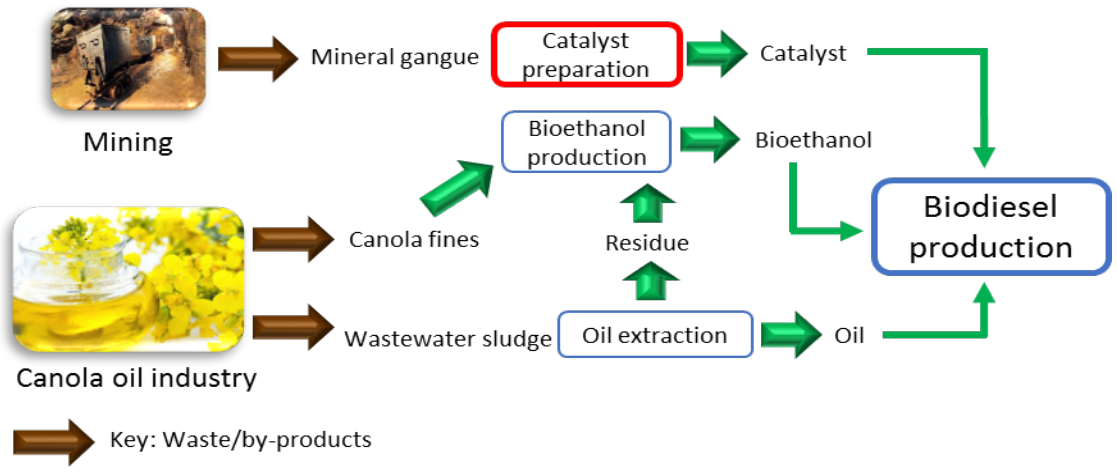

Figure 23: Flow diagram showing the relationship of the catalyst to the other primary study objectives (Objective 3: catalyst preparation)

The catalyst was prepared from unrefined dolomite, a double carbonate of calcium and magnesium, which is considered as an alkaline gangue in the mineral processing process, especially in the concentration process of cupriferous minerals.

As indicated in the introduction (Section 1), the current study aimed to produce biodiesel through a heterogeneous catalytic process. The catalyst should be a nanoparticle to tackle the issue of mass transfer as observed by Alhassan *et al*. (2015) and Di Serio *et al.* (2008), as well as the issue of energy consumption (Utama *et al.,* 2014 and Kouzu *et al.,* 2007), and water usage involved (Wen *et al.*, 2010) during the separation process and recycling step of the catalyst used.

The nano-catalysts prepared (co-precipitation and sol-gel techniques) were characterised for the BET surface area (Brunauer-Emmett-Teller), the BJH (Barrett-Joyner-Halenda) pore and volume size, the TEM (transmission electron microscopy), the SEM (scanning electron microscopy) and the EDS (energy-dispersive X-ray spectroscopy) to support their performance in terms of producing biodiesel from the edible oil wastewater sludge and ethanol under the same conditions. All experiments were done in triplicate.

Three catalysts were prepared by co-precipitation method based on different hematite-double nitrate of calcium and magnesium ratios ($(Fe_3O_4)/(Ca,Mg)(NO_3)_2$), and samples were labelled accordingly as $CMCO_1$ (1:2); $CMCO_2$ (1:3) and $CMCO_3$ (1:4).

As for the sol-gel method, three catalysts were prepared based on different ethylene glycol dosages, and samples were labelled accordingly as $CMSG_1$ (15 ml); $CMSG_2$ (20 ml); $CMSG_3$ (25 ml). The optimum (in terms of biodiesel yield) was supported by zerovalent iron nanoparticles (ZVINPs) on three ZVNIPs/$CMSG_{opt}$ ratios (2:1 / 3:1 and 4:1).

4.3.1 Brunauer-Emmett-Teller (BET) surface area analysis and Barrett-Joyner-Halenda (BJH) pore size and volume analysis (Figures 24-29)

The BET analyses has been used to provide information on the material's specific surface area. This was performed by an evaluation of the catalyst with nitrogen multilayer adsorption, measured as a function of relative pressure using a fully automated analyser. The BJH analysis was also employed to determine pore area and specific pore volume using adsorption and desorption techniques. The BET technique characterises pore size distribution independent of external area due to particle size of the sample, enabling full understanding of the effect of surface porosity and particles size of CMCO catalyst.

The BET technique encompasses external area and pore area evaluations yielding a maximum of 46.3 m^2/g for the catalyst with hematite-Ca, $Mg(NO_3)$ ratio of 1 to 3 (Catalyst $CMCO_2$).

From the indicated results (Figures 24A, 24B, 26A and 26B), it can be observed that the increase in nitric acid to modify the ratio nitrate/hematite slightly improves the surface area of all catalysts, and at the 1:5 ratio the sample could not reach the margin of 40 m^2/g, which in other words will eventually affect the performance of the catalyst on the issue of mass transfer. Previous researchers such as Moreno *et al*. (2016) and Lu *et al.* (2015) prepared zirconium oxide catalyst supported by a magnetic core, and reported the hematite/nitrate ratio as an influential parameter in the catalyst quality of nanomaterial synthesised mainly in mesoporous and microporous conditions.

As described in figure 25, sample $CMCO_2$ exhibited a good surface area; its BJH adsorption cumulative surface area of pores with a width of 52.6 m^2/g and the BJH desorption cumulative surface area of pores generated a sample width of 52.7 m^2/g.

As for the pore size, the adsorption average pore width (4V/A by BET) was 169.3 Å, with the BJH adsorption average pore width (4V/A): 146.7 Å and the BJH desorption average pore width (4V/A): 148.5 Å. These data obtained were quite in line with several studies done on nanocatalysts to be used in the transesterification process to produce biodiesel (Demirbas, 2016; Di serio *et al*., 2008).

For instance, Xie and Fan (2014) had synthesised solid base catalyst and nanoparticles using the co-precipitation method to achieve maximum surface area of 61 m^2/g. A surface area of 59 m^2/g was obtained by Rashtizadeh *et al.* (2014) and Teo *et al*. (2014) when attempting to prepare nanocomposite and mesoporous materials mainly containing calcium oxide. In the current study, the specific BET were calculated and the BJH average (adsorption and desorption) pore diameter were calculated together with the isothermal plots using the Harkins and Jura thickness equation with t-plot and the catalyst size distribution.

The same technique was used for CMSG samples as shown of figures 24-26. The results have indicated that $CMSG_3$ was the optimum with 25 ml ethylene glycol dosage. This particular sample had a cumulative specific surface area of 58.7 m^2/g and the BJH Desorption cumulative specific surface area was 58.9 m^2/g.

The adsorption average pore width by BET was 169.3 Å for $CMCO_2$ with a BJH adsorption average pore width of 145.7 Å and a BJH desorption average pore width of 148.5 Å, compared to 155.1 Å for $CMSG_3$ with BJH Adsorption average pore width of 135.6 Å and BJH desorption average pore width of 153.9 Å.

The calcination temperature in both cases was constant, which is related to particle growth. The effect of synthesis methods on the surface area of CMCO and CMSG was remarkable,

with $CMSG_3$ having a higher surface area as compared to the $CMCO_2$ sample. It should be noted that the sample prepared by precipitation process was obtained without using structure-directing reagents such as surfactants, which tends to cause an expansion of the final catalyst's structure, hence leading to obtain a much higher surface area.

In order to investigate further in terms of improving the catalytic properties of CMSG samples, ZVINPs was employed to support the reusability of the catalyst. The preparation of the hydride catalyst was done based on CMSG/ZVINPs ratios of 2:1, 3:1 and 4:1.

The performance of all these catalysts was evaluated in the biodiesel production process from edible oil wastewater sludge under same reaction's conditions.

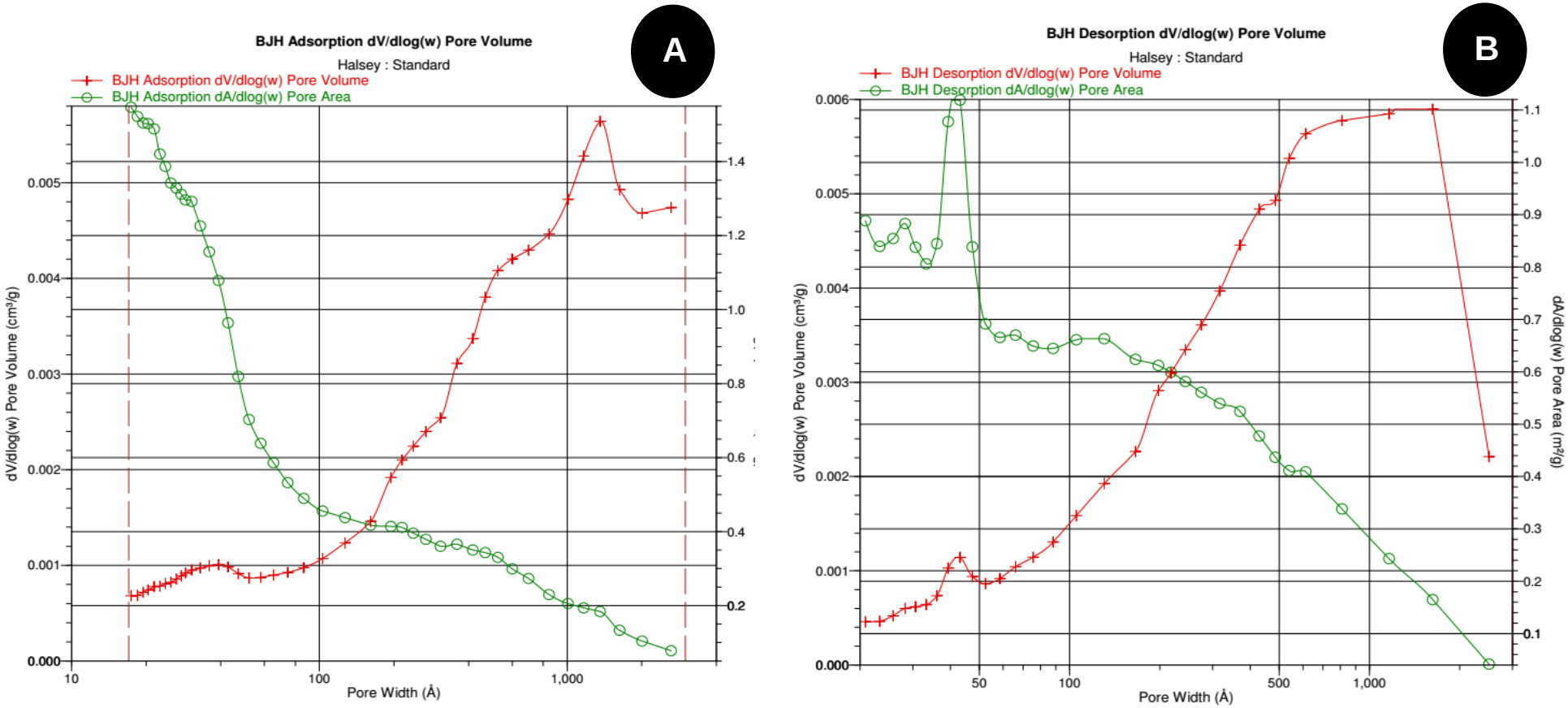

Figure 24: $CMCO_1$ BJH (A) Adsorption - (B) Desorption results

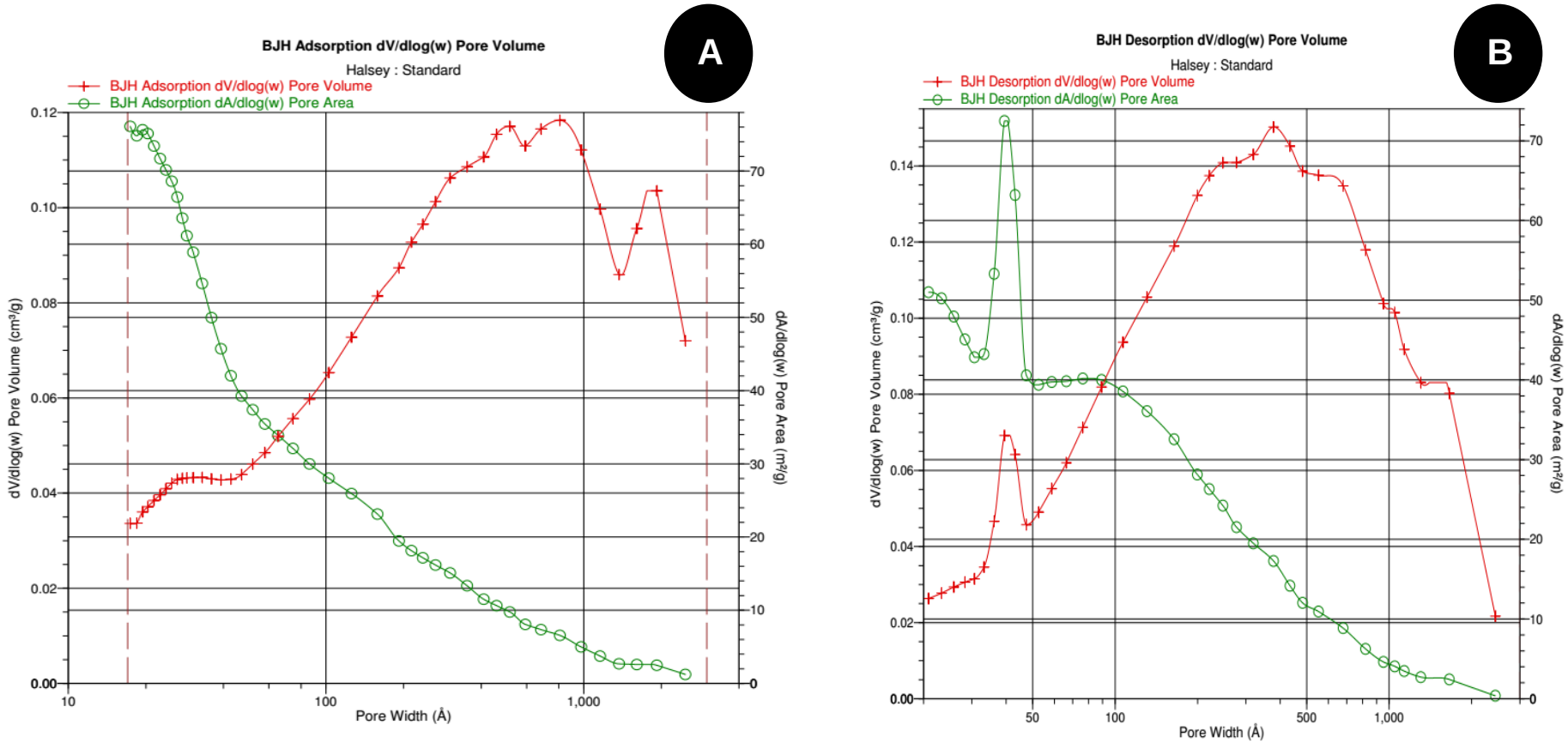

Figure 25: $CMCO_2$ BJH (A) Adsorption - (B) Desorption results

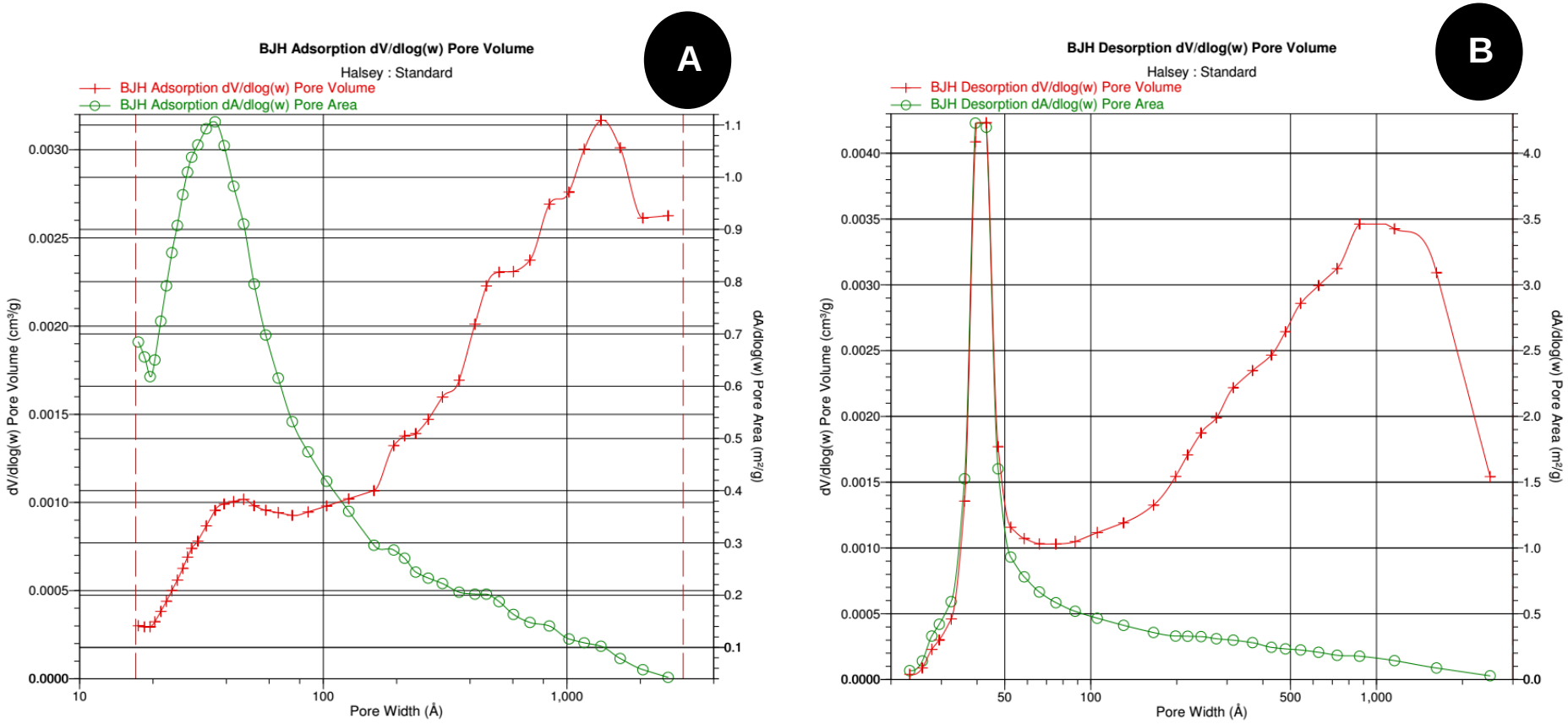

Figure 26: $CMCO_3$ BJH (A) Adsorption - (B) Desorption results

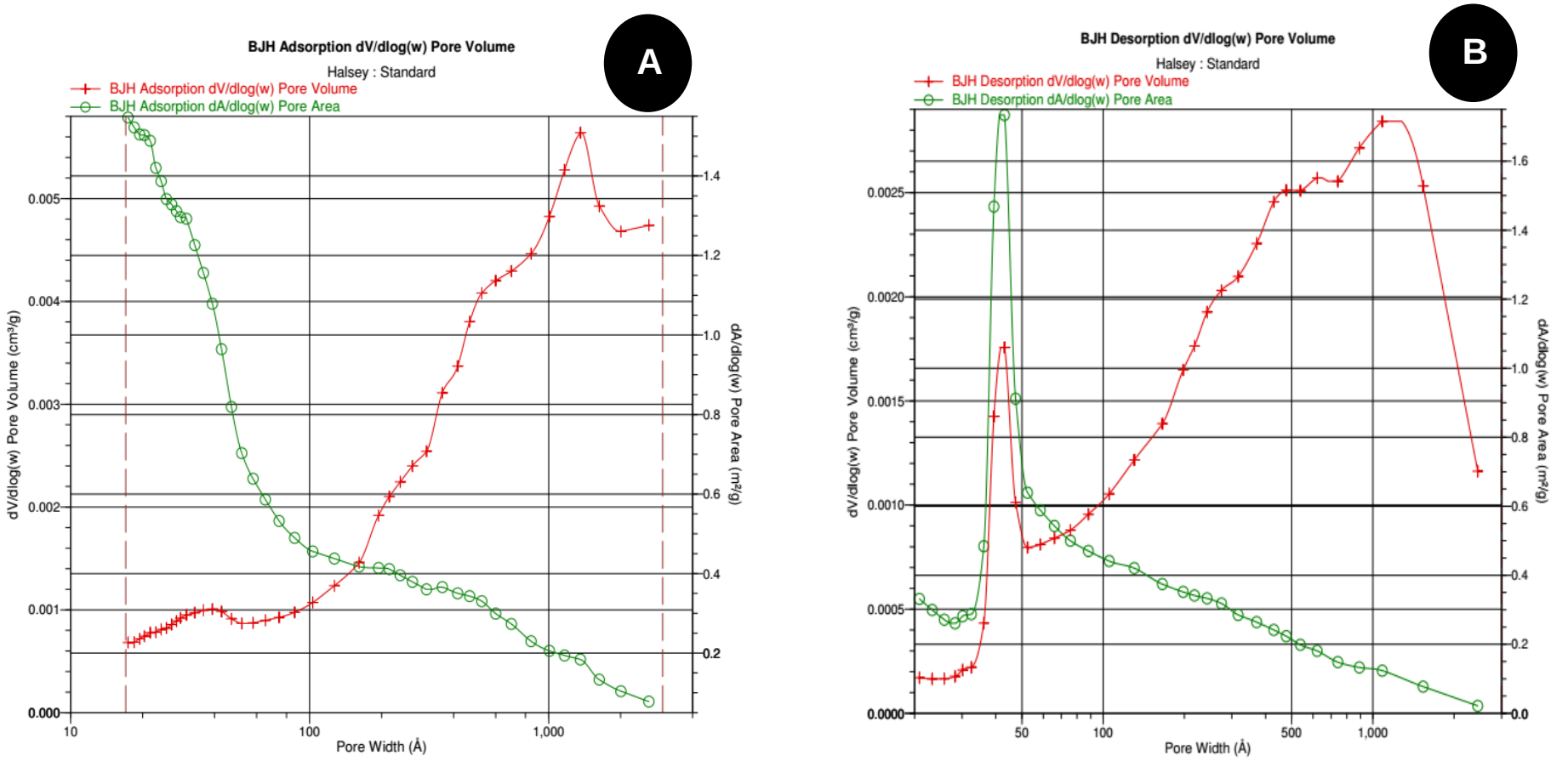

Figure 27: CMSG$_1$ BJH (A) Adsorption - (B) Desorption results

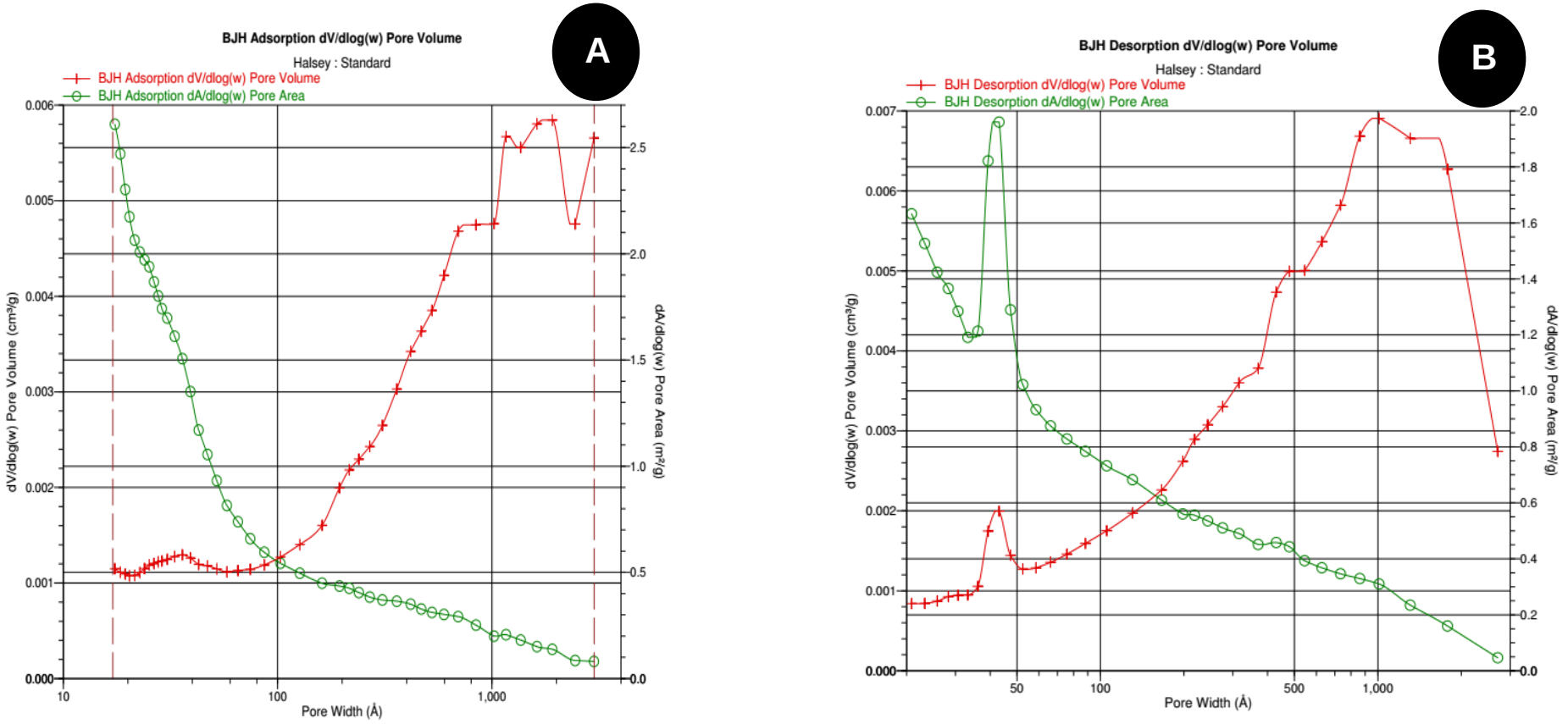

Figure 28: $CMSG_2$ BJH (A) Adsorption - (B) Desorption results

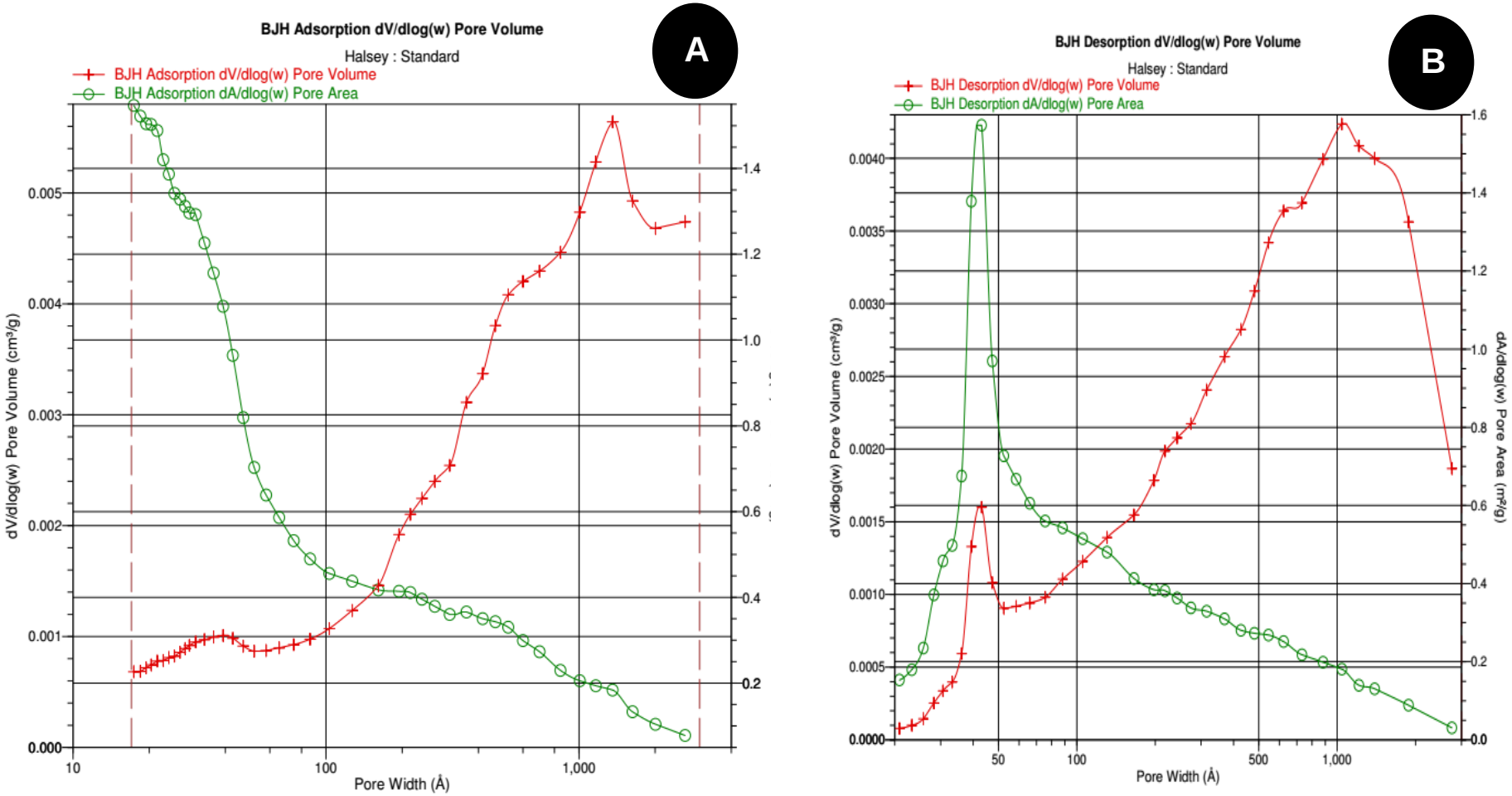

Figure 29: $CMSG_3$ BJH (A) Adsorption - (B) Desorption results

Distribution curves of the pore volumes for all these catalysts were calculated as the pore diameter's function using nitrogen adsorption-desorption data. From each catalyst's surface distribution, the cumulative BJH surface area was derived (Figures 24-29). In the current study, based on the software used for this particular BET analyser, BET t-plot's starting and end-point were arbitrarily selected based on the adsorbent type. And because the adsorbate on the micropore surface is larger than that on non-porous surface, the specific surface area extracted from t-plot graphs is considered to be larger than the actual area (Moreno *et al.,* 2016). BJH relies on Kelvin equation and the universal t-curve for determining pore size distribution (Teo *et al*., 2014).

From these results (CMCOs catalysts (Figures 24-26) and CMSGs (Figures 27-29)), It can be observed that the rate of adsorption was mainly dependent on the change of surface coverage due to adsorption, which is directly linked to the gas vapour pressure and the temperature within the system. The adsorption potential of the catalyst surface area was related to the change of molar free energy, implicated with the variation of vapour pressure from the pure liquid phase to the equilibrium pressure of these catalyst surfaces.

These BJH graphs obtained, summarise a series of derivation process from t-plot graphs at dynamic equilibrium, where the pore distribution in each catalyst's desorption step and the volume of N_2 desorbed will then give an indication of the pore volume based on the geometrical relation obtained after capillary evaporation. CMSGs samples (Figures 27-29) exhibited mesoporous multilayer adsorption Type IV isotherm, and the experimental points on the desorption curve in any range of hysteresis loop corresponded to the adsorbed amount at a relative pressure *p/po*, which was then converted to the pore volume ratio to evaluate the degree of adsorption.

Similarly, CaO as a metal oxide nanomaterial, especially its porosity, were studied by Lu *et al*. (2013). In their reports on the characterisation of mesoporous $SiO_2CaOP_2O_5$ bioactive glass by sol-gel process, they reported the role of capillary condensation phenomenon during monolayer and multilayer adsorption processes for the meniscus of spherical and cylindrical particles. They concluded that the desorption isotherm is used to determine effective capillaries' sizes related to the dimension of cylindrical capillaries. Having determined several values of pore volumes at different pressures, the structural curve of the adsorbents was plotted; then by its differentiation, a curve of capillary volume distribution versus effective diameter was calculated (Figures 24-29). The derivative "dv/d log(w)" of each catalyst, based on the Halsey model, was then compared to the porosity of the catalysts and their respective sizes.

The determined textural parameters can predict a better activity of these new nano-catalysts.

4.3.2 Microscopic observations

Figures 30 (A-F) are SEM 3-D morphology micrographs of the co-precipitated catalyst as well as the sol-gel catalyst prepared from dolomite tailings at the scale of the micrometre, whereas Figures 31 (A-F) are TEM micrographs corresponding to a much higher magnification and obtained from a slice of both catalysts.

Additionally, CMSG have shown to be elongated shape throughout a uniform distribution, besides a significant agglomeration and variation in precipitates' sizes. This is due to the presence an open structure of gelatinous state which is allowing the crystal agglomeration freely with a more spherical and uniform structure as the case of $CMSG_3$ in comparison to $CMCO_2$. Similar observations were reported by Taufiq-Yap and Lee (2013) during their investigation on heterogeneous catalysed processes, especially on the characterisations on various solid base catalysts. Similarly, in the current study the sol-gel obtained catalyst micrographs were quite homogeneous microstructures comprising mainly a well-distributed phase as shown on Figure 30B for $CMCO_2$.

In the CMCO samples, it appears that CaO and MgO aggregates are shown to be larger and distinct. The obtained quantification shows that the size of aggregates, as well as the pores width of pores between the aggregates, at an average of 16 to 17 nanometres ranged in comparison with 15 to 17 nanometres for the CMSG samples.

From the microscopic results obtained there is a clear indication of the specimen being a localisation of metal nanoparticles in relative smaller pores, as it was also observed by Rahstizadeh *et al.* (2014) and Farooq et al. (2013). In the case of nano-MgO catalyst obtained by co-precipitation technique and by the impregnation method, those authors obtained quite similar metal particle sizes from TEM. However, this was at lower activity per site for biodiesel production with nano-MgO catalyst, as compared to the impregnated MgO catalyst supported with ZrO_2 and TiO_2. This was attributed to localisation in the microporous structure (Rahstizadeh *et al*., 2014).

The nitric acid concentration was increased (0.5 to 1.5 M), which resulted in an increase of pH from $CMCO_1$ to $CMCO_3$ samples. This was an attempt to improve the conditions of the co-precipitation method which is highly favoured in an alkaline environment. The optimum concentration was 1M HNO3 for $CMCO_2$ catalyst. It was unclear why $CMCO_3$, obtained under optimum conditions as described by previous studies by Alhassan *et al.* (2015), Shengyang

et al. (2011) and Montero et al. (2010), could not exhibit better microscopic characteristics and ideal surface area compared to $CMCO_2$. In particular, Alhassan *et al.* (2015) suggested that the pH of the solution while adding HNO_3 should be monitored to avoid a pH decrease before completion of the reaction, which can adversely affect the precipitation stage of the metal oxide catalyst. From the CMSG results obtained, the ethylene glycol ($C_2H_6O_2$) increase positively contributed to the quality of the resultant gel, which was in agreement with reports by Zebarjad *et al.* (2013).

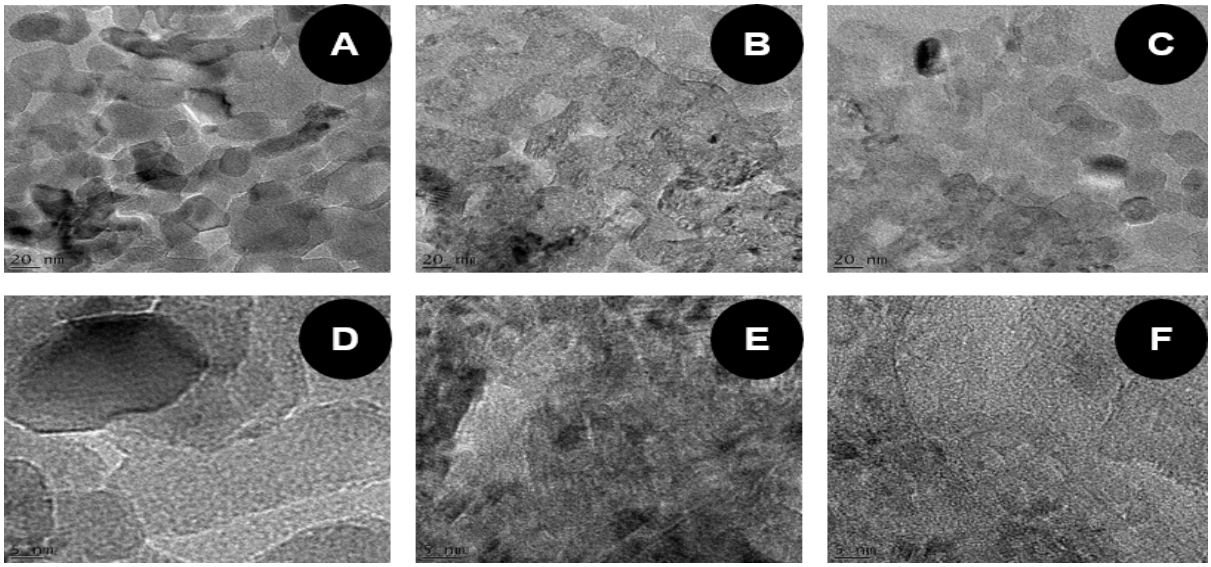

Figure 30: SEM results of the prepared catalyst (A: $CMCO_1$ / B: $CMCO_2$ / C: $CMCO_3$ / D: $CMSG_1$ / E: $CMSG_2$ / F: $CMSG_3$)

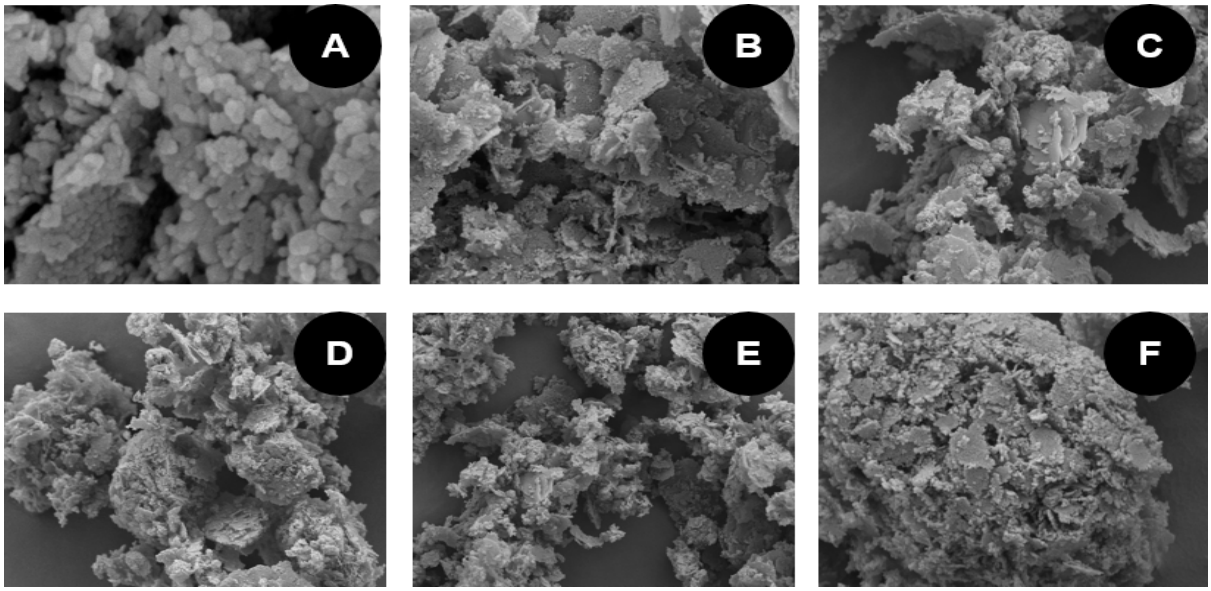

Figure 31: TEM results of the prepared catalyst (A: $CMCO_1$ / B: $CMCO_2$ / C: $CMCO_3$ / D: $CMSG_1$ / E: $CMSG_2$ / F: $CMSG_3$)

Figures 31(A-F), at higher magnification, show the optimum sample ($CMCO_2$) as well as $CMSG_2$ and $CMSG_3$ obtained by the sol-gel method, aggregating very much better as an agglomerated and interconnected specimen, as compared to the catalyst obtained by co-precipitation.

As for the elemental analyses and to check the purity of the catalyst prepared, energy dispersive X-ray spectrometry (EDX or EDS) analyses were conducted. From the results obtained (Figures 32 (A-C)), it can be deduced that magnesium was predominant in the prepared catalyst as compared to calcium. This could be explained by their difference in electronegativity, with magnesium having an electronegativity of 1.32 and calcium an electronegativity of 1 on the Linus Pauling scale (Coulson and Richardson, 2002).

The 0.5 keV and 10 keV peaks maxima were directly related to the alkaline and transitional metal characteristic lines and the presence of nanomaterials as per individual spectrum related to its purity and maximum energy of 9.5 keV. The maximum located on the left part of the spectrum at 0.2 keV clearly comes from carbon and oxygen, which confirms the presence of stabilisers, composed of alkyl chains, with the last peak being copper at approximately 8 keV.

From all three EDX spectrums, magnesium is the most abundant as well as copper. This was due to the predominance of transitional metal in the raw gangue originated from cupriferous minerals. Additionally, the visibility of calcium and iron as compared to magnesium based on a single peak that correlates to the quite uniform material contrast obtained in TEM and SEM. The ratio in terms of abundancy of magnesium and calcium in both CMCO and CMSG catalysts, with a maximum of over 6000 counts in magnesium, were quite close to those obtained by Bergeret *et al.* (2010), they have investigated the preapration of heterogeneous catalyst made of Mg/Al_2O_3 with a lanthanum oxide layer (LaO) for biodiesel production from several feedstock. They reported the EDX profile of magnesium in an abundancy ratio of 6 to 1 as compared to aluminium in the catalyst supported by LaO. Similarly, Amani *et al*. (2014) confirmed higher predominance of magnesium in one of their studies related to the preparation of magnesium oxide, calcium oxide and nanocomposite materials by hydrothermal, ultrasonication, and co-precipitation methods.

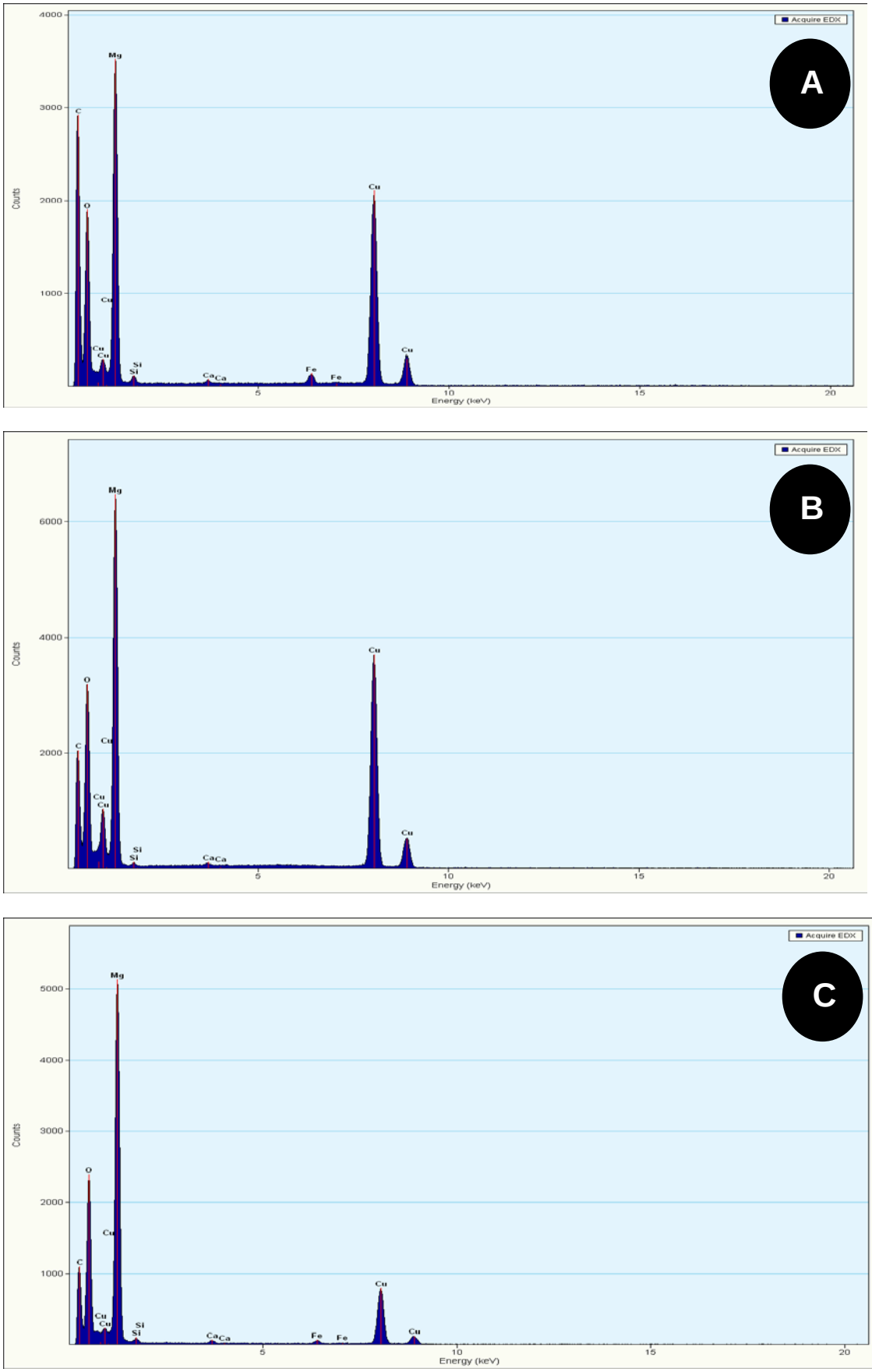

Figure 32: EDX peaks for the prepared catalyst (A: CMCO2 / B: CMSG3 / C: CMSG3/ZVINPs)

4.3.3 Magnetic susceptibility and mass magnetisation calculations

After calculations for all catalyst samples, the magnetic susceptibility was then converted into mass magnetisation to quantify the sample's magnetic strength towards the magnet (Table 20).

Due to the presence of iron in the CMCO sample, it exhibited relatively higher magnetic activity compared to the CMSG catalyst. This was since there was no major hysteresis in the magnetisation for both of samples, suggesting the magnetic particles produced were paramagnetic, but on a different scale as per the results obtained with a maximum mass magnetisation of 173 emu/g for CMSG/ZVINPs$_3$ as compared to only 84 emu/g mass magnetisation of the CMSG sample. This was attributed to the smaller size of both catalysts which were smaller than the superparamagnetic critical size of 27 nm (Zebarjad *et al.*, 2013).

In this instance, to boost the saturation magnetisation of CMSG catalyst while conserving the optimum surface area to address the mass transfer limitation in heterogeneous catalysed processes, the prepared CMSG was coupled by ZVINPs to support and subsequently improve its magnetic ability for separation and regeneration purposes.

Table 23: Mass magnetisation of catalysts prepared

Catalysts	Average pore size (nm)	Average mass magnetisation (emu/g)
CMCO$_1$	15.6±0.92	168±2.45
CMCO$_2$	16.9±0.56	163±1.71
CMCO$_3$	16.1±1.02	159±0.97
CMSG$_1$	16.7±1.35	76±1.94
CMSG$_2$	15.9±1.87	91±1.06
CMSG$_3$	15.4±0.77	84±0.56
CMSG$_3$/ZVINPs$_1$	15.6±0.18	164±2.52
CMSG$_3$/ZVINPs$_2$	16.3±0.43	162±1.27
CMSG$_3$/ZVINPs$_3$	15.8±0.25	173±0.36

Results are expressed as averages ± standard deviation (*n*=2)

In the current study, paramagnetism, that is responsiveness to an applied magnetic field without permanent magnetisation, therefore was tested by placing a magnet near the bottle containing the catalyst (Figure 33). The black particles were attracted toward the neodymium magnet; therefore, CMCO and CMSG/ZVINPs could be easily removed from the vessel containing biodiesel and glycerol. This was achieved under an external magnetic field and coupled with an electrostatic separation to improve the sedimentation of glycerol (Section 4.4).

Figure 33: CMSG/ZVINPs$_3$ catalyst being attracted by to the neodymium magnet

4.4 Biodiesel production

The block flow diagram below (Figure 34) illustrates how biodiesel was produced from edible oil wastewater sludge using the nano-magnetic catalyst prepared from cupriferous tailings.

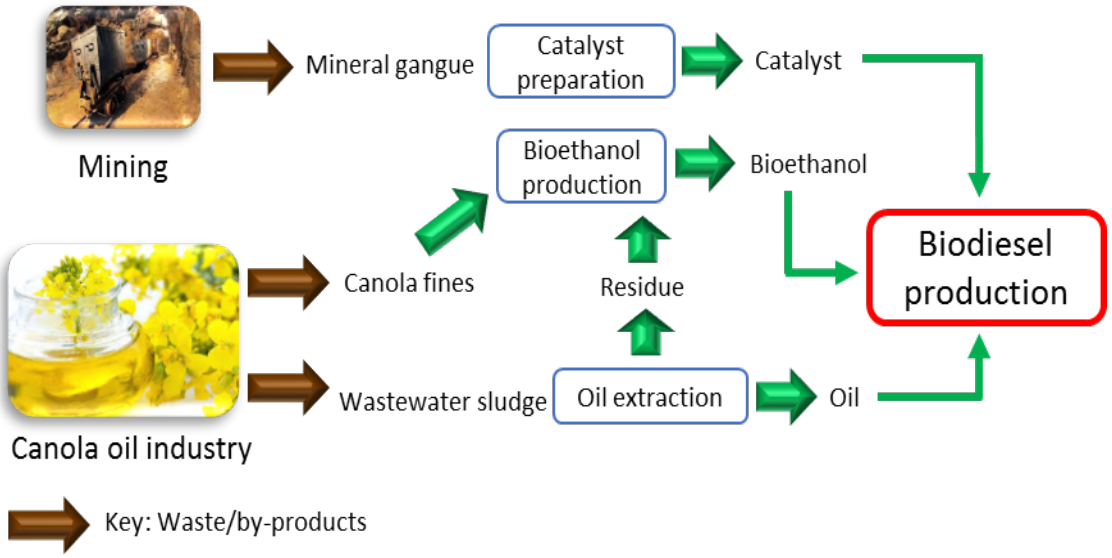

Figure 34: Flow diagram showing the relationship of biodiesel to the other primary study objectives (Objective 4: biodiesel production)

4.4.1 Effect of catalyst dosage and oil/ethanol ratio on the biodiesel produced

The oil to ethanol ratio impact on the biodiesel yield has been reported by many researchers, as discussed in the literature review section (Chapter 2). The transesterification reaction's stoichiometry requires 3 moles of alcohol per mole of triglycerides (Wang *et al*., 2014). In the current study, the oil extracted from wastewater sludge was mixed with ethanol in three different molar ratios (Table 22) and for each oil: ethanol molar ratio at specific catalyst dosage was administered to the system, knowing that in this study the transesterification reaction has involved the use of nine synthesised catalysts (refer to section 2.3).

From the results obtained presented on Table 22, it is shown that an increase in catalyst in the reactants has increased the amount of active basic metal oxide (Ca and Mg), and proportionally increased the biodiesel yield. The catalytic activities of CMCO, CMSG and CMSG/ZVINPs were compared by performing the transesterification reaction of edible oil wastewater sludges. Results showed that all catalysts exhibited higher activity, achieving a biodiesel yield of 74.3% and 77.6% with $CMCO_2$ and $CMSG_3$ respectively.

Table 24: Effect of oil/ethanol (oil/ETOH) ratio and catalyst loading on biodiesel (35°C, 120 min)

Catalyst name	Oil/EtOH ratio	Catalyst loading (wt.%)	Biodiesel yield (%)
$CMCO_1$	1.3	3	57.1±1.22
		5	43.4±0.45
		8	52.2±2.09
	1.6	3	49.4±1.98
		5	58.6±0.98
		8	60.5±0.34
	1.9	3	55.5±0.08
		5	64.6±0.57
		8	62.1±0.56
$CMCO_2$	1.3	3	54.8±0.27
		5	61.3±0.41
		8	69.4±0.78
	1.6	3	60.1±1.53
		5	68.9±1.11
		8	70.5±2.34
	1.9	3	65.7±0.81
		5	**74.3**±2.13
		8	69.9±0.33
$CMCO_3$	1.3	3	68.4±0.15
		5	70.8±0.08
		8	71.6±2.31
	1.6	3	63.2±2.06
		5	52.3±1.21
		8	55.7±1.99
	1.9	3	51.9±1.62
		5	46.6±1.04
		8	50.4±0.07
$CMSG_1$	1.3	3	44.9±0.26
		5	51.7±1.05
		8	60.8±2.88
	1.6	3	65.5±0.60
		5	70±1.65
		8	71.4±0.48
	1.9	3	68.3±0.55
		5	56.9±1.08
		8	62.8±1.33

Table 22: Effect of oil/ETOH ratio and catalyst loading on biodiesel (35°C, 120 min) (*Continued…)*

Catalyst name	Oil/EtOH ratio	Catalyst loading (wt.%)	Biodiesel yield (%)
$CMSG_2$	1.3	3	67.9±1.07
		5	72.3±0.28
		8	70.5±2.09
	1.6	3	71.5±1.77
		5	67.7±1.03
		8	54.3±2.22
	1.9	3	69.9±0.78
		5	72.5±0.26
		8	57.4±0.41
$CMSG_3$	1.3	3	65.5±0.44
		5	69.5±0.67
		8	73±0.92
	1.6	**3**	**77.6**±1.15
		5	72.7±0.72
		8	69±1.09
	1.9	3	56.4±1.66
		5	65.5±1.24
		8	63.4±0.64
$CMSG_3/ZVINPs_1$	1.3	3	66.6±1.21
		5	68.5±2.02
		8	68.1±2.33
	1.6	3	58.7±0.96
		5	59±2.00
		8	59.2±1.48
	1.9	3	65.3±0.57
		5	66.7±0.61
		8	54.4±1.99
$CMSG_3/ZVINPs_2$	**1.3**	3	69.9±0.45
		5	**74.4**±1.53
		8	71.6±0.91
	1.6	3	64.6±2.56
		5	65±1.32
		8	52.3±0.61
	1.9	3	58±0.38
		5	62.5±1.02
		8	67.7±1.29

Table 22: Effect of oil/ETOH ratio and catalyst loading on biodiesel (35°C, 120 min (*Continued…)*

Catalyst name	Oil/EtOH ratio	Catalyst loading (wt.%)	Biodiesel yield (%)
$CMSG_3/ZVINPs_3$	1.3	3	60±0.72
		5	63.3±0.30
		8	62.7±0.59
	1.6	3	68.7±1.88
		5	**75.3**±2.73
		8	70.2±1.26
	1.9	3	64.1±0.78
		5	66.3±0.08
		8	72.6±1.00

Results are expressed as averages ± standard deviation (*n*=3)

From Table 21, it was observed that $CMSG_3$ required only 3 wt.% dosage with a 1:3 oil/ethanol ratio, as compared to other catalysts used in this study, with an optimum catalyst loading of 5 wt.% under 1:6 oil: ethanol ratio for $CMCO_2$ and $CMSG_3/ZVINPs_3$. Similar results were obtained by Bergeret *et al.* (2010) from lanthanum-based mixed oxide ($CaO\text{-}La_2O_3$) and ($MgO\text{-}La_2O_3$) catalysts at 3 wt.% loading, in biodiesel production from soybean oil with methanol. This exhibited 86.5% biodiesel yield under the optimised condition reaction. Their study indicated that catalytic activity was proportional to the increase in CaO/MgO loadings, which increased the basicity of the catalyst. Additionally, Fukuda *et al.* (2009) reported a biodiesel yield of 86.3% for transesterification parameters of 9:1 methanol/oil molar ratio, 5 wt.% catalyst, after 6 h using calcium-nickel oxide (CaO–NiO) as catalyst.

Molar ratio of alcohol to oil is one of the most significant factors affecting the conversion efficiency and the cost involved (Farooq *et al.,* 2015). Furthermore, from the stoichiometric molar ratio of alcohol to oil for the transesterification is 3:1 and the reaction is reversible, higher molar ratios were required to enhance the contact between the alcohol molecule and the triglyceride. Generally, higher ratios have been used to accelerate the rate of reaction by shifting the reaction toward products formation. The reason for the increase in molar ratio is related to the reaction equilibrium based on Le Chatelier's principle (Coulson and Richardson, 2002) where the increase in ethanol concentration will favour the formation of products, thus reducing mass transfer restrictions. Increasing the molar ratio showed the expected results, that is, increase in rate of reaction with increase of ethanol: oil ratio but not proportionally to the catalyst loading used in each run, which was done in triplicate and all data validated using the relative standard deviation method.

A much higher catalytic activity of calcium-based mixed oxide (Chen *et al*., 2014; Teo *et al*., 2014;), as well as magnesium oxide-based catalysts as compared to CaO or MgO usage

individually (Taufiq-Yep and Lee, 2013) were intensively reported. In the study by Taufiq-Yap *et al.* (2011), zinc doped calcium oxide (Zn/CaO) was employed as a catalyst to generate methyl ester from pongamia pinnata oil, at catalyst dosage of 3.4 wt.%. The wet impregnation method was employed to synthesise the catalyst in nanoparticle form. Under optimised reaction conditions, 99% of biodiesel yield was achieved. Wang *et al.* (2009) Indicated in their studies that the biodiesel yield increased by using KF/MgO instead of MgO as catalyst when converting sunflower oil into biodiesel, reaching a maximum yield of 98% at 65°C for after 4 h. These transesterification parameters were considered as a starting point in order to optimise the yield of biodiesel produced with all 4 catalysts at their respective optimal reaction conditions (***highlighted in yellow in Table 21***).
Hence, in the current study, the next parameter to be optimised was the process temperature.

4.4.2 Effect of temperature on the yield of biodiesel produced at 120 minutes

The influence of temperature in this transesterification process was investigated and the time at which the yield of biodiesel was evaluated was set to 120 min for all 4 tested catalysts at their respective and optimum reaction conditions. Which means that the optimisation of the temperature in the transesterification reaction was performed using $CMCO_2$ catalyst (generated from optimum conditions: Oil/EtOH:1.9 / 5 wt.% catalyst loading), $CMSG_3$ catalyst (obtained from optimum conditions: Oil/EtOH:1.6 / 3 wt.% catalyst loading), $CMSG_3/ZVINPs_2$ catalyst (generated from optimum conditions: Oil/EtOH:1.3 / 5 wt.% catalyst loading) and $CMCSG_3/ZVINPs_3$ catalyst (obtained from optimum conditions: Oil/EtOH:1.6 / 5 wt.% catalyst loading).

The temperature in the transesterification reaction is a very crucial parameter as clearly demonstrated in the literature review (Chapter 2). In the current study, the process temperature was set to be 35°C, 50°C, 65°C and 75°C for each catalyst at their respective optimum in terms of oil: ethanol molar ratio as well as catalyst loading while keeping the reaction time constant at 120 min. From the biodiesel yields obtained, it can be observed that the temperature has definitely contributed to a rise of biodiesel yield; in all four scenarios the biodiesel production rate was higher when increasing the reaction temperature.

For instance, in Figure 35, it was observed that the maximum biodiesel yield of 82% was decreasing with the temperature. At a maximum of 90°C, only 69% biodiesel yield could be obtained using $CMCO_2$ as catalyst, which could be explained by ethanol changing phase to vapor before interacting with the other components involved in the transesterification process. Similarly, this phenomenon was observed on the transesterification reaction using $CMSG_3$

(Figure 36) and CMSG/ZVINPs (Figures 37 & 38). An optimum biodiesel yield of 84% was obtained at 75°C using $CMSG_3$ as nano-catalyst.

Therefore, producing biodiesel through a transesterification reaction with solid catalyst should be controlled by mass transfer limitation of reactants in the immiscible ethanol-oil-catalyst system. This problem of mass transfer can be minimised or by using continuous stirring in the vessel (Demirbas *et al*., 2016). The influence of temperature on mass transfer of reactants, especially in immiscible <ethanol-oil-catalyst> system has been investigated and the findings stated that at a fixed stirring rate of 200 rpm, the rate in mass transfer of reactants is directly proportional to the temperature at which the reaction is occurring (Demirbas *et al*., 2016). Similarly, Berchmans *et al.* (2013) have used methanol to produce biodiesel from *Jatropha curcas* waste food. They reported an increase in biodiesel yield from raising the reaction temperature from 30°C to 65°C with a maximum yield of 91%, and attributed this increase in oil conversion to the increased mass transfer of reactants in the immiscible methanol–oil–catalyst systems when the reaction temperature is increased. Additionally, Sirisomboonchai *et al.* (2015) have indicated 65°C as their optimum while attempting to produce biodiesel from waste cooking oil using calcined scallop shell as a catalyst. In the current study, the maximum temperature was chosen as 75°C, closer to the critical temperature (ethanol boiling point: 78.4°C) in the experimental set-up. However, because of heat transfer from the water bath to the heterogeneously mixed reactant in the vessel, the temperature was assumed to be a little bit lower than the critical set temperature, to avoid ethanol in the vessel being vaporised.

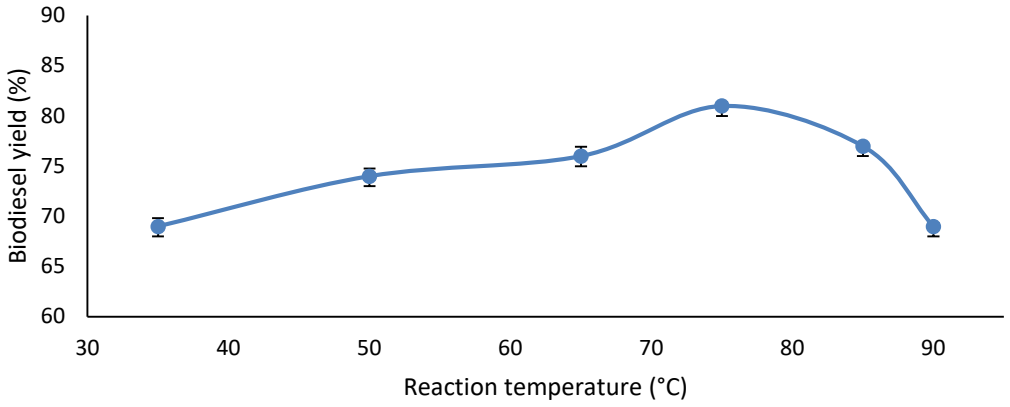

Figure 35: Effect of temperature on the biodiesel yield with $CMCO_2$ catalyst (Oil/EtOH:1.9 / 5 wt.% catalyst loading / 120 min reaction time) (error bars represent the standard deviation from the mean (n = 3))

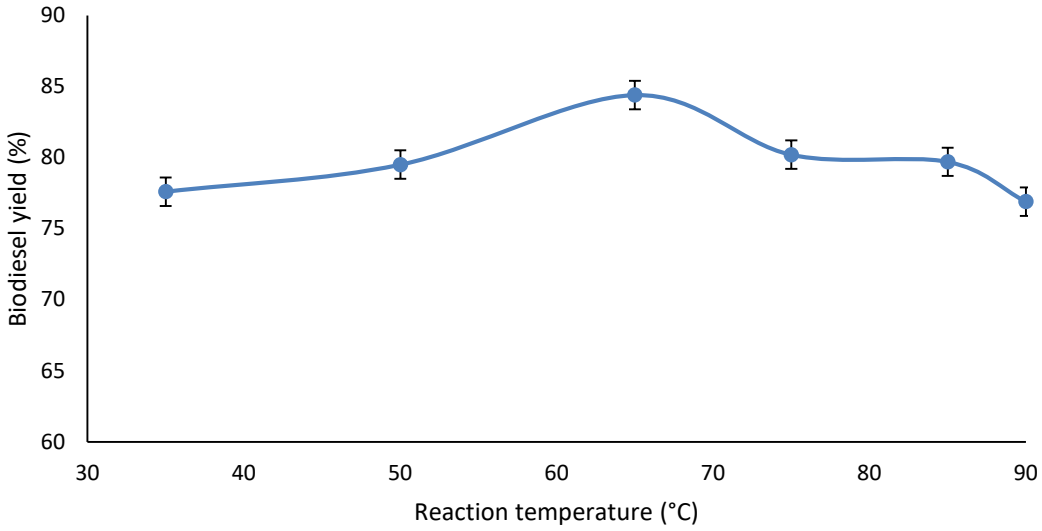

Figure 36: Effect of temperature on the biodiesel yield with $CMSG_3$ catalyst (Oil/EtOH:1.6 / 3 wt.% catalyst loading / 120 min reaction time) (error bars represent the standard deviation from the mean (n = 3))

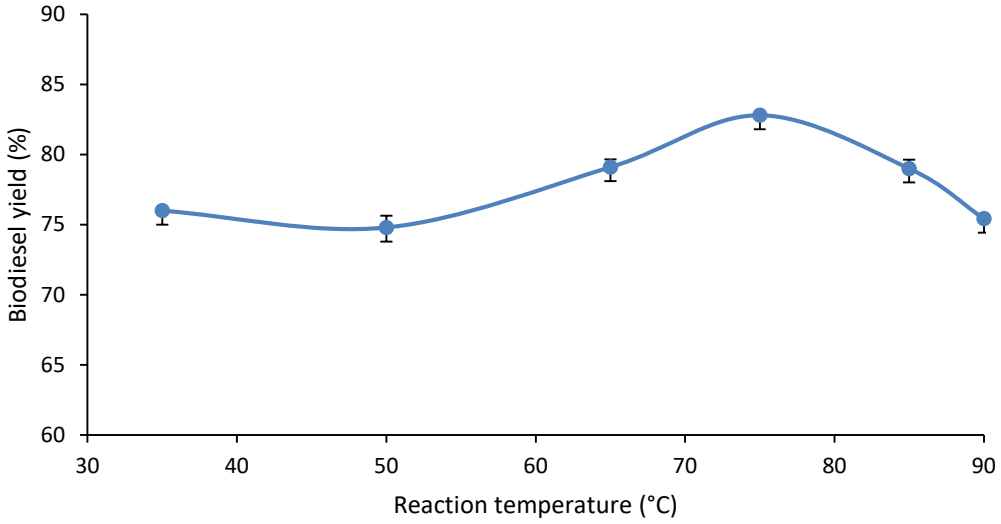

Figure 37: Effect of temperature on the biodiesel yield with $CMSG_3/ZVINPs_2$ catalyst (Oil/EtOH:1.3 / 5 wt.% catalyst loading / 120 min reaction time) (error bars represent the standard deviation from the mean (n = 3))

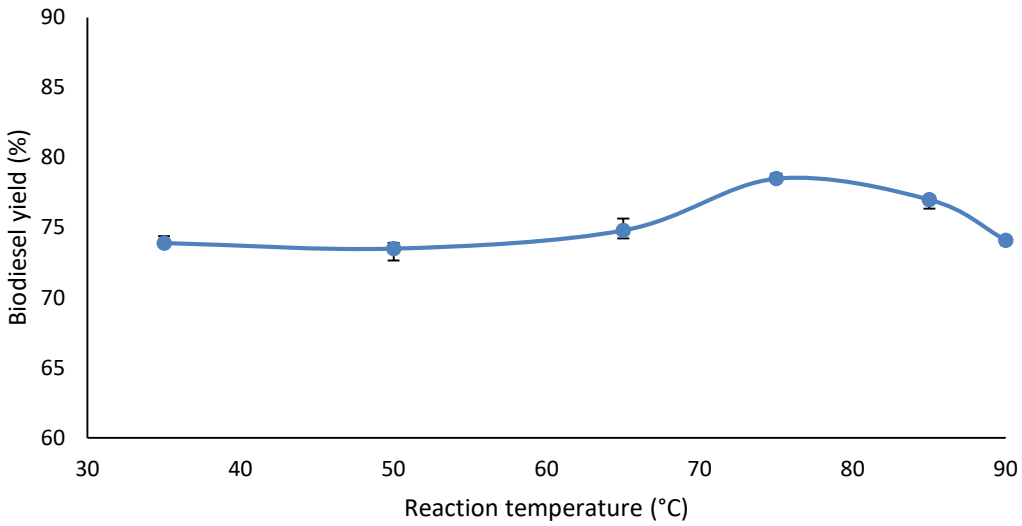

Figure 38: Effect of temperature on the biodiesel yield with CMCSG3/ZVINPs3 catalyst (Oil/EtOH:1.6 / 5 wt.% catalyst loading / 120 min reaction time) (error bars represent the standard deviation from the mean (n = 3))

Afterwards, these catalyst performances were evaluated in terms of the reaction time, comparing edible oil wastewater sludge (EOWWS) and pure canola oil as feedstock for biodiesel production under optimum conditions for each catalyst.

4.4.3 Effect of reaction time for the transesterification process

For each catalyst in comparison with their respective abilities (Figures 39 – 42). (($CMCO_2$: Oil/EtOH:1.9 / 5 wt.% catalyst loading at 75°C); ($CMSG_3$: Oil/EtOH:1.6 / 3 wt.% catalyst loading at 65°C); ($CMSG_3$/$ZVINPs_2$: Oil/EtOH:1.3 / 5 wt.% catalyst loading at 75°C)) and ($CMSG_3$/$ZVINPs_3$: Oil/EtOH:1.6 / 5 wt.% catalyst loading at 75°C) to produce biodiesel from pure canola oil. All experiments were duplicate for both EOWWS and pure canola oil as the main feedstock to produce biodiesel.

With the catalyst loading, oil to ethanol molar ratio and the transesterification temperature having been optimised for each catalyst on their individual performances on the biodiesel yield produced, the next step was to study the effect that the reaction time has on improving the biodiesel yield, and to understand its effect on the transesterification process. In so doing, pure canola oil was used for biodiesel production with these catalysts in order to investigate their respective performances compared to EOWWS, with the duration of the process as a variable. Samples were taken out of the vessel after four hours to compute the yield and express the oil conversion into biodiesel yield. The reaction time is a very important parameter

and closely related to the energy cost of the entire process of producing biodiesel (Demirbas *et al*., 2016).

The results obtained statistically show an increase in ethyl ester production with time, with a maximum of 87% biodiesel yield using $CMCO_2$ (Figure 39) as a catalyst for EOWWS, and with pure canola oil to achieve a biodiesel yield of 89% at 180 min. From figures 39 and 40 it can be observed that the performance of $CMSG_3$ was better than $CMCO_2$, with a maximum yield of biodiesel that reached 98.5% with pure canola oil, and 84% of EOWWS biodiesel only after 4 h. This could be justified by the fact that the catalyst with sol-gel texture, compare to the co-precipitate catalyst, needed some time to be homogenised into the system before the active sites of the catalyst responded to their reactive catalyst-reactant interface. As for the sol-gel/zero valent iron supported nano-catalysts, the results showed an increase of biodiesel yield to 98% at 180 min, slightly decreasing at 240 min for EOWWS biodiesel, while pure canola biodiesel yield kept increasing at that particular time (Figure 41). This was due to the fact that the oil used to make biodiesel that was extracted from wastewater sludge did contain other components that could have increased the mass transfer limitation of the catalyst specifically on the catalyst's basic and active sites, while subsequently minimising the conversion of oil into biodiesel as compared to the same catalyst performance with pure canola oil, whereby the yield kept increasing with transesterification time.

Farooq *et al.* (2015) in their studies also noticed a drastic decrease of biodiesel yield (using waste cooking as feedstock) through a heterogeneous catalytic transesterification using chicken bones. They confirmed that particularly in a chemical reaction using a heterogeneous catalyst, the limitations in mass transfer that occur when the rate at which the reactants are consumed on active sites is faster than the diffusion rate of these reactants towards those active sites, should be very minimal to avoid extensive decrease in the overall rate of the process, thus leading to poor activity of the catalyst. Furthermore, the lower biodiesel yield observed in the current study may have related to a probable occurrence of reversible reactions (ethanolysis) in the vessel, which occurs via three reversible consecutive reactions from triglycerides to diglycerides, diglycerides to monoglycerides and finally ethyl esters (Farooq *et al.,* 2015). Another parameter responsible for lower biodiesel yield may be catalyst leaching (Demirbas *et al.,* 2003).

Fukuda *et al.* (2011) and Metsovitia *et al.* (2013) made similar observations when producing biodiesel through a heterogeneous catalysed transesterification. Additionally, Fabiano *et al.* (2016) investigated on soybean oil as feedstock to produce biodiesel using ethanol and CaO as catalyst with Zn, K and Mg, acting as promotor. They also reported an estimated biodiesel

yield decrease of approximately 7% from the optimum ethyl ester conversion after increasing the reaction time.

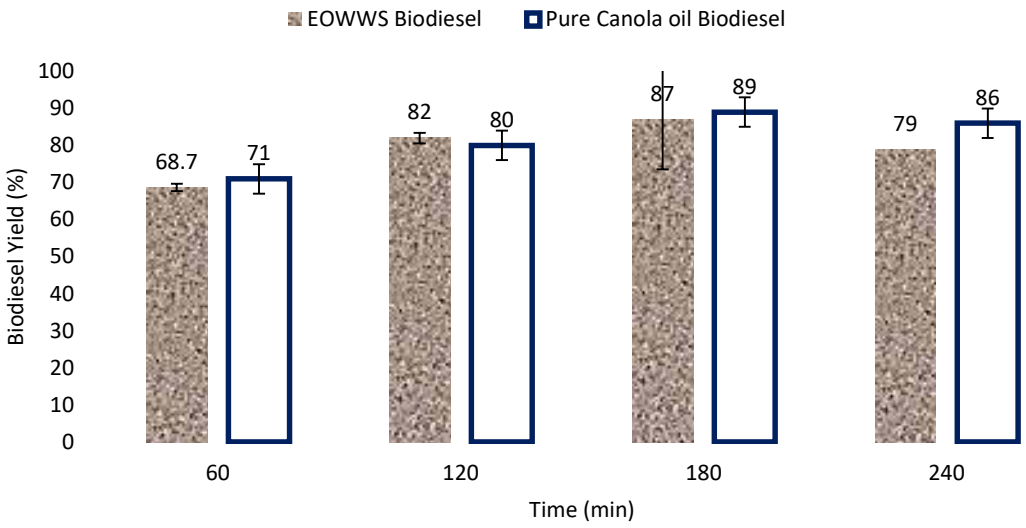

Figure 39: Effect of the reaction time on the biodiesel yield with $CMCO_2$ catalyst (Oil/EtOH:1.9 / 5 wt.% catalyst loading at 75°C) (error bars represent the standard deviation from the mean (n = 3))

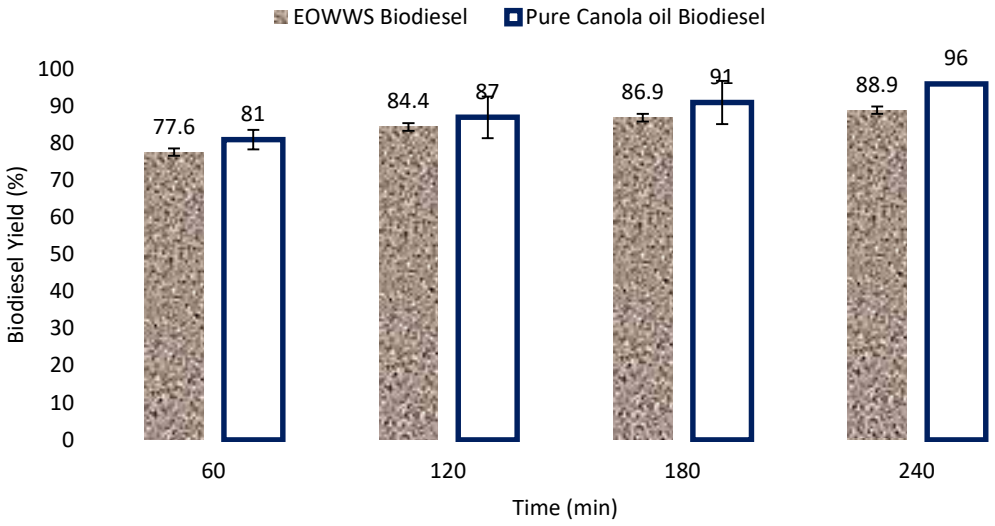

Figure 40: Effect of the reaction time on the biodiesel yield with $CMSG_3$ catalyst (Oil/EtOH:1.6 / 3 wt.% catalyst loading at 65°C) (error bars represent the standard deviation from the mean (n = 3))

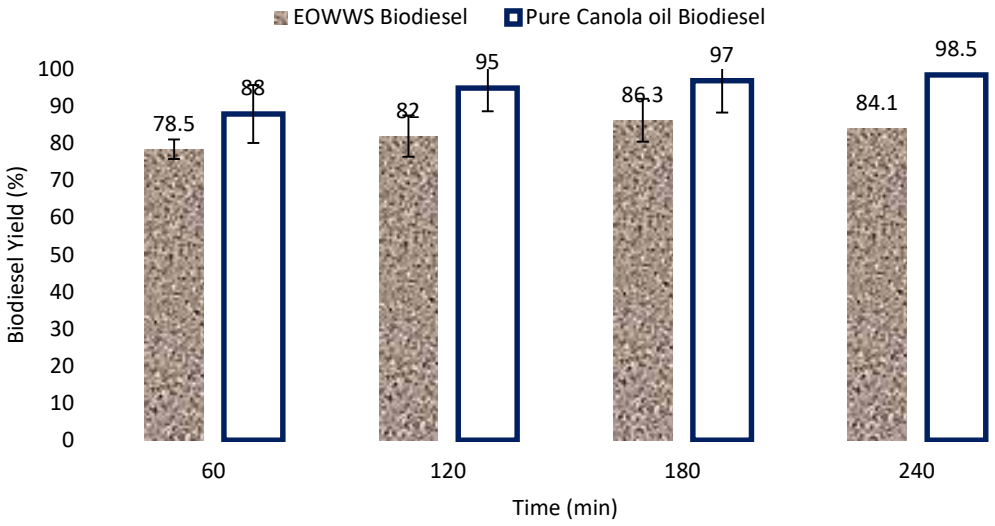

Figure 41: Effect of the reaction time on the biodiesel yield with $CMSG_3/ZVINPs_2$ catalyst (Oil/EtOH:1.3 / 5 wt.% catalyst loading at 75°C) (error bars represent the standard deviation from the mean (n = 3))

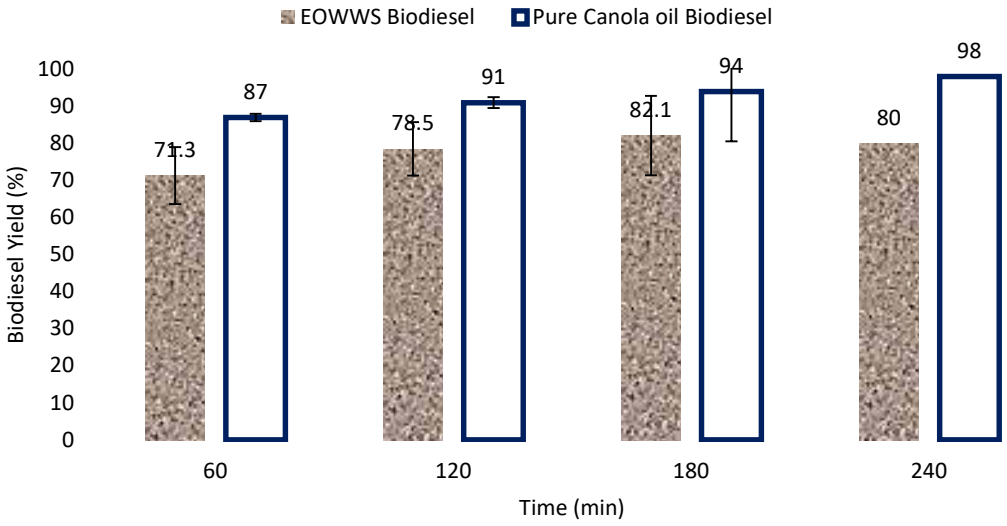

Figure 42: Effect of the reaction time on the biodiesel yield with $CMSG_3/ZVINPs_3$ catalyst (Oil/EtOH:1.6 / 5 wt.% catalyst loading at 75°C) (error bars represent the standard deviation from the mean (n = 2))

4.4.4 Investigation of the reusability of all catalysts for biodiesel production

Once the biodiesel was produced, two electrodes from a normal AC transformer of 1.4 kV were used to accelerate the removal of biodiesel from glycerol (total volume of 1 L). Afterwards, the neodymium magnet was immersed in the flask containing the biodiesel obtained to recover the catalyst used according to its relative magnetic susceptibility to the magnet. The collected catalyst, after being washed using ethanol was placed in an oven at

80°C drying during a maximum period of 2 h. In the current study, a loss in catalyst was observed during this particular process especially due to low mass magnetisation of the sol-gel synthesised catalyst.

Each catalyst was evaluated on the basis of the number of runs (in duplicate each), in terms of each respective biodiesel yield obtained. For this purpose, a maximum of 4 reaction cycles per catalyst were set, in order to investigate catalyst reusability. From the results obtained, all experiments exhibited a decreased biodiesel yield with increasing reaction cycle, with $CMSG_3$ (Figure 44) being the worst performer (by losing its catalytic activity). With a possibility of $CMCO_2$ being regenerated four times while the biodiesel yield dropped from 88% to 64% (Figure 43), and 50% biodiesel yield obtained with $CMSG_3$ as catalyst after the fourth reaction cycle (Figure 44), nanocatalyst with ZVINPs was more stable in terms of reusability, only decreasing from 84% to 69% using $CMSG/ZVINPS_3$ (Figure 45). This was justified by the catalyst mass magnetisation (Section 4.3.3), as it was much easier to reuse this particular catalyst and simultaneously conserve its catalytic activity. Additionally, some other factors such as the loss in catalyst during separation (Frisch and Patzirek, 2008), oversaturation on the catalyst's surface after being used (Dermirbas *et al.,* 2016; Metsovitia *et al.*, 2013; Di Serio *et al*., 2008) and probable catalyst leaching occurring (Farooq *et al*., 2015; Fukuda *et al*., 2011) which could have contributed to the biodiesel yield obtained, especially when using the regenerated catalyst and subsequently lowering its performance during the process.

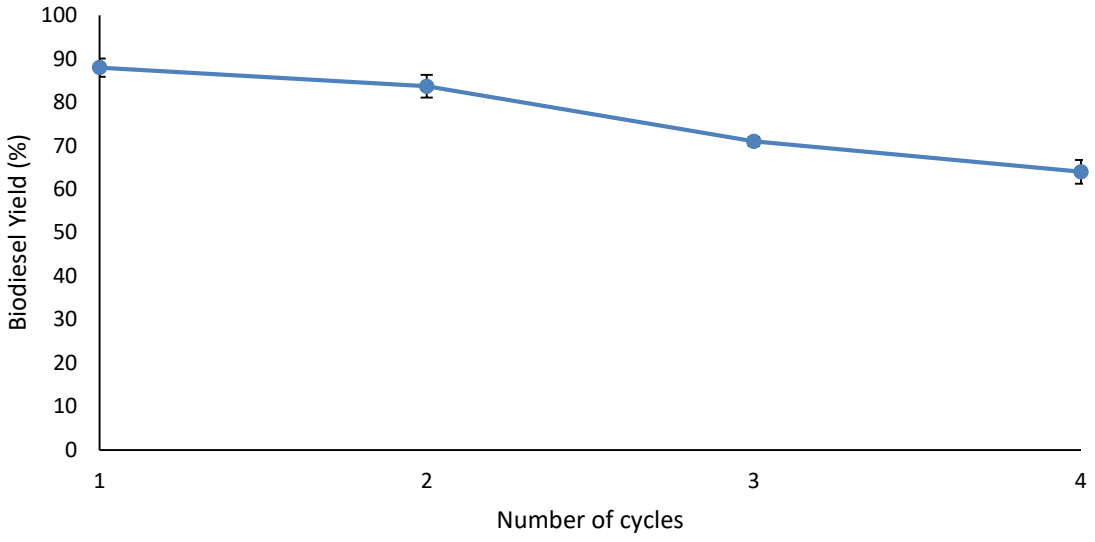

Figure 43: The effect of recycled $CMCO_2$ catalyst (under optimum conditions) on the biodiesel yield (error bars represent the standard deviation from the mean (n = 3))

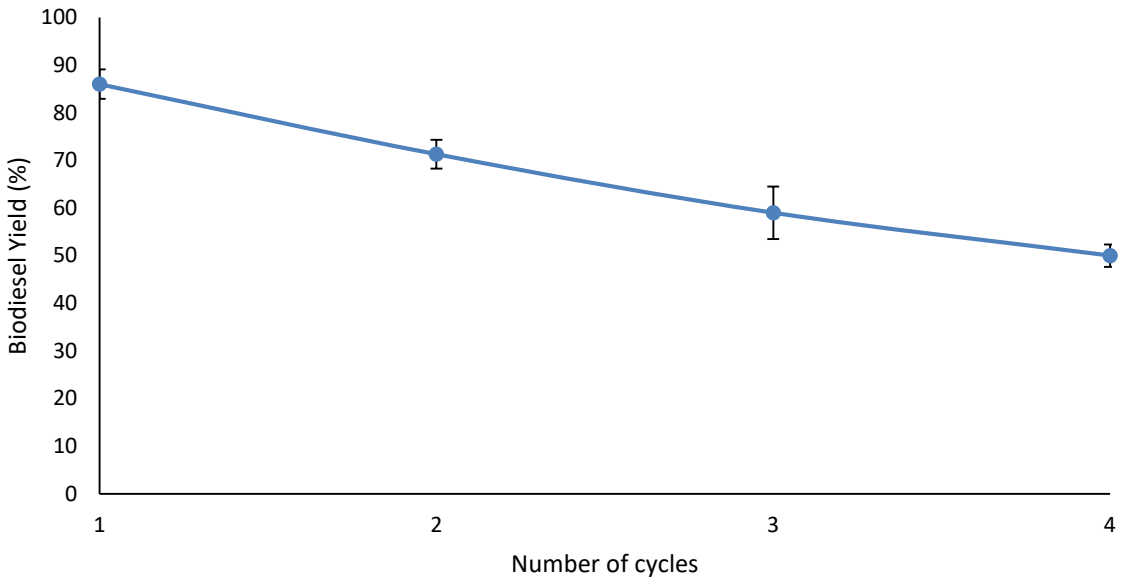

Figure 44: The effect of recycled $CMSG_3$ catalyst (under optimum conditions) on the biodiesel yield (error bars represent the standard deviation from the mean (n = 3))

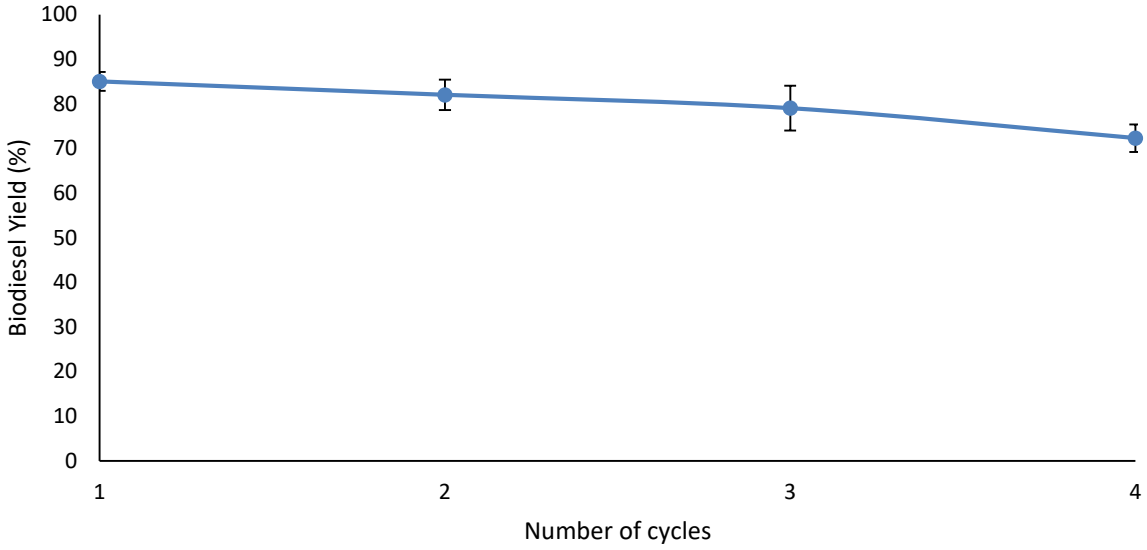

Figure 45: The effect of recycled $CMSG_3/ZVINPs_2$ catalyst (under optimum conditions) on the biodiesel yield (error bars represent the standard deviation from the mean (n = 3))

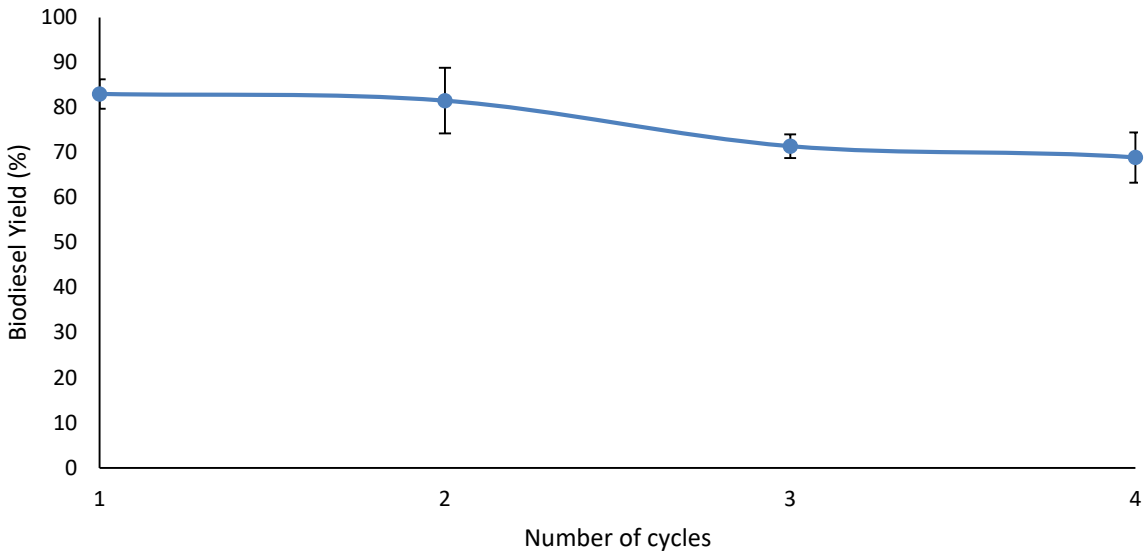

Figure 46: The effect of recycled $CMSG_3/ZVINPs_3$ catalyst (under optimum conditions) on the biodiesel yield (error bars represent the standard deviation from the mean (n = 3))

Furthermore, Vishal *et al.* (2013) have reported the use of *n*-hexane in improving the catalytic activity to convert jatropha oil into biodiesel. They achieved a reduction in biodiesel yield from 98 to 89% after 5 reaction cycles, which ustified the decrease in yield with the loss in catalyst during the separation process and the oversaturation of the catalyst's pores. Additionally, Devarapaga *et al.* (2017) in their investigation of synthesising a reusable catalyst containing tricalcium phosphate, for biodiesel production from an Indian tribal feedstock reported the reusability of the catalyst being affected due to high FFA concentration, hence adversely impacting on the biodiesel yield. They reported major losses in terms of mass transfer of β-tricalcium phosphate after three reaction cycles, which adversely neutralised the catalyst basic sites, thus reducing their effectiveness during the transesterification process.

4.4.5 Properties of biodiesel produced and its thermodynamic evaluation

After the entire transesterification process was evaluated, the EOWWS biodiesel as well as the pure canola biodiesel were analysed to verify their properties as compared to the commercial diesel (50 ppm sulphur), and only the biodiesel with better quality was evaluated in a power generation engine to investigate its thermodynamic properties, to compute the approximate energy generated by this synthesised liquid fuel.

4.4.5.1 Biodiesel properties

As described in Table 23, both EOWWS biodiesel and pure canola biodiesel were analysed in terms of their respective viscosity, specific gravity, high-heating value (HHV) and flash point. Other important properties (cetane number, cloud point, water content and iodine value) were not measured in this study. The quality of biodiesel was mainly discussed on the basis on viscosity and density, which are crucial for engine performance (Bhuiya *et al*., 2016).

Table 25: Comparison of the synthesised biodiesel quality and the commercial diesel

Properties	Unit	Measurement Standards	Commercial Diesel (50ppm sulphur)	EOWWS Biodiesel	Pure Canola Biodiesel
Viscosity at 40ºC	m^2/s	ASTM D445	$3.0*10^{-6}$ ± 0.87	$3.7*10^{-6}$ ± 0.71	$3.2*10^{-6}$ ± 0.38
Density at 15ºC	kg/m^3	ASTM D941	830.0 ± 0.78	832.62 ± 0.69	841.17 ± 0.81
HHV	MJ/kg	ASTM D2015	48.12 ± 1.59	45.75 ± 1.21	46.45 ± 1.34
Flash point	°C	ASTM D93	50.4 ± 0.73	61.3 ± 0.64	58.6 ± 0.86

Results are expressed as averages ± standard deviation (*n*=2)

From the results obtained there is a clear indication that both EOWWS and pure canola oil biodiesel exhibited excellent properties, very similar to commercial diesel, with acceptable viscosity for EOWWS compared to the pure canola biodiesel. For instance, the density of biodiesel, which was measured at 15°C was 0.832 g/cm^3 for EOWWS biodiesel, and 0.841 g/cm^3 for pure canola biodiesel. These values were in the range of biodiesel density (0.8-0.856 g/cm^3) as determined by previous researchers (Rakopoulos *et al., 2*008; Demirbas, 2009; Atabani *et al.,* 2013; Bhuiya *et al*., 2016).

As reported in the literature review (Chapter 2), the viscosity is an important property for the selection of fuel as the quality of combustion directly depends on it. Additionally, the atomisation and spray characteristics. From the obtained results in Table 23 (which were done in duplicate), results showed that the kinematic viscosity of biodiesel was much higher than the conventional or commercial diesel, because of its enormous molecular mass and chemical structure. Normally at low temperature, high viscosity affects the flow of the fuel negatively. Lower viscosity of a fuel increases wear and leakage due to insufficient lubrication. Additionally, an increase in viscosity may lead to incomplete combustion and more difficulties, especially in regions with relatively cold weather conditions, because mostly when the temperature decreases, the viscosity increases (Atabani *et al., 2*013; Bhuiya *et al.,* 2016).

Furthermore, Chen *et al.* (2009) performed on the performance the combustion and the evaluation of a diesel engine using biodiesel obtained from soybean oil. They reported that the formation of large droplet due to higher viscosity of the fuel is during the injection in the combustion chamber, which further deteriorates the combustion quality by emitting much more exhausts emissions.

HHV and flash point results from Table 23 clearly show that the biodiesel obtained was of good quality, though it needed to be tested to evaluate the amount of energy produced, based on thermodynamic considerations of the power generation of the engine used.

4.4.5.2 Performance of biodiesel in a power engine

It was observed that the average indicated thermal efficiency used to calculate the overall thermal efficiency for the prepared biodiesel was 30.75%, and 26.92% for commercial diesel. These results can be translated from their respective viscosity values (Section 4.4.5.1). The higher the viscosity of fuel, the higher the indicated thermal efficiency, and the lower the mechanical efficiency (Sarala *et al.*, 2012).

The reasonable mechanical efficiency of 73.88% with EOWWS biodiesel can be explained and illustrated by the working principles of an IC engine, more particularly depending on the brake power within the system, which is defined as the product of the inverse in brake specific fuel consumption and the measure mass flow rate of air (as shown in the calculations below) at a specific fuel/air ratio. The specific fuel consumption is effectively a measure of the engine's ability to convert the chemical energy to mechanical energy (Cengel *et al.*, 2008 and Ganessan, 2003). To illustrate this, when the piston approaches the top of its stroke it slows, and afterwards comes to rest and then moves back down. Depending on the viscosity which is influencing the whole compression process, heat will be released (combustion) generating an increase in pressure which pushes the piston's last upward movement. The opposition to the piston's movement represents a loss in efficiency, which is computed in Table 24.

Table 26: Thermal and mechanical efficiency of EOWWS biodiesel and diesel

Indicated Thermal Efficiency (%)		**Mechanical Efficiency (%)**	
EOWWS Biodiesel	**Commercial Diesel**	**EOWWS Biodiesel**	**Commercial Diesel**
30.75 ± 1.28	26.91 ± 1.06	73.88 ± 1.79	90.55 ± 1.25

Results are expressed as averages ± standard deviation (*n*=2)

Sarala *et al.* (2012) in his work on internal combustion engines has confirmed that one should avoid delaying the heat release which will eventually allow a significant part of the load (air/fuel mixture) to explode with delays, and causing loss of energy through the hotter exhaust stream. Hence, in the current study, an offsetting technique on the crankshaft angle to the piston axis was performed; and definitely improved the efficiency of the engine. In their investigation Monyem *et al.* (2001) analysed the performance of biodiesel/fuel blend (0-100% biodiesel) in terms of their emissions and IC engine mechanical efficiencies. They reported that the main sources contributing to a decrease in mechanical efficiency and heat losses were: (i) the air/fuel compression ratio and the friction between moving parts as well as the type of materials used (such as the piston rings on the cylinder walls); (ii) the required power required to run the valve gear and all the pumps controlling the cylinder's inlets and outlets of gases.

The approximate contributions breakdown in energy balances is as follows: crankshaft and seals (12.4%); pistons, rings, pins and rods (45.5%); valve train (22.7%); oil pump (5.8%); water pump and alternator (12.6%). In this current study, this particular model was not applied due to the simplicity of the IC engine used, and because the main objective was to determine the thermal and mechanical efficiency. From the obtained results for EOWWS biodiesel and diesel (Tables 24), their respective mechanical efficiencies were fairly close to the results reported by Ganessan (2003) and Srivinivasaan (2001) with an average thermal efficiency of 26-29% for biodiesel.

From the heat balance obtained, the change of maximum combustion temperature, the exhaust gas temperature and the engine load are interconnected with the fuel consumption in the engine. Hence, maximum combustion temperature increases (from 60°C) with increase in load; this can be referred to increase in heat release rate due to increase in fuel supply at higher loads (Sarala *et al.*, 2012). In addition, the temperature in the exhaust stream also increases with an augmentation in engine load, accounted for an average of 15.5%. Because of high loads there are an increases in fuel richness, and combustion slightly progresses to the afterburning stage, leading to increase in exhaust temperature (Mofijur *et al*., 2015; Ozsezen and Canakci, 2011).

The diesel engine used in this study was fully insulated but not equipped with any additional regulator of heat lost, such as turbo machinery to retrieve the heat loss in the exhaust gas streams (Swaminathan and Sarangan, 2012). Practically, in an engine cycle, a major part of the energy within the system is generally lost with the exhaust gases because it can be released at an ambient temperature (Chong *et al*., 2015; Ozsezen and Canakci, 2011).

4.4.5.3 GHGs emissions evaluation of biodiesel produced

This was an additional milestone in order to address the issue of commercial diesel produced from fossil fuel being responsible for GHGs emissions, which negatively impact our environment. EOWWS biodiesel and commercial diesel were fed into the IC engine, which was equipped with a device checking the quality of gases in the outlet stream after combustion. The emissions of gas for each run were recorded on a selected set of engine speeds (Table 27). In the current study, only carbon monoxide (CO) and nitrogen oxides (NOx) were analysed. This approach was adapted from Mofijur *et al*. (2015), they explained that the main concern with diesel engines and their emissions is with nitrogen dioxide (NO_2), a compound of NOx (Nitrogen oxide). NO_2 has a strong capacity to absorb infrared rays; therefore, it is a major contributing factor to global warming (250 times worse than CO_2 at the same concentration) (Chong *et al*., 2015; Mofijur *et al*., 2015).

Table 25: NOx and CO emissions of EOWWS Biodiesel and commercial diesel in the IC engine

Engine Speed (rpm)	**CO Emission index (ppm/g/h)**		**NOx Emission index (ppm/g/h)**	
	EOWWS Biodiesel	**Commercial Diesel**	**EOWWS Biodiesel**	**Commercial Diesel**
800	**249.3 ± 3.01**	**310.4 ± 1.45**	**227.3 ± 0.76**	**289.3 ± 0.56**
1000	231.1 ± 0.32	251.8 ± 1.76	196.1 ± 0.83	253.2 ± 1.22
1200	189.9 ± 0.78	198.7 ± 2.09	151.2 ± 0.11	210.4 ± 0.88
1400	156.8 ± 0.46	172.3 ± 0.61	107.8 ± 0.39	187.5 ± 0.93
1600	138.5 ± 1.56	148.2 ± 1.37	90.6 ± 1.87	150.9 ± 2.01
1800	111.4 ± 1.91	139.2 ± 0.81	65.8 ± 1.44	104.6 ± 1.93
2000	**98.2 ± 0.89**	**131.6 ± 1.27**	**51.5 ± 1.06**	**89.9 ± 0.88**

Results are expressed as averages ± standard deviation (*n*=2)

From Table 25, it was found that under same conditions, EOWWS biodiesel exhibited minimum amount of CO and NOx emissions in comparison to commercial diesel, with both showing a linear decrease of gas emissions proportionately to the increase in engine speed, reaching an average 51.5 ppm/g/h of NOx emissions for EOWWS biodiesel and 89.9 ppm/g/h for the diesel sample at 2000 rpm engine speed. In terms of amounts of CO measured, the EOWWS biodiesel showed 249.3 ppm and the commercial diesel 310.4 ppm at the lowest

speed (800 rpm) used to run these tests to investigate their prospective impacts on the environment. These results were very similar to findings reported by several researchers.

Alhassan *et al.* (2015), in their work on IC engines with diesel and biodiesel, did a comparitive study of nitrogen oxide emission for diesel and biodiesel in terms of their respective compression ratios in the cylinder, and established a link with NOx and CO emissions. They found that biodiesel produced lower NOx emissions from the engine compared to diesel at 960 ppm and 1093 ppm respectively. Additionally, they reported that NOx emissions decreased for biodiesel under full load conditions but slightly increased under partial load condition.

Öztürk (2015) used different blend ratios of biodiesel (canola oil based biodiesel to commercial diesel) in an IC engine and evaluated their performances. When investigating on the performance of a single cylinder diesel engine fed with biodiesel blend of 80% canola oil, he reported a significant decrease the ignition delay and heat release rate and improve the injection and combustion duration. This was very similar with the findings in the current study whereby EOWWS biodiesel had a higher HHV as compared to the canola oil/biodiesel blend, and realised better thermal efficiency in the IC engine (*Section 4.4.5.2*).

Additionally, Labeckas and Slavinskas (2006) reporting on the performance and emission of a diesel engine fed at 5-30% by volume blends of rapeseed and jet fuel at engine speed varying from 1400 to 2200 rpm, have indicated that brake thermal efficiency of blended fuels was maximally 3.6% higher than clean jet fuel. And these findings show how environment-friendly prepared biodiesel was in comparison to commercial fossil fuel.

CHAPTER FIVE: CONCLUSIONS AND RECOMMENDATIONS

Monounsaturated oil and fermentable sugars were successfully extracted from edible oil waste water sludge for biodiesel production. A maximum biodiesel yield of 88% was obtained with a nano-magnetic heterogeneous catalyst prepared from cupriferous mineral processing gangue. The prepared biodiesel performance was evaluated in a diesel engine and the thermal efficiency obtained was 30.75% (compared to 28.4% and 26.95 for conventional biodiesel and petroleum-based commercial diesel, respectively). The fuel consumption was higher than commercial diesel at a maximum brake power of 12.8 kW (0.15 and 0.31 kg/kW.h for commercial diesel and wastewater sludge biodiesel respectively).

This study showed that it is feasible to produce biodiesel from oil extracted from wastewater sludge using a novel nano-magnetic catalyst prepared from carbonaceous tailings (dolomite) from cupriferous mineral processing. This technology has the potential to reduce material costs (using wastes as raw materials), energy consumption (avoiding centrifugation for catalyst separation) and water usage (homogenised transesterification) associated with conventional biodiesel production technologies. Additionally, this study demonstrated that producing bioethanol and biodiesel from edible oil wastewater sludge can contribute positively to waste reduction (from the water and the mining sector), serving as sustainable resource recovery (nano-catalyst, bioethanol and biodiesel), and addressing the issue of food insecurity.

Prior scaling-up this process, further research is required to improve the yield of bioethanol and biodiesel as well as the reusability of catalysts. Furthermore, a proper techno-economic analysis should be performed in order to assess the detailed feasibility of this study.

REFERENCES

Abdullah, Sianipar, R.N.R., Ariyani, D., and Nata, I.F. 2017. Conversion of palm oil sludge to biodiesel using alum and KOH as catalysts. *Sustainable Environment Research*, 27(1):291-295.

Abdul-Majeed, W.S., AAl-Thani, G.S., and Al-Sabahi, J. N. 2016. Application of flying jet plasma for production of biodiesel fuel from wasted vegetable oil. *Plasma Chemistry Plasma Processing.* 36:1517-1531.

Adewale, P., Vithanage, L.M., and Christopher, L. 2017. Optimization of enzyme-catalyzed biodiesel production from crude tall oil using Taguchi method. *Energy Conservation and Management*. 154:81-91.

Agarwal, A.K. and Rajamanoharan K. 2009. Experimental investigations of performance and emissions of Karanja oil and its blends in a single cylinder agricultural diesel engine. *Applied Energy*. 86(1):106–112.

Akoh, C.C., Chang, S.W., Lee, G.C., and Shaw, J.F. 2007. Enzymatic approach to biodiesel production. *Journal of Agricultural and Food Chemistry.* 55:8995-9005.

Alba-Rubio, A.C., Gonzalez, J.S. and Josefa, M. 2010. Heterogeneous Transesterification Processes by using CaO supported on zinc oxide as basic catalysts. *Catalysis Today.* 149:281-28.

Al-Hamamre, Z., Foerster, S., Hartmann, F., Kröger, M., and Kaltschmitt, M. 2012. Oil extracted from spent coffee grounds as a renewable source for fatty acid methyl ester manufacturing. *Fuel.* 96:70–76.

Alhassan, F.H., Rashid, U., and Taufiq-Yap, Y.H. 2015. Synthesis of waste cooking oil-based biodiesel via effectual recyclable bi-functional Fe2O3MnOSO42−/ZrO2 nanoparticle solid catalyst. *Fuel.* 142:38–45.

Allioux, F.-M., He, L., She, F., Hodgson, P. D., Kong, L., and Dumée, L. F. 2015. Investigation of hybrid ion-exchange membranes reinforced with non-woven metal meshes for electro-dialysis applications. *Journal of Separation and Purification Technology.* 147:353–363.

Almeida, J.R.M., Modig, T., Petersson, A., Hahn-Hagerda, l.B., Lidén, G., and Gorwa-Grauslund, M.F. 2007. Increased tolerance and conversion of inhibitors in lignocellulosic hydrolysates by Saccharomyces cerevisiae. *Journal of Chemical Technology and Biotechnol*ogy 82(4):340-349.

Al-Sakkari, E.G., El-Sheltawy, S.T., Attia, N.K., and Mostafa, S.R. 2017. Kinetic study of soybean oil methanolysis using cement kiln dust as a heterogeneous catalyst for biodiesel production. *Appl Catal B*. 206:146-157.

Alsalme, A., Kozhevnikov, E.F. and Kozhevnikov IV. 2008. Heteropoly acids as catalysts for liquid-phase esterification and transesterification. *Applied Catalysis A: General.* 349 :170-176.

Althor, G., Watson, J.E.M. and Fuller, R.A. 2016. Global mismatch between greenhouse gas emissions and the burden of climate change. *Scientific Reports*. 5:72-81.

Althuri, A.A., Sanjeev, K., Knawang, C.S. and Banerjee, R. 2016. Bioconversion of hemicelluloses of lignocellulosic biomass to ethanol: an attempt to utilize pentose sugars. *Biofuels in the future bioeconomy.* (1):431-444 .

Al-Zuhair, S. 2007. Production of biodiesel, possibilities and challenges. *Biofuels, Bioproducts and Biorefining*. 1:57-66.

Amani, H., Ahmad, Z. and Hameed, B.H. 2014. Synthesis of fatty acid methyl esters via the methanolysis of palm oil over Ca3.5xZr0.5yAlxO3 mixed oxide catalyst. *Renewable Energy.* 66:680–685.

Amini, Z., Ilham, Z., Ong, H.C., Mazaheri, H., and Chen, W.H. 2017. State of the art and prospective of lipase-catalyzed transesterification reaction for biodiesel production. *Energy Conversion and Management.* 141:339-353.

Aransiola, E., Daramola, M., Ojumu, T., Solomon, B. and Layokun, S. 2013. Homogeneously catalyzed transesterification of nigerian jatropha curcas oil into biodiesel: a kinetic study. *Modern Research in Catalysis.* 2:83-89.

Arrieta, A.R.A., Garrido, J.A.P. and Castellanous, F.J.S. 2005. Palm oil transesterification with methanol via heterogeneous catalysyst. *Ingenieria e Investigacion.* 25 :1-77.

Arzamendi, G., Arguinarena, E., Campo, I., Zabala, S. and Gandia, L.M. 2008. Alkaline and alkaline-earth metals compounds for the methanolysis of sunflower oil. *Catalysis Today.* 133:305-313.

Asif, S., Ahmad, M., Bokharie, A., Chuahg, L.F., Klemeš, J.J., Akbarj, M.M., Sultana, S. and Yusupe, S. 2017. Methyl ester synthesis of Pistacia khinjuk seed oil by ultrasonic-assisted cavitation system. *Industrial Crops Production*. 108:336-347.

Association of Official Analytical Chemists (AOAC). 2005. AOAC 996.06. Oils and Fat. 18th Edition.

ASTM, American Society for Testing and Materials, International Standards Worldwide, 2016, http://www.astm.org/Standards/D6751.htm.

ASTM. 2001. Standards. A. International. 100 Barr Harbor Drive, PO Box C700, West Conshohocken, Pennsylvania, USA 19428-2959, ASTM International.

Atabani, A.E. and César, A.S. 2014. Calophyllum inophyllum L.: A prospective non-edible biodiesel feedstock. Study of biodiesel production, properties, fatty acid composition, blending and engine performance. *Renewable and Sustainable Energy Reviews.* 37(55):644.

Atabani. A. E., Silitonga, A.S., Badruddina, I.A., Mahliaa, T.M.I., Masjukia, H.H., Mekhilefd, S. 2012. A comprehensive review on biodiesel as an alternative energy resource and its characteristics. *Renewable and Sustainable Energy Reviews.* 16:2070– 2093.

Atadashi, I.M., Aroua, M.K. and Abdul, A. 2011. Biodiesel Separation and Purification: A review. *Renewable Energy*. 36 (1): 437-443.

Atadashi, I.M., Aroua, M.K., Abdul Aziz, A.R. and Sulaiman, N.M.N. 2011. Membrane biodiesel production and refining technology: a critical review. *Renew. Sustain. Energy Reviews.* 15, 5051–5062.

Avhad, M.R. and Marchetti, M. 2015. A review on recent advancement in catalytic materials for biodiesel production. Renewable and Sustainable *Energy reviews.* 50:696-718.

Awang, R., Ghazuli, M.R. and Basri, M. 2007. Immobilization of lipase from Candida rugosa on palm-based polyurethane foam as a support material. *American Journal of Biochemistry and Biotechnology*. 3:163-166

Awolu, O.O. and Layokum, S.K. 2013. Optimization of two-step transesterification production of biodiesel from neem (Azadirachtaindica) oil. *International Journal of Energy and Environmental Engineering*. 4:39-48.

Azcan, N. and Yilmaz, O. 2014. Energy consumption of biodiesel production from microalgae oil using homogeneous and heterogeneous catalyst. *IAENG Transactions on Engineering Technologies*. 247:651-664.

Bailis, R., Ezzati, M. and Kammen, D.M. 2005. Mortality and greenhouse gas impacts of biomass and petroleum energy futures in Africa. *Science 308*. 5718:98-103.

Bajaj, A., Lohan, P., Jha, P. N. and Mehrotra, R. 2010. Biodiesel production through lipase catalysed transesterification: an overview. *Journal of Molecular Catalysis B*. 1(62):9-14.

Balat, M. and Balat, H. 2009. Recent trends in global production and utilization of bioethanol fuel. *Applied Energy.* 86:2273–2282.

Balat, M. and Balat, H. 2010. Progress in biodiesel processing. *Applied Energy.* 87:1815-1835.

Banerjee, A., Chakraborty, R. and Bepari, S. 2011. Application of calcined waste fish (Labeorohita) scale as low-cost heterogeneous catalyst for biodiesel synthesis. *Bioresourc and Technology.* (8) 102:3610.

Barot, V.B. and Andher, S.S. 2015. Application of some available formulas of specific refraction for edible oils. *Research Journal of Physical Sciences* 3(10): 2320–4796.

Baskar, G., Selvakumari, A.E., Aiswarya, R. 2017. Biodiesel production from castor oil using heterogeneous Ni doped ZnO nanocatalyst. *Bioresour Technol*. 250:793-798.

Berchmans, H.J. and Hirata.S. 2008. Biodiesel production from crude Jatropha curcas L.seed oil with a high content of free fatty acids. *Bioresource and Technology.* 99:1716–1721.

Berchmans, H.J., Morishita, K. and Takarada, T. 2013. Kinetic study of hydroxide-catalyzed methanolysis of Jatropha curcas–waste food oil mixture for biodiesel production. *Fuel*. 104 :46–52.

Bergeret, G., Desmartin-Chomel, A., Palomeque, J. and Essayem, N. 2010. Basic properties of MgLaO mixed oxides as determined by microcalorimetry and kinetics. *Catalysis Today.* 152:110-114.

Bergquist, P.L., Teo, V.S.J., Gibbs, M.D., Curah, N.C. and Nevalainen, K.M.H. 2004. Recombinant enzymes from thermophilic micro-organisms expressed in fungal hosts. *Biochemical Society Transaction*. 32(2):293–297.

Beydoun, D., Amal, R., Low, G.K.C. and McEvoy, S. 2000. Novel photocatalyst: titania-coated magnetite: activity and photo dissolution. *The Journal of Physical Chemistry B*. 104(96):438796.

Bhuiya, M., Rasul and M., Khan, M. 2016. Prospects of 2nd generation biodiesel as a sustainable fuel–Part 2: properties, performance and emission characteristics. *Renew Sustain Energy Reviews.* 46–55.

Bhuiya, M.M.K., Rasul, M.G. and Khan and M.M.K. 2014. Second generation biodiesel: potential alternative to-edible oil-derived biodiesel. *Energy Processing*. (19):61–72.

Bhushan, I., Parshad, R., Gazi, G. and Gupta, V.K. 2008. Immobilization of lipase by entrapment in ca-alginate beads. *Journal of Bioactive and Compatible Polymers*. 23:552-562.

Bobade, V.V., Kulkarni, K.S. and Kulkarni, A.D. 2011. Application of heterogeneous catalyst for the production of biodiesel. *International Journal of Advanced Engineering Technology*. 2(1):184-185.

Boulbabac, L., Belgaib, J. and Benamor, N.H. 2017. Production of bio-ethanol from three varieties of dates. *Biofuels in the Future Bioeconomy*. 4(8):41-50

Butler, A.P., Brook, C., Godley, A., Lewin, K. and Young, C.P. 2003. Attenuation of landfill leachate in unsaturated sandston. *Ninth International Landfill Symposium*, CISA Publisher.

Canakci, M., 2007. The potential of restaurant waste lipids as biodiesel feedstocks. *Bioresource Technology.* 98: 183-190.

Capolupo, L. and Faraco, V. 2016. Green methods of lignocellulose pretreatment for biorefinery development. *Applied Microbiology and Biotechnology.* 100:9451–9467.

Centi, G. and Perathoner, S. 2008. Catalysis by layered materials: A review. *Microporous and Mesoporous Materials*. 107(2):3-15

Chen, S.Y., Mochizuki, T., Abe Y., Toba, M. and Yoshimura, Y. 2014. Ti-incorporated SBA-15 mesoporous silica as an efficient and robust Lewis solid acid catalyst for the production of high-quality biodiesel fuels. *Applied Catalysis B. Environment.* 148:344–356.

Chinnusamy, T.R., Murugesan, A., Umarani, C., Krishnan, M., Subramanian, R. and Neduzchezhain, N. 2009. Production and analysis of bio-diesel from non-edible oils. *Renewable and Sustainable Energy Reviews* 13: 825–834.

Coulson, J.M. and Richardson, J.F. 2002. Coulson's and Richardson's Chemical Engineering Handbook. In. R.P Chhabra, Basavaraj Gurappa (Ed). . Butterworth-Heinemann, United kingdom.

Cowie, A., Soimakallio, S. and Brandao, M. 2016. Environmental Risks and Opportunities of Biofuels. In Bouthillier, Y.L., Cowie, A., Martin, P., McLeod-Kilmurray, H., Eds. *The Law and Policy of Biofuels*. Cheltenham: Edward Elgar.

Darnoko, D., & Cheryan, M. 2000. Continuous production of palm methyl esters. *Journal of the American Oil Chemists' Society*. 77:1263-127.

Demirbas, A. 2001. Biomass resource facilities and biomass conversion processing for fuels and chemicals. *Energy Conversion and Management.* 42 (11):1357-1378.

Demirbas, A. 2003. Biodiesel fuels from vegetable oils via catalytic and non-catalytic supercritical alcohol transesterifications and other methods: a survey. *Energy Conversion and Management.* 44 (13):2093-2109.

Demirbas, A. 2003. Biodiesel fuels from vegetable oils via catalytic and non- catalytic supercritical alcohol transesterifications and other methods: /a survey. *Energy Convers Manage*. 44:2093-109.

Demirbas, A. 2007. Importance of biodiesel as transportation fuel. *Energy Policy*. 35:4661-4670.

Demirbas, A. 2009. Biodiesel from waste cooking oil via base catalytic and supercritical methanol transesterification. *Energy Conversion and Management.* 50:923-927.

Demirbas, A., Bafail, A., Ahmad, W. and Sheikh, M. 2016. Biodiesel production from non-edible plant oils. *Energy Exploration and Exploitation*. 34:290–318.

Demirbas, A.H. and Demirbas, I. 2007. Importance of rural bioenergy for developing countries. *Energy Conversion and Management*. 48: 2386-2398.

Department of Environmental Affairs (DEA). 2014. GHG Inventory for South Africa: 2000 - 2010. Compilation under the United Nations Framework Convention on Climate Change, Pretoria: DEA.

Department of Water Affairs (DWA). 2017. Minimum Requirements for Handling. Classification and Disposal of Hazardous Waste. Pretoria.

Di Serio, M., Cozzolino, M., Giordano, M., Tesser, R., Patrono, P. and Santacesaria, E. 2007. From homogeneous to heterogeneous catalysts in biodiesel production. *Industrial & Engineering Chemistry Research*. 46:6379-6384.

Di Serio, M., Tesser, R., Pengmei, L. and Santacesaria, E. 2008. Heterogeneous catalysts for biodiesel production*. Energy Fuels*. (207):17-22.

Dias, J.M., Alvim-Ferraz, MC. M., Almeida, M.F. 2008. Comparison of the performance of different homogeneous alkali catalysts during transesterification of waste and virgin oils and evaluation of biodiesel quality. Journal/volume/issue/page range?

Dorado M. P., Ballesteros E., Almeida J. A., Schellert C., Lohrlein H. P. and Krause R. 2002. An alkali-catalysed transesterification process for high free fatty acid waste oils. *Transactions of ASAE*. 45(3):525.

Dossin, T.F., Reyniers, M.F., Berger, R.J. and Marin, G.B. 2006. Simulation of heterogeneously MgO-catalyzed transesterification for fine-chemical and biodiesel industrial production. *Applied. Catalysis. B. Environmental* .67:136-148.

Dufreche, S., Hernandez, R., French, T., Sparks, D., Zappi, M. and Alley E. 2007. Extraction of Lipids from Municipal Wastewater Plant Microorganisms for Production of Biodiesel. *J American Oil Chemical Society*, 84:181-187.

Duval, Y. 2001. Environmental impact of modern biomass cogeneration in Southeast Asia*. Biomass and Bioenerg.* 20(4):287-295.

Elfimov, I.S., Yunoki S. and Sawatzky, G.A. 2002. Possible path to a new class of ferromagnetic and half-metallic ferromagnetic materials. *Physical Review Letters.* 89:216-403.

Ellermann, T., Nøjgaard, J.K., Nordstrøm, C., Brandt, J., Christensen, J., Ketzel, M., Jansen, Massling, A. and Jensen, S. S. 2013. *The Danish Air Quality Monitoring Programme. Annual Summary for 2012*. Publisher?

Elumalai, S. and Thangavelu, V. 2010. Simultaneous sacccharification and fermentation (SSF) of pretreated sugarcane bagasse using cellulase and Saccharomyces cerevisiae. Kinetics and modeling. *Chemical Engineering Research Bullettin*. 14(1):29-35.

Endalew, A.K., Kiros, Y. and Zanzi, R. 2011. Inorganic heterogeneous catalysts for biodiesel production from vegetable oils. *Biomass and Bioenergy*. 35:3787-3809.

Faaij, A. 2006. Modern Biomass Conversion Technologies. Mitigation and Adaptation. *Strategies for Global Change.* 2(11):335-367.

Fadhil A. 2013. Biodiesel production from beef tallow using alkali-catalyzed transesterification. *Arab J Sci Eng.* (38)41–47.

Fan, M., Huang, J., Yang, J. and Zhang, P. 2013. Biodiesel production by transesterification catalyzed by an efficient choline ionic liquid catalyst. *Applied Energy.* 108:333–339.

Farooq M, Ramli A and Subbarao D. 2013. Biodiesel production from waste cooking oil using bifunctional heterogeneous solid catalysts*. Journal of Cleaner Production*. 59: 131–140.

Farooq, M., Ramli, A. and Naeem, A. 2015. Biodiesel production from low FFA waste cooking oil using heterogeneous catalyst derived from chicken bones. *Renewable Energy.* 76(8):362.

Farrell, A., Plevin, R.J., Turner, B.T., Jones, A.T., O'Hare, M. and Kammen, D.M. 2006. Ethanol Can Contribute to Energy and Environmental Goals. *Science. 311*(27)::506-508.

Feng, Y., He, B., Cao, Y., Li, J., Liu, M., Yan, F. and Kiang, X. 2010. Biodiesel production using cation-exchange resin as heterogeneous catalyst. *Bioresource Technology.* 101:1518-1521.

Feng, Y., Qiu, T., Yang, J., Li, L., Wang, X. and Wang, H. 2017. Transesterification of palm oil to biodiesel using Brønsted acidic ionic liquid as high-efficient and eco-friendly catalyst. *Chinese Journal of Chemical Engineering.* 25:1222-122.

Figiel, S. and Hamulczuk, M. 2014. The effects of increase in production of biofuels on world agricultural prices and food security. *European Scientific Journal.* (10) 9:10–17.

FitzPatrick, M., Champagne, P., Cunningham, M., F. and Whitney, R.A. 2010. A biorefinery processing perspective: Treatment of lignocellulosic materials for the production of value addued products. *Bioresource Technology.* 101(23):8915-8922.

Fjerbaek, L., Christensen, V.K. and Norddahl, B. 2009. A review of the current state of biodiesel production using enzymatic transesterification. *Biotechnology and Bioengineering*. 102:1298-1315.

Frisch, A. and Pizarek, T. 2008. Two methods for determining the moment of a magnet inside a cue ball, *Wabash. Journal of Physics.* volume/issue/page range

Fukuda, H., Kondo, A. and Noda, H. 2009. Biodiesel fuel production by transesterification of oils. *Journal of Bioscience and Bioengineering*. 92: 405-416.

Fulton, L., Howes, T. and Hardy, J. 2004. *Biofuels for Transport: An International Perspective*. Paris: International Energy Agency.

Gan, S., Ng, J-H. and Ng, H.K., 2012. Characterisation of engine-out responses from a light-duty diesel engine fuelled with palm methyl ester (PME). *Applied Energy.* 90:58–67.

Gao, G., Feng, Y., Guo, H. and Liu, S. 2011. Synthesis, structure characterization, and engine performance test of ethylene glycol-n-propyl ether palm oil monoester as biodiesel. *Energy and Fuels.* 25:4686-4692.

Gao, X., Yu, K.M.K., Tam, K.Y. and Tsang, S.C. 2003. Colloidal stable silica encapsulated nano magnetic composite as a novel bio-catalyst carrier*. Chemical Communications*. 24(9):2998.

Gao, Y., Xu J., Zhang, Y., Yu, Q., Yuan, Z. and Liu, Y. 2013. Effects of different pretreatment methods on chemical composition of sugarcane bagasse and enzymatic hydrolysis. *Bioresource Technology*. 144:396-400.

Gaurav, K., Srivastava, R. and Singh R. 2013. Exploring biodiesel, chemistry, biochemistry and microalgal source*. International Journal of Green Energy*. 10:775-796.

Gaurav, K., Srivastava, R., Sharma, J.G., Singh, R. and Singh, V. 2016. molasses based growth and lipid production by Chlorella pyrenoidosa, a potential feedstock for biodiesel*. International Journal of Green Energy*.13: 320-327.

Gaurav, P., Rathod, R., Kagdi D., Nileshkumar R.J., Ahmedabad T.J. and Patel, M. 2015. Effect of blend ratio of plastic pyrolysis oil and diesel fuel on the performance of single cylinder CI engine. *International Journal of Science Technology & Engineering*. 1(11):2349-784.

Georgogianni, K.G., Katsoulidis, A.P., Pomonis, P.J. and Kontominas, MG. 2009. Transesterification of soybean frying oil to biodiesel using heterogeneous catalysts. *Fuel Process Technol*ogy. 90:671-676.

Ghadge S. V., and Raheman H. 2008. Biodiesel production from mahua (Madhuca indica) oil having high free fatty acids. *Biomass and Bioenergy.* (28):601-605.

Ghanei, R., Moradi, G.R., Kalantari, T.R. and Arjmandzadeh E. 2011. Variation of physical properties during transesterification of sunflower oil to biodiesel as an approach to predict reaction progress. *Fuel Processing Technology.* 92:1593-1598.

Gildemeister, B., Thiex, N. and Anderson, S. 2003. Crude fat, diethyl ether extraction, in feed, cereal grain, & forage (Randall/ Soxtec/Submersion method): a collaborative study. *JAOAC Int.* 86:899–908.

Ginzburg B. Z. 1993. Liquid fuel (oil) from halophilic algae: a renewable source of non-polluting energy. *Renewable Energy*. (3):249-252.

Granados, M.L., Poves, M.D.Z., Alonso, D.M., Mariscal, R., Galisteo, R.F.C., Moreno, R., Santamaría, J. and Fierro, J.L.G. 2007. Bio-diesel from sunflower oil by using activated calcium oxide. *Applied Catalysis B, Environmental.* 73:317-326.

Guillen J., Lany, S., S. Barabash, S.V. and Zunger, A. 2006. Model for ferromagnetism in d^0 materials. *Physical Review Letters.* (96):107-203.

Guldhe, A., Singh, B., Rawat, I., Permaul, K. and Bux, F. 2015. Biocatalytic conversion of lipids from microalgae Scenedesmus obliquus to biodiesel using Pseudomonas fluorescens lipase. *Fuel*.147:117-124.

Guldhe, A., Singh, P., Faiz Ahmad Ansari, F.A., Singh, B. and Bux, F. 2017. Biodiesel synthesis from microalgal lipids using tungstated zirconia as a heterogeneous acid catalyst and its comparison with homogeneous acid and enzyme catalysts. *Fuel.* 187:180-188.

Guo, W., Li, H., Ji, G. and Zhang, G. 2012. Ultrasound-assisted production of biodiesel from soybean oil using Brønsted acidic ionic liquid as catalyst. *Bioresource Technology.* 125:332–334.

Gupta, A.R., Yadav, S.V. and Rathod, V.K. 2015. Enhancement in biodiesel production using waste cooking oil and calcium diglyceroxide as a heterogeneous catalyst in presence of ultrasound*. Fuel*. 158:800-806.

Gupta, R., Gupta, N. and Rathi, P. 2004. Bacterial lipases: an overview of production, purification and biochemical properties. *Appl Microbiol Biotechnol.* 64:763–781.

Gutiérrez, L., Óscar F., Sánchez, J., Carlos A. and Cardona. 2009. Process integration possibilities for biodiesel production from palm oil using ethanol obtained from lignocellulosic residues of oil palm industry. *Bioresource Technology*. 100:1227-1237.

Hassani, M., Najafpour, G.D., Mohammadi, M. and Rabiee, M. 2014. Preparation, characterization and application of zeolite-based catalyst for production of biodiesel from waste cooking oil. *Journal of Scientific and Industrial Research.* 73:129-133.

Hazell, P. and Pachauri, R.K. 2006. Bioenergy and Agriculture: Promises and Challenges. *International Food Policy Research Institute 2020 Focus.* 14:41-58.

Helwani, Z., Othman, M.R., Aziz, N., Fernando, W.J.N. and Kim, J. 2009. Technologies for production of biodiesel focusing on green catalytic techniques, A review*. Fuel Processing Technology*. 90:1502-1514.

Helwani, Z., Othman, M.R., Aziz, N., Kim, J. and Fernando, W.J.N. 2009. Solid Heterogeneous Catalysts for Trans-esterification of Triglycerides with Methanol. *Applied Catalysis A*. 363(2009):1-10.

Herrera, V.A.C., Gómez-Rodríguez, J., Hayward-Jones, P.M., Dulce María Barradas-Dermitz, D.M. and Aguilar-Uscanga, M.G. 2017. In-situ monitoring of Saccharomyces cerevisiaeITV01 bioethanol process using near-infrared spectroscopy NIRS and chemometrics. *Biotechnology Progress*. 32:510-517.

Herrera, W., Rivera, E., Alvarez, L.A., Plazas Tovar, L., Tamayo Rojas, S., Yamakawa, C. and Bonomi, A., Maciel Filho, R. 2016. Modelling and control of a continuous ethanol fermentation using a mixture of enzymatic hydrolysate and molasses from sugarcane. *Chemical Engineering Transactions*. 50:169-174.

Hu, S., Guan, H., Wang, Y. & Han, H. 2011. Nano-magnetic catalyst KF/CaO–Fe_3O_4 for biodiesel production. *Applied Energy*. 88(1):2688-268.

Hu, S., Li, Y. and Lou, W. 2017. Novel efficient procedure for biodiesel synthesis from waste oils with high acid value using 1-sulfobutyl-3-methylimidazolium hydrosulfate ionic liquid as the catalyst. *Chinese Journal of Chemical Engineering.* 25:1519-1523.

Huang, H.-J., Ramaswamy, S., Tschirner, U. and Ramarao, B. 2008. A review of separation technologies in current and future biorefineries. *Journal of Separation and Puriication Technology.* 62:1–21.

International Energy Agency. 2017. Renewables – Bioenergy. International Energy Agency (IEA), Paris. Avaliable at: http//:www.iea.org/Topics/Renewables/Subtopics (Retrieved on 11th November 2017).

Iroba, K.L. and Tabil, L.G. 2013. Lignocellulosic biomass feedstock characteristics, pretreatment methods and pre-processing of biofuel and bioproduct applications. *Biomass Processing, Conversion and Biorefinery.* 10:61–98.

Iroba, K.L., Tabil, L.G., Sokhansanj, S. and Meda, V. 2014. Producing durable pellets from barley straw subjected to radio frequency-alkaline and steam explosion pretreatments*. International. Journal of Agriculture and Biology Engineering*. 7:68–82.

Issariyakul, T., Kulkarni, M.G., Meher, L.C., Dalai, A.K. and Bakhshi, N.N. 2008. Biodiesel production from mixtures of canola oil and used cooking oil. *Chemical Engineering Journal.* 140:77–85.

Jamil F, Al-Muhtaseb AH, Al-Haj L, Al-Hinai MA, Hellier P, Rashid U. 2016. Optimization of oil extraction from waste “Date pits” for biodiesel production. *Energy Conversion Manage*. 117 :264–272.

Janssen, R., Turhollow, A.F., Rutz, D. and Mergner, R. 2013. Production facilities for second-generation biofuels in the USA and the EU—current status and future perspectives. *Biofuels, Bioprodaction and Biorefining*. 7:647–665.

Jiménez-Morales, I., Santamaría-González, J., Maireles-Torres, P. and Jiménez-López, A. 2014. Calcined zirconium sulphate supported on MCM-41 silica as acid catalyst for ethanolysis of sunflower oil. *Applied Catalysis B and Environmental.* 103(1):91-98.

Kammen, D., Kapadia, K. and Fripp, M. 2004. Putting renewables to work: how many jobs can the clean energy industry generate. *Report of the Renewable and Appropriate Energy Laboratory*, Energy and Resources Group/Goldman School of Public Policy at University of California, Berkeley. Insert URL.

Kang, K.E., Chung, D.-P. and Kim. 2015. High-titer ethanol production from simultaneous saccharification and fermentation using a continuous feeding system. *Fuel.* 145:18–24.

Kang, Q., Appels, L., Tan, T and Dewil, R. 2014. Bioethanol from lignocellulosic biomass: Current findings determine research priorities. *Sci. World J.* 7:211-220.

Kangala B. C. and Krystyna M. 2008. Characterization of the fate of lipids in activated sludge. *Journal of Environmental Sciences*. 20:536-54.

Karaosmanoglu, F., Cigizoglu, K.B., Tüter, M. and Ertekin, S. 1996. Investigation of the refining step of biodiesel production. *Energy & Fuels*. 10:890-895.

Karmee S.K., Raffel Dharma P. R. and Sze K. L. C. 2015. Techno-economic evaluation of biodiesel production from waste cooking oil - a case study of Hong Kong. *International Journal of Molecular Sciences. 16*(3):4362-4371.

Karmee, S.K., Chandna, D., Ravi, R. and Chadha, A. 2006. Kinetics of base-catalyzed transesterification of triglycerides from Pongamia oil. *Journal of the American Oil Chemists Society.* 83:873-877.

Kawashima, A., Matsubara, K. & Honda, K., 2008. Development of heterogeneous base catalysts for biodiesel production. *Bioresource Technology.* 99:3439-3443.

Kim S., Dale B.E. 2004. Global potential bioethanol production from wasted crops and crop residues. *Biomass Bioenergy.* 26(4):361-375.

Kim, M., Yan, S., Salley, S. and Ng, K.Y.S. 2010. Competitive transesterification of soybean oil with mixed methanol/ethanol over heterogeneous catalysts. *Bioresource Technology.* (101):4409-441.

Kim, S., and Dale, B. 2004. Global potential bioethanol production from wasted crops and crop residues. *Biomass and Bioenergy.* 26(4):361-375.

Kiss, A. A. 2010. Separative reactors for integrated production of bioethanol and biodiesel. *Computers and Chemical Engineering*. (34):812-820.

Kiss, F. and Boskovic, G. 2012. Life cycle energy requirements of biodiesel produced from rapeseed oil in Serbia. *Processing and Energy in Agriculture* (16):28-3

Knothe, G. 2008. Designer biodiesel: optimizing fatty ester composition to improve fuel properties. *Energy Fuels.* 22:1358–1364.

Knothe, G. and Razon, L.F. 2017. Biodiesel Fuels. *Progress in Energy and Combustion Science*. 58:36-59.

Koçar, G. and Civas, N. 2013. An overview of biofuels from energy crops: Current status and future prospects. *Renew Sustain Energy Rev*. 28:900–916.

Konaka, A., Tago, T., Yoshikawa, T., Shitara, H., Nakasaka, Y. and Masuda, T. 2013. Conversion of biodiesel-derived crude glycerol into useful chemicals over a zirconia–iron oxide catalyst. *Industrial and Engineering Chemistry Research*. 52:15509–15515.

Kose, O., Tuter, M., and Aksoy, H. A. 2002. Immobilized *Candida Antarctica* lipase catalysed alcoholysis of cotton seed oil in a solvent-free medium. *Bioresource Technology*. 83:125–129.

Kouzu M, Kajita A and Fujimori A. 2016. Catalytic activity of calcined scallop shell for rapeseed oil transesterification to produce biodiesel. *Fuel*. 182: 220–226.

Kouzu, M., Kasuno, T., Tajika, M., Yamanaka, S. and Hidaka, J. 2007. Active phase of calcium used as solid base catalyst for transesterification of soybean oil with refluxing methanol. *Applied Catalysis A*. (334):357.

Krishnan, D. 2012. A kinetic study of biodiesel in waste cooking oil. *African Journal of Biotechnology*. 11:9797-9804.

Kulkarni, M. G., Dalai, A. K., and Bakhshi, N. N. 2007.Transesterication of canola oil in mixed methanol/ ethanol system and use of esters as lubricity additive. *Bioresource Technolology*. (98):2027-2033.

Kumar, D., Singh, V. 2016. Dry-grind processing using amylase corn and superior yeast to reduce the exogenous enzyme requirements in bioethanol production. *Biotechnol Biofuels.* 9:228.

Kumar, P., Barrett, D.M., Delwiche, M.J. and Stroeve, P. 2009. Methods for pretreatment of lignocellulosic biomass for efficient hydrolysis and biofuel production. *Industrial & Engineering Chemistry Research.* 48(8):3713-3729.

Kumar, R. and Wyman, C.E. 2009. Effect of xylanase supplementation of cellulase on digestion of corn stover solids prepared by leading pretreatment technologies. *Bioresour Technol.* 100:4203–4213.

Kumar, S.P.J. and Banerjee, R. 2013. Optimization of lipid enriched biomass production from oleaginous fungus using response surface methodology. *Indian Journal for Experimental Biology.* 51:979–983.

Kusdiana, D. and Saka, H. 2004. Effects of water on biodiesel production by supercritical methanol treatment. *Bioresource Technology.* 91:289.

Laopaiboon, L., Thanonkeo, Jaisil, P. and Laopaiboon, P. 2007. Ethanol production from sweet sorghum juice in batch and fed-batch fermentations by Saccharomyces cerevisiae, *World Journal of Microbiology and Biotechnology.* 23:1497–1501.

Lavarack, B.P., Griffin, G.J. and Rodman, D. 2002. The acid hydrolysis of sugarcane bagasse hemicellulose to produce xylose, arabinose, glucose and other products. *Biomass and Bioenergy.* 23:367-380.

Leung, D. Y. C., Koo, B. C. P. and Guo, Y. 2006. Degradation of biodiesel under different storage conditions*. Bioresource Technology*. 97(2): 250-256.

Lida, H., Takayanagi, K., Nakanishi, T. and Osaka, T. 2007. Synthesis of Fe_3O_4 nanoparticles with various sizes and magnetic properties by controlled hydrolysis*. Journal of Colloid Interfaces in Sciences*. 80:274-314.

Liu X, He H, Wang and Zhu S. 2007. Transesterification of soybean oil to biodiesel using SrO as a solid base catalyst. *Catalysts Communications.* 8:1107-1111.

Liu, X., Piao, X., Wang, Y., Zhu, S. and He, H. 2008. Calcium methoxide as a solid base catalyst for the transesterification of soybean oil with methanol. *Fuel.* 87:716-717.

Liu, Y., Lu, H., Nyarko, K.A., MacDonald, T., Tavlarides, L.L., Liu, S. and Liang, B. 2016. Kinetic studies on biodiesel production using a trace acid catalyst. *Catalysis today*. 264:55-62.

Liu, Y., Tu, Q., Knothe, G. and Lu, M., 2017. Direct transesterification of spent coffee grounds for biodiesel production. *Fuel* 199, 157–161.

Long, Y-D., Fang, Z., Su, T-C. and Yang, Q. 2014. Co-production of biodiesel and hydrogen from rapeseed and Jatropha oils with sodium silicate and Ni catalysts. *Applied Energy.* 113:1819-1825.

Lotero, E., Liu, Y., Lopez, D.E., Suwannakarn, K., Bruce, D.A. & Goodwin Jr, J.G. 2005. Synthesis of biodiesel via acid catalysis. *Industrial & Engineering Chemistry Research*. 44:5353-5363.

Lu, A.H., Salabas, E.L. and Schiith, F. 2007. Magnetic nanoparticles: synthesis, protection, functionalization, and application. *Cheminternationale*. 46(44) :1222.

Lu, L., Deng, L., Zhao, R., Zhang, R., Wang, F. and Tan, T. 2010. Pretreatment of immobilized Candida sp.99/125 lipase to improve its methanol tolerance for biodiesel production. *Journal of Molecular Catalysis B. Enzymatic.* 62:5-18.

Lynd, L. 1996. Overview and evaluation of fuel ethanol from cellulosic biomass: technology, economics, the environment, and policy. *Annual Review of Energy and the Environment.* 21(1):403-465.

Ma, F. and Hanna, M. A. 1999. Biodiesel production: a review. *Bioresour. Technol.*70:1–15.

Ma, F., Clements, L.D., & Hanna, M.A. 1998. The effects of catalyst, free fatty acids, and water on transesterification of beef tallow. *Transactions of the ASAE-American Society of Agricultural Engineers*. 41:1261-1264.

Mani, S., Tabil, L.G., Sokhansanj, S. 2006. Effects of compressive force, particle size and moisture content on mechanical properties of biomass pellets from grasses. *Biomass Bioenergy.* 30:648–654.

Mann, M. K. and Spath, P.L. 1997. Life cycle assessment of a biomass gasification combined cycle power system. technical report. *National Renewable Energy Lab.* Golden, Colorado. Insert URL

Mardhiah, H.H., Ong, H.C., Masjuki, H.H., Lim, S. and Lee, H.V. 2017. A review on latest developments and future prospects of heterogeneous catalyst in biodiesel production from non-edible oils. *Renew Sustain Energy Rev.* 67:1225-1236

Mardhiah, H.H., Ong, H.C., Masjuki, H.H., Lim, S. and Lee, H.V. 2017. A review on latest developments and future prospects of heterogeneous catalyst in biodiesel production from non-edible oils. *Renewable and Sustainable Energy Reviews.* 67:1225–1236.

Marinkovic, D.M., Avramovic´, J.M., Stankovic, M.V., Stamenkovic, O.S., Jovanovića, D.M. and Veljković, V.B. 2017. Synthesis and characterization of spherically-shaped CaO/γ-Al2O3 catalyst and its application in biodiesel production. *Energy Conversion and Management* 144:399-413.

Mário, L.R. and José, R.S. 2011. Exhaust emissions from a diesel-powered vehicle fueled by soybean biodiesel blends (B3-B20) with ethanol as an additive (B20E2-B20E5*). Fuel.* 90:98-103.

McNeff, C. V., McNeff, L. C., Yan, B., Nowlan, D. T., Rasmussen, M., Gyberg, A. E., Khron, J., Fedie, R. and Hoye, T. R. 2008. A continuous catalytic system for biodiesel production. *Applied Cataysis A*. (343):39-42.

Meher, L.C., Sagar, D.V. and Naik, S.N. 2006. Technical aspects of biodiesel production by transesterification – a review. *Renewable and Sustainable Energy Reviews*. 10:248–268.

Miao X. and Wu Q. 2006, Biodiesel production from heterotrophic microalgal oil. *Bioresource Technology.* 97:841–846.

Micic R. D., Tomic M. D., Kiss E. F., Nikolic-Djoric E. B., Mirko Đ. and Simikic M. D. 2014. Influence of reaction conditions and type of alcohol on biodiesel yields and process economics of supercritical transesterification. *Energy Conversion and Management*. 86:717-726.

Mofijur M, Masjuki HH, Kalam MA, Atabani AE, Shahabuddin M, Palash SM and Hazrat MA. 2013. Effect of biodiesel from various feedstocks on combustion characteristics, engine durability and materials compatibility: a review. *Renewable and Sustainable Energy Reviews*. 28: 441–455.

Mofijur M, Masjuki HH, Kalam MA, Hazrat MA, Liaquat AM, Shahabuddin M, and Varman M. 2012. Prospects of biodiesel feom Jatropha in Malaysia. *Renew Sustain Energy Rev*. 16: 5007–5020.

Mofijur, M., Rasul, M.G. and Hyde, J. 2016. Role of biofuel and their binary (diesel–biodiesel) and ternary (ethanol–biodiesel–diesel) blends on internal combustion engines emission reduction. *Renew Sustain Energy Reviews.* 53:78–265.

Mofijur, M., Rasul, M.G., Hassan, N.M.S., Masjuki, H.H., Kalam, M.A. and Mahmudul, H.M. 2016. Assessment of physical, chemical and tribological properties of different biodiesel fuel. *Clean Energy for Sustainable Development.* 61(1):441.

Montero, J. M., Brown, R., Gai, P. L., Lee, A. F. and Wilsonc, K. 2010. *In situ* studies of structure-reactivity relations in biodiesel synthesis over nanocrystalline MgO. *Chemical Engineering Journal.* (161):332-336.

Montero, J., Wilson, K. and Lee, A. 2010. Cs promoted triglyceride transesterification over MgO nanocatalysts. *Topics in Catalysis.* 53:737-745.

Montero, J., Wilson, K. and Lee, A.F. 2014. Identifying the active phase in Cs-promoted MgO nanocatalysts for triglyceride transesterification. *Journal of Chemical Technology and Biotechnology*. 89:73-80.

Morais, S., Mata, T. M., Martins, A. A., Pinto, G. A. and Costa, C. A. 2010. Simulation and lifecycle assessment of process design alternatives for biodiesel production from waste vegetable oils. *Journal of Cleaner Production.* 18:1251-1259.

Moreira, A.L., Dias J.M., Almeida, M.F. and Alvim-Ferraz, M.C.M. 2010. Biodiesel production through transesterification of poultry fat at 30◦C. *Energy and Fuels*. 24:5717-5721.

Murphy, F., Devlin, G. and McDonnell, K. 2013. The evaluation of flash point and cold filter plugging with blends of diesel and cyn-diesel pyrolysis fuel for automotive engines. The Open *Fuel and Energy Science Journal*. 6:1-8.

Murugesan, A., Umarani, C., Chinnusamy, T.R., Krishnan, M., Subramanian, R. and Neduzchezhain, N. 2009. Production and analysis of biodiesel from non-edible oils, a review. *Renewable and Sustainable Energy Review*. 13**:**825-834.

Nayebzadeh, H., Saghatoleslami, N., Haghighi, M. and Tabasizadeh, M. 2017. Influence of fuel type on microwave-enhanced fabrication of KOH/Ca12Al14O33 nanocatalyst for biodiesel production via microwave heating. *Jornal of Taiwan Institute of Chemical Engineering.* 75:148-155.

Ngamcharussrivichai C, Nunthasanti P, Tanachai S and Bunyakiat K. 2010. Biodiesel production through transesterification over natural calciums. *Fuel Procesing and Technology.* 91(15):1409.

Ngamcharussrivichai, C., Benjapornkulaphong, S. and Bunyakiat, K. 2009. Al_2O_3-supported alkali earth metal oxides for transesterification of palm kernel oil and coconut oil. *Chemical Engineering Joutrnal*. 145:468-474.

Ngamcharussrivichai, C., Totarat, P., and Bunyakiat, K. 2009. K, Ca and Zn mixed oxide as a heterogeneous base catalyst for transesterification of palm kernel oil. *Applied Catalysis A*. 366:154-159.

Nguyen, T.Y., Cai, C.M., Osman, O., Kumar, R. and Wyman, C.E. 2016. CELF pretreatment of corn stover boosts ethanol titers and yields from high solids SSF with low enzyme loadings. *Green Chemistry*. 18:1581–1589.

Nisar, J., Razaq and R., Farooq, M., Iqbal, M., Ali Khan, R., Sayed, M., Shah, A., rahman I. 2017. Enhanced biodiesel production from Jatropha oil using calcined waste animal bones as catalyst. *Renewable Energy*. 101:111-119.

Öhgren, K., Rudolf A., Galbe, M. and Zacchi, G. 2006. Fuel ethanol production from steam-pretreated corn stover using SSF at higher dry matter content. *Biomass Bioenergy*. 30(10):863-869.

Oliveira, D. and Oliveira, J.D. 2001. Enzymatic alcoholysis of palm kernel oil in n-hexane. *Supercritical Fluids*. 19:141–148.

Olkiewicz, M., Fortuny, A., Stuber F., Fabregat, A., Font, J., Bengoa, Ch. 2012. Evaluation of different sludges from WWTP as a potential source for biodiesel production. *Procedia Engineering*. 42:634-643.

Olofsson, K., Bertilsson, M. and Lidén, G. 2008. A short review on SSF – an interesting process option for ethanol production from lignocellulosic feedstocks. *Biotechnology for Biofuels.* 1(7):1-14.

Olsson, L. and Hahn-Hägerdal, B. 1996. Fermentation of lignocellulosic hydrolysates for ethanol production. *Enzyme and Microbial Technology*. 18:312-331.

Olsson, L., Jørgensen, H., Krogh, K.B.R. and Roca, C. 2004. Bioethanol production from lignocellulosic material. In Severian Dumitriu (Ed.) *Polysaccharides: structural diversity and functional versatility*. New York: Marcel Dekker Inc. 957-993

Opara, C. 2002. Mixed culture fermentation is a *biochemical* process involving two or more microorganisms in a nutrient substance. *Biochemical and Microbiological Engineering*. 1:144-146.

Organiation of Economic Co-operation and Development (OECD). 2017. A Review of Policy Measures Supporting Production and Use of Bioenergy. www.oecd.org/eco/surveys/economic-survey-southafrica.htm. Retrived on 11th November 2017

Osborn, D., Xu F, Ding, H., Tejirian, A., Brown, K., Albano, W., Sheehy, N. and Langston, J. 2008. Partition of enzymes between the solvent and insoluble substrate during the hydrolysis of lignocellulose by cellulases. *Journal of Molecular Catalysis. B: Enzyme.* 51(1-2): 42-48.

Osborn, D., Xu, F., Ding, H., Tejirian, A., Brown, K., Albano, W., Sheehy, N. and Langston, J. 2008. Partition of enzymes between the solvent and insoluble substrate during the hydrolysis of lignocellulose by cellulases. *Journal of Molecular Catalysis B: Enzymatic.* 51(2):42-48.

Owen, N.A., Oliver, R. and King, D. 2010. The status of conventional world oil reserves. Hype or cause for concern? *Energy Policy*. 38(8):4743.

Ozsezen, A.N. and Canakci, M. 2011. Determination of performance and combustion characteristics of a diesel engine fueled with canola and waste palm oil methyl esters. *Energy Conversion Management.* 52:108–16.

Phisalaphong, M., Srirattana, N., and Tanthapanichakoon, W. 2006. Mathematical modelling to investigate temperature effect on kinetic parameters of ethanol fermentation. *J. Biochem. Eng.* 28: 36–43.

Pimentel, D., and Patzek, T. 2005. Ethanol production using corn, switchgrass, and wood; biodiesel production using soybean and sunflower. *Natural Resources Research.* 14(1):65-76.

Polyon, C., Photharin, S., and Wiangnon, K. 2010. Experimental study of a longitudinal magnetic filter. *PIERS Proceedings*. 1(1): 1783

Potter, H.A.B. and Yong, R.N., 1993. Waste disposal by landfill in Britain: problems, solutions and the way forward. In: R.W. Sarsby (Ed.), *Waste Disposal by Landfill*. Rotterdam: Balkema: 167-173

Rahim, R., Mamat, R., Taib, M.Y. and Abdullah. A.A. 2013. Influence of fuel temperature on a diesel engine performance operating with biodiesel blended. *Journal of Mechanical Engineering and Sciences*. 2:226-236.

Rakopoulos, C.D., Rakopoulos, D.C. and Hountalas, D.T. 2008. Performance and emissions of bus engine using blends of diesel fuel with bio-diesel of sunflower or cottonseed oils derived from Greek feedstock*. Fuel.* 87:147–57.

Ramaswammy, B., Kar, D. and De, S. 2007. A study on recovery of oil from sludge containing oil using froth flotation. *Journal of Environment and Management*. 85 :150-154.

Ramos, M.J., Casas, A., Rodriguez, L., Romero, R. and Perez, A. 2008. Transesterification of sunflower over Zeolites using different metal loading: A case of leaching and agglomeration studies. *Applied Catalysis A: General.* 346:79-85.

Rashid, U., Knothe, G., Yunus, R. and Evangelista, R.L. 2014. Kapok oil methyl esters. *Biomass and Bioenergy*. 66:419–425.

Rashtizadeh, E., Farzaneh, F. and Talebpour, Z. 2014. Synthesis and characterization of Sr3Al2O6 nanocomposite as catalyst for biodiesel production. *Bioresource Technol*ogy. 1:154: 32–37.

REN 21 2017. Global Status Report. Available at www.ren21.net. Retrieved on 10th November 2017.

Rengasamy, M., Mohanraj, S. and Vardhan, S.H. 2014. Transesterification of castor oil using nanosized iron catalyst for the production of biodiesel. *Journal of Chemistry and Pharmaceutical Sciences* 2:108–112.

Robinson, J., Keating, J.D., Mansfield, S.D. and Saddler, J.N. 2013. The fermentability of concentrated softwood-derived hemicellulose fractions with and without supplemental cellulose hydrolysates. *Enzymatic and Microbial Technolology.* 33:757-765.

Rounce, P., Tsolakis, A., Leung, P. and York, A.P.E. 2010. A comparison of diesel and biodiesel emissions using dimethyl carbonate as an oxygenated additive. *Energy Fuels*. 24:4812–4819.

Rousseau, R.W. and Felder, R.M. 2005. Elementary Principles of Chemical Processes. 3rd Edition. In. John Wiley & Sons. Inc. Hoboken, N.J. United States.

Sahoo, P. K., Das, L. M., Babu, M. K. G. and Naik, S. N. 2007. Biodiesel development from high acid value polanga seed oil and performance evaluation in a CI engine. *Fuel*. 86(3):448-454.

Samanya, J. 2011. Thermal stability of sewage sludge pyrolysis oil. *International Journal for Renewable Energy Research*. 1:175-183.

Sarala, R., Rajendran, M. and Sutharson, B. 2012. Experimental studies on the performance and emission characteristics of a diesel engine fuelled with Heliant oil methyl ester and its diesel blends. *European Journal of Scientific Research*. 93:400-407.

Sassner, P., Galbe, M. and Zacchi, G. 2006. Bioethanol production based on simultaneous saccharification and fermentation of steampretreated Salix at high dry-matter content. *Enzyme Microbial Technology.* 39(4):756-762.

Sassner, P., Galbe, M. and Zacchi, G. 2007. Techno-economic evaluation of bioethanol production from three different lignocellulosic materials. *Biomass Bioenergy*. 10:14-16.

Sekmen, P. and Yilbasi, Z. 2011. Application of energy and exergy analyses to a CI engine using biodiesel fuel. *Mathematical and Computational Applications*. 16:797-808.

Shahir, S.A., Masjuki, H.H., Kalam, M.A., Imran, A., Fattah, I.M.R. and Sanjid, A. 2014. Feasibility of diesel–biodiesel–ethanol/bioethanol blend as existing CI engine fuel: an assessment of properties, material compatibility, safety and combustion. *Reneable and Sustainable Energy Reviews.* 32:379–395.

Sharma, Y.C. and Singh, B. 2007. Development of biodiesel from karanja, a tree found in rural India. *Fuel.* 87:1740-1742.

Sharon, H., Karuppasamy, K., Soban Kumar, D.R. and Sundaresan, A. 2012. A test on DI diesel engine fueled with methyl esters of used palm oil. *Renew Energy*. 47:160–6.

Shengyang, H., Yanping G., Wang Y. and Heyou H. 2011. Nano-magnetic catalyst KF/CaO-Fe2O3 for biodiesel production. *Applied Energy*. 88:2685-2690.

Silitonga, A.S., Atabani, A.E., Mahlia, T.M.I., Masjuki, H.H., Badruddin, IA and Mekhilef, S. 2011. A review on prospect of Jatropha curcas for biodiesel in Indonesia. *Renewable and Sustainable Energy Reviews.* 15:3733–3756.

Singh, A., He, B., Thompson, J. and Van Gerpen, J. 2006. Process optimization of biodiesel production using alkaline catalysts. *Applied Engineering in Agriculture.* 22:597-600.

Singh, A.P., He, B.B., Thompson, J.C. and Gerpen, J.H. 2006. Process Optimization of Biodiesel production using alkaline catalysts. *Applied Engineering in Agriculture*. 22:597-600.

Singh, V. and Sharma, Y.C. 2017. Low cost guinea fowl bone derived recyclable heterogeneous catalyst for microwave assisted transesterification of Annona squamosa L. seed oil. *Energy Conversion and Management.*138:627-637.

Singh, V., Yadav, M. and Sharma, Y.C. 2017. Effect of co-solvent on biodiesel production using calcium aluminium oxide as a reusable catalyst and waste vegetable oil*. Fuel.* 203:360-369.

Sivakumar, P., Anbarasu, K., Renganathan, S. 2011. Biodiesel production by alkali catalyzed transesterification of dairy waste scum. *Fuel*. 90:147-151.

Sluiter, J.B., Ruiz, O.R., Scarlata, C.J. and Sluiter, A. 2010. Compositional Analysis of Lignocellulosic Feedstocks. 1. Review and Description of Methods. *Journal of Agricultural and Food Chemistry.* 58(16):9043-9053.

Soma, Y., Nakajima, M. and Yoshida, K. 2007. The application of coconut-oil methyl ester for diesel engine. *SAE Technical Paper*; 2007-32-0065.

Sun C., Qiu F., Yang D. and Ye B. 2014. Preparation of biodiesel from soybean oil catalyzed by Al–Ca hydrotalcite loaded with K2CO3 as heterogeneous solid base catalyst. *Fuel Procesing Techno*logy. 126:383–91.

Sun, Y., Li, X., Zhang, W. and Wang, H. 2007. A Method for the preparation of stable dispersion of zero-valent iron nanoparticles. *Colloids Surface A*. 308:6-60.

Suresh, P.S., Kumar, A., Kumar, R., Singh, V. P. 2008. An in-silico approach to bioremediation: laccase as a case study. *Journal of Molecular Graphics and Modelling*. 26(5):845–849.

Suryawanshi, J. 2006. Performance and emission characteristics of CI engine fueled by coconut oil methyl ester. *SAE Technical Paper*; 2006-32-0077.

Swaminathan, C. and Sarangan, J. 2012. Performance and exhaust emission characteristics of a CI engine fueled with biodiesel (fish oil) with DEE as additive. *Biomass Bioenergy.* 39:168–74.

Taherzadeh, M.J. and Karimi, K. 2008. Pretreatment of lignocellulosic wastes to improve ethanol and biogas production: a review. *International Journal of Molecular Sciences*. 9:162.

Taherzadeh, M.J., Nilsson, A. and Liden, G. 2001. Use of dynamic step response for control of fed-batch conversion of lignocellulosic hydrolyzates to ethanol. *J Biotechnol.* 89(1):41-53.

Tan, K. T. and Lee, K. 2014. A review on supercritical fluids (SCF) technology in sustainable biodiesel production: Potential and challenges. *Renewable and Sustainable Energy Reviews*. 5(15):2452-2456.

Tan, Y.H., Abdullah, M.O. and Nolasco-Hipolito, C. 2015. The potential of waste cooking oil-based biodiesel using heterogeneous catalyst derived from various calcined eggshells coupled with an emulsification technique: A review on the emission reduction and engine performance. *Renew Sust. Energy Reviews*. 47:589-603.

Tang, Z., Du, Z., Min, E., Gao, L., Jiang, T., and Han, B. 2006. Phase equilibria of methanol–triolein system at elevated temperature and pressure. *Fluid Phase Equilibrium*. 239:8–11.

Tangviroon P. and Svang-Ariyaskul A., 2014. Life Cycle Assessment Comparison between Methanol and Ethanol Feedstock for the Biodiesel from Soybean Oil. *International Scholarly and Scientific Research & Innovation.* 8(5):124-132

Tashtoush, G. M., Widyan, M. I. and Jarrah, M. M. 2004. Experimental study on evaluation and optimization of conversion of waste animal fat into biodiesel. *Energy Conversion and Management*. (45):2697– 2711.

Taufiq-Yap YH and Lee HV. 2013. Higher grade biodiesel production by using solid heterogeneous catalysts. In Pogaku, Sarbatly RH (Ed). Springer: United States.

Taufiq-Yap YH, Teo SH, Rashid U, Islam A, Hussien MZ and Lee KT. 2014. Transesterification of Jatropha curcas crude oil to biodiesel on calcium lanthanum mixed oxide catalyst: effect of stoichiometric composition. *Energy Conversion and Management*. 88: 1290–1296.

Teo S.H., Rashid, U. and Taufiq-Yap, Y.H. 2014. Biodiesel production from crude Jatropha Curcas oil using calcium based mixed oxide catalysts. *Fuel*. 136: 244–252.

Thangaraj, B., Ramachandran, K.B. and Raj, S.B. 2014. Homogeneous catalytic transesterification of renewable Azadirachta indica (Neem) oil and its derivatives to biodiesel fuel via acid/alkaline esterification processes. *International Journal of Renewable Energy and Biofuels*. 11:1-16.

Thomsen, A.B., Martín, C. and Klinke, H.B. 2007. Wet oxidation as a pretreatment method for enhancing the enzymatic convertibility of sugarcane bagasse*. Enzyme and Microbial Technology.* 40:426-432

Thomsen, M.H, Oleskowicz, P.P., Przemyslaw, L. and Holm-Nielsen, J.B. 2008. Ethanol production from maize silage as lignocellulosic biomass in anaerobically digested and wet-oxidized manure. *Bioresource Technology.* 99:13-34.

Tinprabatha P., Hespelb C., Chanchaonac S. and Foucherb F. 2016. Impact of cold conditions on diesel injection processes of biodiesel blends. *Renewable Energy*. 96:270–280.

Tiwari, A. K., Kumar, A. and Raheman, H. 2007. Biodiesel production from Jatropha oil (Jatropha Curcas) with high free fatty acids:an optimized process. *Biomass and Bioenergy*. 31:569-575.

Toka, A., Iakovou, E., Vlachos, D., Tsolakis, N., and Grigoriadou, A-L. 2014. Managing the diffusion of biomass in the residential energy sector: an illustrative real-world case study. *Applied Energy*. 129:56–69.

Tudu, K., Murugan, S. and Patel, S.K. 2016. Experimental analysis of a DI diesel engine fuelled with light fraction of pyrolysis oil. *Int. J. Oil, Gas Coal Technology*. 11:318–338.

Ugarte, D.G. 2006. Developing bioenergy: economic and social issues in bioenergy and agriculture: promises and challenges. *International Food Policy Research Institute 2020 Focus 14*:71-73.

Ugursal V.I. 2014. Energy consumption, associated questions and some answers. *Appl Energy.* 130:783–792.

United States Department of Agriculture (USDA). 2017 Oilseeds. Available at http://www.fas.usda.gov/data/oilseeds-world-markets-andtrade. Retrieved on 10th November 2017

Utama, N.A., Fathoni, A.M., Kristianto, M.A. and McLellan, B.C. 2014. The end of fossil fuel era: supply-demand measures through energy efficiency. *Process and Environmental Sciences.* 20:40–45.

Van Eijck, J., Batidzirai, B. and Faaij, A. 2014. Current and future economic performance of first and second generationbiofuels in developing countries. *Applied Energy*. 135:115–141.

Van Zyl, J.M., Van Rensburg, E., Van Zyl, W.H., Harms, T.M. and Lynd, L.R. 2011. A kinetic model for simultaneous saccharification and fermentation of Avicel with Saccharomyces cerevisiae. *Biotechnology and Bioengineering*. 108(4):924-33.

Viikari, L., Alapuranen, M., Puranen, T., Vehmaanperä, J. and Siika-aho, M. 2007. Thermostable enzymes in lignocellulose hydrolysis*. Advances in Biochemical Engineering/Biotechnology*. 108:121-145.

Vujicic, D., Comic, D., Zarubica, A., Micic, R., and Boskovic, G. 2010. Kinetics of biodiesel synthesis from sunflower oil over CaO heterogeneous catalyst. *Fuel*. 89:2054-2061.

Wang L, Dong X, Jiang H, Li G, Zhang M. 2014. Ordered mesoporous carbon supported ferric sulfate: a novel catalyst for the esterification of free fatty acids in waste cooking oil. *Fuel Procesing Technology*. 128:10-16.

Wang, J., Chen, Y., Wang, X. and Cao, F. 2009. Aluminumdodecatungstophosphate (AL0.9H0.3PW12O40) nanotube as a solid acid catalyst one-pot production of biodieselfrom waste cooking oil. *BioResources*. 4:1477-1486.

Wang, L., Dong, X., Jiang, H., Li, G. and Zhang M. 2014. Ordered mesoporous carbon supported ferric sulfate: a novel catalyst for the esterification of free fatty acids in waste cooking oil. *Fuel Process Technol*. 128:10-16.

Wang, Y., Hu S., Wen, L., Guan, Y. and Han, H. 2009. Preparation of mesoporous nano-sized KF/CaO/MgO catalysts and their application for biodiesel synthesis via transesterification. *Catalysis Letters.* 131(8):574.

Wang, Y., Wu, H. and Zong, M.H. 2008. Improvement of biodiesel production by lipozyme TLIM-catalysed methanolysis using surface methodology and acyl migration enhancer. *Bioresource and Technol*ogy. (99):7232.

Warabi, Y., Kusdiana, D. and Saka, S. 2004. Reactivity of triglycerides and fatty acids of rapeseed oil in supercritical alcohols. *Bioresource Technology*. (91):283-287.

Watanabe, H. and Tokuda, G. 2010. Cellulolytic system in insects. *Annual Review of Entomology*. 55:609-632.

Welz, P.J., Ramond, J.-B., Cowan, D.A., Prins, A. and Burton, S.G. 2011. Ethanol degradation and the benefits of incremental priming in pilot-scale constructed wetlands. *Ecological Engineering*. 37:1453–1459.

Wen, L.B., Wang, Y., Lu, D.L., Hu, S.Y. and Han, H.Y. 2010. Preparation of KF/CaO nanocatalyst and its application in biodiesel production from Chinese tallow seed oil. *Fuel.* 89(71):2267.

Wen, M., Qi, H., Zhao, W., Chen, J., Li, L. and Wu, Q. 2008. Phase transfer catalysis: synthesis of mono dispersed Fe-Pt nanoparticles and its electrocatalytic activity. *Colloids Surface A*. 312:8-73.

Wen, Z., Yu, X., Tu, S-T., Yan, J. and Dahlquist, E. 2010. Biodiesel production from waste cooking oil catalyzed by TiO2–MgO mixed oxides. *Bioresource Technology.* 101:9570–9576.

Widyan M. I. and Shyoukh A. O. 2002. Experimental evaluation of the transesterification of waste palm oil into biodiesel. *Bioresource Technology.* 85(3):253.

Woodford, J.J., Parlett, C.M.A., Dacquin, J.P., Cibin, G., Dent, A., Montero, J., Wilson, K.. and Lee, A.F. 2014. Identifying the active phase in Cs-promoted MgO nanocatalysts for triglyceride transesterification. *Journal of Chemical Technology and Biotechnology*. 89:73-80.

Wu, H., Zhang J., Liu, Y., Zheng, J. and Wei, Q. 2014. Biodiesel production from Jatropha oil using mesoporous molecular sieves supporting K2SiO3 as catalysts for transesterification*. Fuel Processing Technology.* 119:114–120.

Wyman, C. 1999. Biomass ethanol: technical progress, opportunities, and commercial challenges. *Annual Review of Energy and the Environment.* 24(1):189-226.

Wyman, C.E. 2003. Potential synergies and challenges in refining cellulosic biomass to fuels, chemicals and power. *Biotechnology Progress.* 19:254-262.

Wyman, C.E., Balan, V., Dale, B.E., Elander, R.T., Falls, M., Hames, B., Holtzapple, M.T., Ladisch, M.R., Lee, Y.Y., Mosier, N., Pallapolu, V.R., Shi J., Thomas, S.R. and Warner, R.E. 2011. Comparative data on effects of leading pretreatments and enzyme loadings and formulations on sugar yields from different switchgrass sources. *Bioresource Technology.* 102:11052–11062.

Xiang, Y., Xiang, Y. and Wang, L. 2017. Microwave radiation improves biodiesel yields from waste cooking oil in the presence of modified coal fly ash. *Journal of Taibah University for Science*. 11:1019-1029.

Xie W. and Fan M. 2014. Biodiesel production by transesterification using tetraalkylammonium hydroxides immobilized onto SBA-15 as a solid catalyst. *Chem Eng J.* 239: 60–67.

Xie W. and Wang J. 2014. Enzymatic production of biodiesel from soybean oil by using immobilized lipase on Fe3O4 / poly (styrene-rnethacrylic acid) magnetic microsphere as a biocatalyst. *Energy Fuel.* 28: 2624–2631.

Xie W. and Yang X., Fan M. 2015. Novel solid base catalyst for biodiesel production: mesoporous SBA-15 silica immobilized with 1,3-dicyclohexyl-2-octylguanidine. *Renewable Energy*. 80:230–237.

Xie W., Wang H. and Li H. 2012. Silica-supported tin oxides as heterogeneous acid catalysts for transesterification of soybean oil with methanol. *Industrial and Engineering Chemistry Research*. 51: 225–231.

Xie, W. and Ma, N. 2009. Immobilized lipase on Fe_3O_4 nanoparticles as biocatalyst for biodiesel production. *Energy Fuels*. 23(53):1347.

Xie, W. and Yang, Z. 2007. Ba-ZnO catalysts for soybean oil transesterification. *Catalysis Letters.* (117):159.

Xie, W., Yang, X. and Fan, M. 2015. Novel solid base catalyst for biodiesel production: mesoporous SBA-15 silica immobilized with 1,3-dicyclohexyl-2-octylguanidine. *Renewable Energy*. 80:230–237.

Xu, L., Wang, Y., Yang, X., Yu X., Guo, Y. and Clark, J.H. 2008. Preparation of mesoporous polyoxometalate-tantalum pentoxide composite catalyst and its application for biodiesel production by esterification and transesterification. *Green Chemistry*. 10:746-745.

Yang, Z. and Xie, W. 2007. Soybean oil transesterification over ZnO modified with alkaline earth metals. *Fuel processing technology*. 88:631-638

Ying, M. and Chen, G.Y. 2007. Study on the production of biodiesel by magnetic cell biocatalyst based on lipase-producing Bacillus subtilis. *Applied Biochemistry and Biotechnol*ogy. 137:793-803.

Zabed, H., Faruq, G. and Sahu, J.N. 2014. Bioethanol production from fermentable sugar juice. *The Scientific World Journal*. 1:1–11.

Zakaria, H., Khalid, A., Sies, M.F. and Mustaffa, N. 2014. Overview effect of biodiesel storage on properties and characteristics. *Applied Mechanics and Materials*. 466:260-264.

Zhang, L., Sun, S., Xin, Z., Sheng, B. and Liu, Q. 2010. Synthesis and component confirmation of biodiesel from palm oil and dimethyl carbonate catalyzed by immobilized-lipase in solvent-free system. *Fuel*. 89:3960–3965

Zhang, Y., Dube, M.A., McLean, D.D. and Kates, M. 2003. Biodiesel production from waste cooking oil: Process design and technological assessment. *Bioresource Technology*. 89(1):1-16.

Zhu, H., Wu, Z., Chen, Y., Zhang, P., Duan, S., Liu, X. and Mao, Z. 2006. Preparation of biodiesel catalyzed by solid super base of calcium oxide and its refining process. *Chinese Journal of Catalysis.* 27:391–396

APPENDICES

Sample calculations for heat balances around the engine and biodiesel thermal properties

- ***Data recorded***

Torque radius = 318 mm

Hanger weight (or Hanging Load) = 248 N

Friction load = 76 N at 1788 rpm

Friction load = 260 N at 2107 rpm

Applied load = 475 N at 2107 rpm

Brake load = 475 - 260 = 215 N

Coefficient of discharge = 0.6

Air box orifice size = 32 mm

Temperature of exhaust gas leaving the engine = 60°C

Temperature of exhaust gas leaving the calorimeter = 57°C

Temperature of water entering the exhaust calorimeter = 41°C

Temperature of water leaving the exhaust calorimeter = 55°C

Temperature of water entering the engine = 67°C

Temperature of water leaving the engine = 76°C

Water flowing through the exhaust calorimeter = 3.6 L/min

Water flowing through engine = 20 L/min

- ***Calculations and Equations***

Table 1: Calculations of the mass flow rate of EOWWS Biodiesel

Volume (m^3)	Time (s)	Mass flow rate (m^3/s)
50×10^{-6}	33.7	1.484×10^{-6}
100×10^{-6}	67.1	1.490×10^{-6}
200×10^{-6}	133.5	1.498×10^{-6}
Average	0.0014907×10^{-3} m^3/s	
$\dot{m}_f$	$0.0014907 \times 10^{-3} \times 840 = 1.252 \times 10^{-3}$ kg/s	

a) Mass flow rate of the air

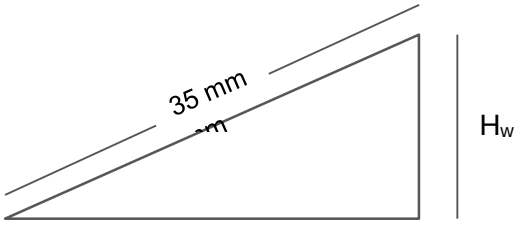

$$H_w = 0.035 \times \sin 30$$
$$= 0.0175m$$

$$A = \frac{\pi \times 0.039^2}{4}$$
$$= 0.001195\ m^2$$

$$H_a = \frac{\rho_w \times h_w}{\rho_a}$$
$$= \frac{1000 \times 0.0175}{1.23}$$
$$= 14.227\ m$$

$$m_a = C_d \times \rho_a \times A \times \sqrt{2gh_a}$$
$$= 0.6 \times 1.23 \times 0.001195 \times \sqrt{2 \times 9.81 \times 14.227}$$
$$= 0.01476\ kg/s$$

b) The theoretical air mass flow rate

$$\dot{m}_t = 1.23 \times 0.001195 \times \sqrt{2 \times 9.81 \times 14.227}$$
$$= 0.02456\ kg/s$$

c) The air fuel ratio

$$The\ air\ fuel\ ratio = \frac{\dot{m}_a}{\dot{m}_f}$$

$$= \frac{0.01476}{1.252 \times 10^{-3}}$$

$$= 11.8:1$$

d) The brake power

$$Bp = \frac{2\pi NFR}{60}$$

$$= \frac{2\pi \times 1788 \times 215 \times 0.318}{60}$$

$$= 12\,801\ W$$

e) The indicated power using the motoring test

$$Ip = Bp + Fp$$

$$Fp = \frac{2\pi NF_\mu R}{60}$$

$$= \frac{2\pi \times 1788 \times 76 \times 0.318}{60}$$

$= 4525\,W$

$Ip = 12801 + 4525 = 17326\,W$

f) The mechanical efficiency

$$\eta_{mechanical} = \frac{Bp}{Bp + Fp}$$

$$= \frac{Bp}{Bp + Fp}$$
$$= \frac{12801}{12801 + 4525}$$
$$= 0.7388 = 73.88\%$$

$$ite = \frac{Ip}{\dot{m}_f \times CV}$$

$$= \frac{17326}{0.001252 \times 45 \times 10^6}$$

$$= 0.3075$$

$$= 30.75\%$$

g) The brake thermal efficiency

$$bte = \frac{Bp}{\dot{m}_f \times CV}$$

$$= \frac{12801}{0.001252 \times 45 \times 10^6}$$

$$= 0.2272$$

$$= 22.72\%$$

h) Efficiency ratio based on brake thermal

$$\eta = \frac{bte}{ite}$$

$$= \frac{0.2272}{0.3075}$$

$= 0.7388$

$= 73.88\%$

Table 2: Heat balance for the test performed in kJ/min

Heat In	$= \dot{m}_f \times CV \times 60$ $= 0.001252 \times 45 \times 10^6 \times 60$ $= 3380\ kJ/min$	100%	**Heat Out**	$Brake\ power \quad = Bp \times 60$ $= 12801 \times 60$ $= 768\ kJ/min$	**22.7%**
				$Cooling\ water \quad = M_{cw} \times 4.2 \times (t_o - t_i)$ $= 20 \times 4.2 \times (76 - 67)$ $= 756\ kJ/min$	**22.4%**
				$Exhaust\ gas \quad = (\dot{m}_a + \dot{m}_f) \times C_p(t_e - t_a)$ $= [(0.01476 + 0.001252) \times 60] \times 1.005(600 - 57)$ $= 524\ kJ/min$	**15.5%**
				Unaccounted=3380 - (768 +756 + 524)	**39.4%**